

# IOWA STATE UNIVERSITY

## Digital Repository

---

Graduate Theses and Dissertations

Iowa State University Capstones, Theses and  
Dissertations

---

2013

## A laboratory study of the effects of bio-stabilization on geomaterials

Shengting Li  
*Iowa State University*

Follow this and additional works at: <https://lib.dr.iastate.edu/etd>



Part of the [Civil Engineering Commons](#), and the [Geotechnical Engineering Commons](#)

---

### Recommended Citation

Li, Shengting, "A laboratory study of the effects of bio-stabilization on geomaterials" (2013). *Graduate Theses and Dissertations*. 13100.  
<https://lib.dr.iastate.edu/etd/13100>

This Thesis is brought to you for free and open access by the Iowa State University Capstones, Theses and Dissertations at Iowa State University Digital Repository. It has been accepted for inclusion in Graduate Theses and Dissertations by an authorized administrator of Iowa State University Digital Repository. For more information, please contact [digirep@iastate.edu](mailto:digirep@iastate.edu).



[www.manaraa.com](http://www.manaraa.com)

**A laboratory study of the effects of bio-stabilization on geomaterials**

by

**Shengting Li**

A thesis submitted to the graduate faculty

In partial fulfillment of the requirements for the degree of  
**MASTER OF SCIENCE**

Major: Civil Engineering (Geotechnical Engineering)

Program of Study Committee:  
David J. White, Major Professor  
Peter C. Taylor  
Jian Chu  
Thomas E. Loynachan

Iowa State University

Ames, Iowa

2013

Copyright © Shengting Li, 2013. All rights reserved.

*For*

*My loving parents, Li Ren and Li Xinhua*

## TABLE OF CONTENTS

LIST OF TABLES .....	vi
LIST OF FIGURES .....	vii
LIST OF SYMBOLS .....	x
ACKNOWLEDGEMENTS .....	xi
ABSTRACT .....	xii
<b>CHAPTER 1. INTRODUCTION .....</b>	<b>1</b>
Industry problem .....	1
Technical problem .....	2
Goal of the research .....	3
Objectives .....	3
Significance of the research .....	3
Organization of the document.....	3
<b>CHAPTER 2. BACKGROUND AND LITERATURE REVIEW .....</b>	<b>4</b>
Bio-stabilization for geotechnical applications.....	4
Soil .....	4
Concrete .....	5
Other applications .....	5
Bio-treatment methods.....	6
Bio-reactions, processes, and bio-species .....	6
Methods.....	7
Characterization of untreated and treated materials.....	8
Scanning electron microscopy .....	8
X-ray diffraction .....	9
Benefits of bio-stabilization .....	10
<b>CHAPTER 3. METHODS .....</b>	<b>11</b>
Research design .....	11
Bio-stabilization methods .....	12
Laboratory processes .....	12
Rehydrate freeze-dried <i>Bacillus pasteurii</i> .....	12
Streak out lines to get a single colony in solid medium .....	13
Inoculate single colony into culture medium.....	13
Dilute.....	15
Re-suspend in new culture medium.....	15
Mix the culture medium and bacteria with soil (Figure 6) .....	15
Sample preparation .....	15
Lab tests .....	16
Unconfined compression .....	16
Scanning electron microscope (SEM) .....	17
Energy dispersive X-ray spectroscopy (EDS) .....	18
Mercury intrusion porosimetry .....	19

Iowa pore index.....	20
Resistance of concrete to rapid freezing and thawing .....	21
Soundness of aggregate by freezing and thawing.....	22
Soil index tests .....	23
<b>CHAPTER 4. MATERIALS .....</b>	<b>24</b>
Bio-stabilization materials .....	24
<i>Bacillus pasteurii</i> .....	24
Liquid incubation medium .....	25
Porous ceramic disks.....	27
Geomaterials .....	27
Standard Silica Sand .....	28
Surface material from an unpaved road on 160 <sup>th</sup> Street in Boone County, Iowa .....	29
Surface material from an unpaved road on Vail Avenue in Hamilton County, Iowa.....	31
Concrete pavement coarse aggregate.....	34
<b>CHAPTER 5. RESULTS AND DISCUSSION.....</b>	<b>37</b>
Increasing strength of granular soil.....	37
Bio-treatment media and treatment cycles.....	37
Unconfined compression tests .....	38
Compressive strengths from the NH <sub>4</sub> Cl liquid medium .....	39
Compressive strengths from the (NH <sub>4</sub> ) <sub>2</sub> SO <sub>4</sub> liquid medium.....	40
Summary of unconfined compression tests .....	42
Scanning electron microscopy (SEM) .....	43
X-ray diffraction (XRD) test.....	52
Plugging pores in concrete aggregate .....	55
Bio-treatment cycles .....	55
Iowa pore index test .....	55
Mercury intrusion porosimetry .....	56
Freezing and thawing test .....	62
Compression test.....	66
Scanning electron microscopy (SEM) test.....	67
Energy dispersive X-ray spectroscopy (EDS) test.....	91
<b>CHAPTER 6. CONCLUSIONS AND RECOMMENDATIONS .....</b>	<b>99</b>
Key findings from soil strength tests .....	99
Key findings from aggregate tests .....	99
Summary of conclusions.....	100
Recommendations.....	101
Recommendations for future research .....	101
<b>WORKS CITED .....</b>	<b>102</b>
<b>APPENDIX A. Unconfined compressive strength .....</b>	<b>105</b>
<b>APPENDIX B. Concrete coarse aggregate properties .....</b>	<b>111</b>
<b>APPENDIX C. Concrete mix design .....</b>	<b>112</b>
<b>APPENDIX D. Index properties of concrete .....</b>	<b>114</b>

APPENDIX E. Compressive strength of concrete.....	115
APPENDIX F. Freezing and thawing raw data .....	116
APPENDIX G. Mercury intrusion porosimetry raw data.....	120
APPENDIX H. Plan for field testing .....	131

## LIST OF TABLES

Table 1. Microbial induced cementation treatment and formula (DeJong et al. 2006) .....	8
Table 2. XRD quantitative analysis of the final weight fractions of sand samples .....	10
Table 3. Formula for making 1.0 L of the culture medium .....	12
Table 4. Grading requirement of aggregates.....	23
Table 5. Sieve size for determination of weight loss .....	23
Table 6. Formula for making 1.0 L of the incubation liquid medium .....	26
Table 7. Quantity of ingredients for different reagents (as stated on bottle labels).....	26
Table 8. Specifications of porous ceramic disks.....	27
Table 9. Silica sand index properties .....	28
Table 10. Silica sand sieve analysis results .....	29
Table 11. 160 <sup>th</sup> Street soil index properties .....	30
Table 12. 160 <sup>th</sup> Street soil sieve analysis results.....	30
Table 13. Vail Avenue soil index properties .....	32
Table 14. Vail Avenue soil sieve analysis results.....	33
Table 15. Concrete pavement coarse aggregate index properties.....	34
Table 16. Concrete pavement coarse aggregate sieve analysis results .....	35
Table 17. Specific gravity and absorption of coarse aggregate .....	36
Table 18. Silt and clay content of granular soil .....	43
Table 19. Elemental analysis of untreated silica sand .....	51
Table 20. Elemental analysis for bio-treated silica sand.....	51
Table 21. Mohs' scale of hardness (Mohs, 1773–1839) .....	54
Table 22. Iowa pore index of concrete aggregates .....	55
Table 23. Quality of aggregates refer to secondary pore index (Iowa DOT manual, 2010) ..	56
Table 24. Mercury intrusion porosimetry data summary.....	57
Table 25. Compressive strengths of silica sand treated with NH <sub>4</sub> Cl without bacteria .....	105
Table 26. Compressive strengths of silica sand after single bio-treatment with NH <sub>4</sub> Cl.....	105
Table 27. Compressive strengths of silica sand after double bio-treatment with NH <sub>4</sub> Cl .....	106
Table 28. Compressive strength of SM soil after single bio-treatment with NH <sub>4</sub> Cl .....	106
Table 29. Compressive strength of SM soil after double bio-treatment with NH <sub>4</sub> Cl .....	107
Table 30. Compressive strength of silica sand treated with (NH <sub>4</sub> ) <sub>2</sub> SO <sub>4</sub> without bacteria ....	107
Table 31. Compressive strength of silica sand after single bio-treatment with (NH <sub>4</sub> ) <sub>2</sub> SO <sub>4</sub> .	108
Table 32. Compressive strength of silica sand after double bio-treatment with (NH <sub>4</sub> ) <sub>2</sub> SO <sub>4</sub> .....	108
Table 33. Compressive strength of SM soil after single bio-treatment with (NH <sub>4</sub> ) <sub>2</sub> SO <sub>4</sub> .....	109
Table 34. Compressive strength of SM soil after double bio-treatment with (NH <sub>4</sub> ) <sub>2</sub> SO <sub>4</sub> ....	109
Table 35. Compressive strength of silica sand after double bio-treatment with NH <sub>4</sub> Cl.....	110
Table 36. Specific gravity and absorption of untreated aggregate.....	111
Table 37. Specific gravity and absorption of bio-treated aggregate .....	111
Table 38. Untreated concrete mix design sheet .....	112
Table 39. Bio-treated aggregate concrete mix design sheet .....	113
Table 40. Index properties of untreated concrete.....	114
Table 41. Index properties of bio-treated aggregate concrete.....	114
Table 42. Compressive strength of untreated concrete .....	115
Table 43. Compressive strength of bio-treated aggregate concrete .....	115
Table 44. Freezing and thawing raw data .....	116

## LIST OF FIGURES

Figure 1. SEM of treated silica sand particles (Reproduced from DeJong et al. 2010).....	9
Figure 2. <i>Bacillus pasteurii</i> from ATCC .....	12
Figure 3. Solid medium for <i>Bacillus pasteurii</i> .....	13
Figure 4. Culture medium for <i>Bacillus pasteurii</i> .....	14
Figure 5. Flask with culture medium in incubator shaker .....	14
Figure 6. Introduce the culture medium into soil specimen.....	15
Figure 7. Unconfined compression test device .....	17
Figure 8. FEI Quanta FEG250 SEM equipment (a. basic component, b. working stage) .....	18
Figure 9. Quantitatively determination of chemical compositions (right screen) .....	19
Figure 10. Iowa pore index testing equipment.....	20
Figure 11. Humboldt H-3185 rapid freeze-thaw cabinet .....	21
Figure 12. Soundness of aggregate testing in freeze-thaw cabinet .....	22
Figure 13. <i>Bacillus pasteurii</i> (ATCC catalog No. 6453) .....	24
Figure 14. Microscopy view of <i>Bacillus pasteurii</i> .....	25
Figure 15. Ceramic hydrophilic porous disk after bio-treatment.....	27
Figure 16. Standard silica sand without bio-treatment .....	28
Figure 17. Surface material from 160th Street in Boone County, Iowa .....	29
Figure 18. 160 <sup>th</sup> Street soil particle size distribution .....	31
Figure 19. Surface material from Vail Avenue in Hamilton County, Iowa.....	32
Figure 20. Vail Avenue soil particle size distribution .....	33
Figure 21. Concrete coarse aggregates without bio-treatment.....	34
Figure 22. Concrete pavement coarse aggregate particle size distribution .....	35
Figure 23. Liquid medium with bacteria contains NH <sub>4</sub> Cl (left) and (NH <sub>4</sub> ) <sub>2</sub> SO <sub>4</sub> (right).....	38
Figure 24. Failed silica sand sample after unconfined compression .....	39
Figure 25. UC strength of samples with NH <sub>4</sub> Cl medium treatment .....	40
Figure 26. UC strength of samples with (NH <sub>4</sub> ) <sub>2</sub> SO <sub>4</sub> medium treatment.....	41
Figure 27. UC strength of SM soil samples at different oven-dried temperature .....	42
Figure 28. 50x magnification of untreated silica sand .....	43
Figure 29. 300x magnification of untreated silica sand .....	44
Figure 30. Silica sands without bio-treatment (3000x).....	44
Figure 31. Silica sands with bio-treatment (50x).....	45
Figure 32. Silica sands with bio-treatment (100x).....	46
Figure 33. Silica sands with bio-treatment (200x).....	46
Figure 34. Silica sands with bio-treatment (300x).....	47
Figure 35. Silica sands with bio-treatment (350x).....	48
Figure 36. Silica sands with bio-treatment (600x).....	48
Figure 37. Silica sands with bio-treatment (1000x).....	49
Figure 38. Silica sands with bio-treatment (1400x).....	49
Figure 39. Silica sands with bio-treatment (1500x).....	50
Figure 40. Silica sands with bio-treatment (3000x).....	52
Figure 41. XRD results for untreated silica sand .....	53
Figure 42. XRD results for bio-stabilized silica sand .....	54
Figure 43. Cumulative intrusion versus pore size at different treatment cycles .....	58

Figure 44. Incremental intrusion versus pore size at different treatment cycles .....	59
Figure 45. Differential intrusion versus pore size at different cycles .....	60
Figure 46. Log differential intrusion versus pore size at different cycles .....	61
Figure 47. Pore size distribution at different treatment cycles .....	62
Figure 48. Variation of relative dynamic modulus after freeze and thaw .....	63
Figure 49. Variation of weight change after freeze and thaw .....	64
Figure 50. Untreated concrete beam at different freezing thawing cycles .....	65
Figure 51. Bio-treated aggregate concrete beam at different freezing and thawing cycles ....	66
Figure 52. Compressive strength of concrete .....	67
Figure 53. Ceramic plate without bio-treatment, 100x .....	68
Figure 54. Ceramic plate without bio-treatment, 300x .....	69
Figure 55. Ceramic plate without bio-treatment, 1000x .....	69
Figure 56. Ceramic plate without bio-treatment, 3000x .....	70
Figure 57. Ceramic plate without bio-treatment, 10000x .....	70
Figure 58. Ceramic plate with bio-treatment, 100x .....	71
Figure 59. Ceramic plate with bio-treatment, 300x .....	72
Figure 60. Ceramic plate with bio-treatment, 700x .....	72
Figure 61. Ceramic plate with bio-treatment, 1000x .....	73
Figure 62. Ceramic plate with bio-treatment, 1200x .....	73
Figure 63. Ceramic plate with bio-treatment, 3000x .....	74
Figure 64. Section of ceramic plate with bio-treatment, 150x.....	75
Figure 65. Section of ceramic plate with bio-treatment, 500x.....	75
Figure 66. Section of ceramic plate with bio-treatment, 1000x.....	76
Figure 67. Section of ceramic plate with bio-treatment, 3000x.....	76
Figure 68. Fort Calhoun aggregates without bio-treatment, 150x .....	77
Figure 69. Fort Calhoun aggregates without bio-treatment, 500x .....	78
Figure 70. Fort Calhoun aggregates without bio-treatment, 1500x .....	78
Figure 71. Fort Calhoun aggregates without bio-treatment, 5000x .....	79
Figure 72. Fort Calhoun aggregates without bio-treatment, 15000x .....	79
Figure 73. Fort Calhoun aggregates with 1 cycle bio-treatment, 150x.....	80
Figure 74. Fort Calhoun aggregates with 1 cycle bio-treatment, 500x.....	81
Figure 75. Fort Calhoun aggregates with 1 cycle bio-treatment, 1500x.....	81
Figure 76. Fort Calhoun aggregates with 1 cycle bio-treatment, 5000x.....	82
Figure 77. Fort Calhoun aggregates with 1 cycle bio-treatment, 15000x.....	82
Figure 78. Winterset Ledge aggregates without bio-treatment, 1500x .....	83
Figure 79. Winterset Ledge aggregates without bio-treatment, 5000x .....	84
Figure 80. Winterset Ledge aggregates with 1 cycle bio-treatment, 1500x .....	85
Figure 81. Winterset Ledge aggregates with 1 cycle bio-treatment, 5000x .....	85
Figure 82. Winterset Ledge aggregates with 10 cycles' bio-treatment, 1500x .....	86
Figure 83. Winterset Ledge aggregates with 10 cycles' bio-treatment, 5000x .....	87
Figure 84. Hardened concrete without bio-treatment, 150x .....	88
Figure 85. Hardened concrete without bio-treatment, 500x .....	88
Figure 86. Hardened concrete with bio-treatment, 50x .....	89
Figure 87. Hardened concrete with bio-treatment, 168x .....	90
Figure 88. Hardened concrete with bio-treatment, 500x .....	90

Figure 89. Hardened concrete with bio-treatment, 1500x .....	91
Figure 90. Elemental composition of untreated aggregates .....	92
Figure 91. Elemental composition of 1 cycle bio-treated aggregate .....	92
Figure 92. SEM of 1 cycle bio-treated aggregate .....	93
Figure 93. Elemental mapping of 1 cycle bio-treated aggregate .....	94
Figure 94. Elemental composition of 10 cycles bio-treated aggregate .....	95
Figure 95. SEM of 5 cycles' bio-treated concrete .....	95
Figure 96. Elemental mapping of 5 cycles' bio-treated concrete .....	96
Figure 97. SEM of bio-treated aggregate exposed to cement .....	97
Figure 98. Elemental mapping of bio-treated aggregate exposed to cement .....	98
Figure 99. Variation of relative dynamic modulus after freeze and thaw .....	118
Figure 100. Variation of weight after freeze and thaw .....	119
Figure 101. MIP data of raw aggregates .....	120
Figure 102. MIP data of 1-treatment aggregates .....	121
Figure 103. MIP data of 2-treatment aggregates .....	122
Figure 104. MIP data of 3-treatment aggregates .....	123
Figure 105. MIP data of 4-treatment aggregates .....	124
Figure 106. MIP data of 5-treatment aggregates .....	125
Figure 107. MIP data of 6-treatment aggregates .....	126
Figure 108. MIP data of 7-treatment aggregates .....	127
Figure 109. MIP data of 8-treatment aggregates .....	128
Figure 110. MIP data of 9-treatment aggregates .....	129
Figure 111. MIP data of 10-treatment aggregates .....	130
Figure 112. Schematic diagram of field-use bio-stabilization equipment .....	131

## LIST OF SYMBOLS

<b>Symbol</b>	<b>Description</b>	<b>Unit</b>
A	Average cross-sectional area	ft <sup>2</sup>
$c_c$	Coefficient of curvature	—
$c_u$	Coefficient of uniformity	—
d	Apparent pore diameter being intruded	μm
$D_{10}$	Diameter corresponding to 10% finer	mm
$D_{15}$	Diameter corresponding to 15% finer	mm
$D_{30}$	Diameter corresponding to 30% finer	mm
$D_{50}$	Diameter corresponding to 50% finer	mm
$D_{60}$	Diameter corresponding to 60% finer	mm
$D_{85}$	Diameter corresponding to 85% finer	mm
$D_{90}$	Diameter corresponding to 90% finer	mm
n	Fundamental transverse frequency	Hz
P	Applied load	lbs
$P_{ABS}$	Absolute pressure causing the intrusion	kPa
$P_c$	Relative dynamic modulus of elasticity	—
pH	Hydrogen ion concentration	—
$\sigma^c$	Unconfined compressive strength	psf
T	Surface tension of the mercury	N/m
	Angle	°

## ACKNOWLEDGEMENTS

I would like to express the deepest appreciation to my major professor, Dr. David White. Without his guidance, enthusiasm, patience, knowledge and persistent help this thesis would not have been possible. I would like to thank him for the financial support and opportunity that allowed me to obtain a Master of Science degree. I would also like to thank my committee member, Dr. Thomas Loynachan. He generously provides his laboratory to me. I would also like to thank the other members of my committee, Dr. Peter Taylor and Dr. Jian Chu for improving my research by providing their advice and suggestions.

I would also like to thank everyone at the Center for Earthworks Engineering Research, especially Dr. Christianna White, for all the time she spent helping me improve my writing and communication skills.

Lastly, I am grateful for my loving parents and their selfless support that allowed me to accomplish my studies.

## ABSTRACT

This study was designed to test the effects of bio-stabilization on geomaterials as an alternative to chemical and mechanical stabilization. Microbially induced precipitation was used as a method of bio-stabilization. An indigenous microorganism, *Bacillus pasteurii*, was used to prompt calcite and other precipitates that stabilized geomaterials. A standard procedure for bacteria cultivation and bio-treatment soil stabilization and aggregate coating was developed. Two types of liquid incubation medium, one containing NH<sub>4</sub>Cl and one containing (NH<sub>4</sub>)<sub>2</sub>SO<sub>4</sub>, were tested. After conducting unconfined compression tests, it was discovered that both medium work well for bacteria incubation and treated samples have similar strength performance. In addition, double bio-treated samples were stronger than single treated samples, and oven-dried bio-treated samples were stronger than air-dried treated samples.

In aggregates, lower porosity helps to resist the negative effects of freezing and thawing. Mercury intrusion porosimetry confirmed that bio-treatment decreased the porosity of aggregates. At five to six bio-treatment cycles the lowest porosity values were achieved. More than six cycles of bio-treatment showed an increase in porosity. Scanning electron microscopy and X-ray diffraction were conducted and confirmed that bio-treatment produces precipitate coatings on the surfaces of aggregate. Dynamic modulus tests of concrete beams with bio-treated aggregates showed that treated aggregate improved the durability of the concrete. Freeze-thaw soundness tests on the treated aggregate confirmed these results. This is believed to be the first study of its kind.

## CHAPTER 1. INTRODUCTION

This chapter presents the industry and technical problems addressed in this project, the research goals and objectives, and a discussion of the benefits of this research. The final section of this chapter forecasts the organization of the thesis.

### **Industry problem**

Earth materials constitute the major component of roadway infrastructure systems. Soils are used for embankment fills and subgrades, and aggregates are used for pavement bases and in Portland cement concrete and asphalt. The quality of soils and aggregates directly affects the cost and productivity of construction and the long-term performance of the infrastructure systems. The demand for quality civil infrastructure materials is high and expected to continue to increase in the near term (GAO-13-32R report) especially in large population areas, like major cities in the United States, India and China (DeJong et al. 2010). At sites with marginal or weak soils, mechanical (e.g., geosynthetics) and chemical stabilization (e.g., cement, lime, and fly ash) technologies are often used. Although usually effective, cost, suitability, availability, constructability, and environmental issues are some of the factors that inhibit use of mechanical and chemical stabilization technologies. The many products available on the market reinforce that new solutions are needed to the age old problem of marginal soils.

Aggregate quality is another factor for which new solutions are needed. Typically, aggregate quality is assessed by salt susceptibility quality, secondary pore index (relates to porosity and absorption), and durability factor (Iowa DOT Level I & II aggregate reference manual). One of the common problems is low freeze and thaw resistance if aggregates have high porosity for use in PCC. Aggregate treatments use sodium silicate solutions to seal the pores of concrete by chemical reaction (Cisman 2007). However, sodium silicate solutions will put the concrete at risk for low strength development and surface durability issues due to sodium silicate solutions will result in chemical reaction with concrete (Cisman 2007).

On another side, the quality of geomaterials is not entirely satisfactory. For example, concrete is playing an increasingly important role in civil engineering. But because of the unsatisfactory quality of coarse aggregates, the durability of concrete is influenced seriously. A major deterioration of concrete is D-cracking that is caused by susceptible to freezing and

thawing effects (Aberdeen Group, 1988). Nondurable carbonate aggregates associated with D-cracking pavements exhibit a predominance of 0.04–0.2 um diameter pore size (Vernon and Wendell, 1982). Thus increase the quality of aggregates especially control the D-cracking susceptible pore size is a method to extend durability of concrete.

Utilizing biological process to modify the engineering properties of subsurface and geomaterials has emerged in these few years (DeJong et al. 2006). This method has high potential to satisfy the requirements of environmentally friendly and sustainable ground improvement. Bio-stabilization has the potential to change the physical and mechanical properties of geomaterials through precipitation in such a way that weak and unstable soils can be made sufficiently strong and durable for construction, and filling pores in geomaterials. All additives used in bio-stabilization are environmental friendly (Ramakrishnan et al. 2005).

### **Technical problem**

Bio-stabilization and bio-coating can be considered under the term of bio-treatments. Bio-stabilization bonds soil particles together by using some biologically produced precipitates. Bio-coating plugs the pores of coarse aggregates via biologically produced precipitates to decrease the susceptibility to concrete D-cracking. Because bio-stabilization and bio-coating is a relatively new development, there are still many technical challenges. So before bio-treatments can be used widely, these questions must be addressed:

- How do the engineering properties of bio-stabilized soils compare to traditional chemical and mechanical stabilization;
- How can bio-stabilization be implemented into field construction practice and what equipment is needed;
- What are the optimum field conditions requirements (i.e., pH, aerobic environment, temperature, nutrients) to support microorganism processes that stabilize the soil;
- Is it possible to make bio-precipitates penetrate or coat pore spaces in aggregates;
- How can durability of bio-coating treatments on aggregate surface be evaluated;
- What requirements are needed for engineers and workers to safely handle and develop to culture bacteria and treat the soil.

### **Goal of the research**

The main goal of this research is to develop the laboratory methods and test bio-stabilization for few different soils and evaluate the bio-coating for porous aggregates.

### **Objectives**

The research objectives are to:

- Develop a standard procedure for bacteria cultivation and bio-treatment for soil stabilization and aggregate coating;
- Review the literature to compare and investigate the effects of bio-stabilization and bio-coating;
- Introduce biological additives into geomaterial specimens to test the strength and other geotechnical properties of soil;
- Analyze the micro structures of untreated and bio-treated specimens.

### **Significance of the research**

Finding alternatives to traditional stabilizers for soil stabilization and improving the quality of geomaterials in a more sustainable and reliable way.

### **Organization of the document**

Following this introduction chapter, the thesis is organized into five additional chapters. Chapter 2 provides a review of relevant literature and a background for this research. Chapter 3 presents the test methods and chapter 4 presents the analysis of the properties of the geo materials used in this study. Chapter 5 describes and discusses the results, and chapter 6 presents conclusions and recommendations.

## CHAPTER 2. BACKGROUND AND LITERATURE REVIEW

This chapter discusses recent research on a new stabilization technique that uses bacteria to precipitate a binding agent. The chapter discusses bio-stabilization applications for geomaterials, bio-treatment methods, characterization of bio-treated materials, and the benefits of bio-stabilization.

According to NRC (2006) geotechnical engineers need a new understanding of geomechanics to reduce the damage to the environment. Interdisciplinary research, especially the interaction between biology and geotechnical engineering, explores the use of biological methods to solve geomechanical problems such as using microorganisms to stabilize geomaterials. This new concept is called bio-stabilization. This project examines the effects of bio-stabilization on the engineering properties of geomaterials.

### **Bio-stabilization for geotechnical applications**

Bio-stabilization involves injecting naturally occurring or engineered microorganisms that produce a polymer or cause precipitation of inorganic cementing material using biological processes (NRC 2006). DeJong et al. (2010) defined that the bio-stabilization system is “a chemical reaction network that is managed and controlled within soil through biological activity and whose byproducts alter the engineering properties of soil.”

Concepts for bio-stabilization are being developed to stabilize soils (DeJong et al. 2006), improve concrete durability (Ramakrishnan et al. 2005), and mitigates liquefaction (Burbank et al. 2011).

Experiments involving biological processes for soil strengthening have been largely confined to laboratory studies of the precipitation of carbonate as a cementation material for sand stabilization. Much more research is needed to fully evaluate the full potential for soil stabilization, concrete material improvement, and improvement at levels necessary for their routine use in infrastructure construction.

### **Soil**

Microbial activities can directly or indirectly affect the physical properties of soils on a permanent or temporary basis. Some fungal colonies produce microscopic, hair-like hyphae,

and have an effect similar to plant roots grasping soil. Some bacteria precipitate extracellular polymeric materials that bind soil particles together (Gray and Sotir, 1996).

Bachmeier et al. (2001) investigated microbial urease activity in calcite precipitation. They used two types of microorganisms in experiments, *Bacillus pasteurii* and *Escherichia coli*. These two microorganisms have ability to precipitate calcite. To verify the application of these microorganisms for civil engineering problems, the authors designed two groups of experiments using the same culture medium and same environmental conditions. In addition, they used *Bacillus pasteurii* which was immobilized in polyurethane (PU) foam to compare the efficiency of calcite precipitation between the free and immobilized enzymes. After the process of MICP, SEM was used to evaluate the experiment results. SEM images identified calcite precipitation throughout the matrices of PU. In comparison SEM images of calcite precipitation induced by the PU-immobilized urease showed smaller and less organized crystals on the surface, and PU foam has well organized crystals within the matrices.

### **Concrete**

Jonkers et al. (2010) investigated the potential ability of bacteria to repair concrete cracks. They added bacteria directly into cement paste mixture, and found a continuous decrease in pore size diameter during concrete curing. The bacteria produced substantially more crack-plugging minerals than the control groups. In their research, Mercury intrusion porosimetry tests were used to determine pore size distribution. Mercury intrusion porosimetry analysis indicated two major cement matrix pore diameter size ranges, 0.01–0.1 $\mu\text{m}$  and 0.1–1.0 $\mu\text{m}$ . Results showed that the pore size distribution changed from large to small with treatment. And there was a large difference in pore size diameters between young specimens cured 3 and 7 days and old specimens cured 28 days. Pores volume was significantly decreased after 28 days curing. The incremental intrusion volume of 3 days is 0.39 mL/g, after 7 days pore volume was decreased to 0.22 mL/g, 28 days curing can make the pore volume reach to 0.1 mL/g.

### **Other applications**

Burbank et al. (2011) conducted laboratory and in situ bio-treatment experiments on saturated soils from different depths that could liquefy due to seismic vibration. They treated the soils with indigenous microorganisms that precipitate calcite and concluded that this kind

of treatment increases the resistance to seismic induced liquefaction. The CPT data showed the tip resistance for calcite precipitation levels as low as 1.8 to 2.4% can reach to 4.9 to 5.9 MPa. The maximum tip resistance of untreated soil is 2.5 MPa.

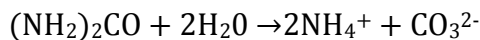
Meyer et al. (2011) designed and conducted experiments utilizing indigenous microorganism – *Sporosarcina pasteurii* to verify the workability of this type microorganism for dust control. Meyer et al. (2011) examined the dust control effects on different concentrations of microorganism for different temperature and humidity levels. From their study, microbial dust control showed potential to be effective. Under 20% humidity, 45°C environments, dust control achieved was optimum. The effect of dust control reached to maximum when the concentration of microorganism was  $1 \times 10^6$  cells/mL in liquid medium. After wind tunnel testing, the mass loss can be limited to 1% or less compare to mass loss with no treatment.

### **Bio-treatment methods**

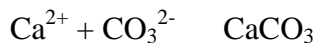
Bio-treatment utilizes calcite precipitation to bond soil particles and fill the pores of aggregates. The following section introduces the primary chemical reactions, bio-species, and some methods literature review.

### **Bio-reactions, processes, and bio-species**

MICP is a process that one mole of urea,  $(\text{NH}_2)_2\text{CO}$ , is hydrolyzed to two moles of  $\text{NH}_4^+$  and one mole of  $\text{CO}_3^{2-}$  per mole of urea by the enzyme urease indicated in the following simplified reaction (Burbank et al. 2011);



$\text{NH}_4^+$  will increase the pH of liquid medium, and  $\text{CO}_3^{2-}$  can react with calcium ions ( $\text{Ca}^{2+}$ ) and precipitate calcium carbonate ( $\text{CaCO}_3$ ).



DeJong et al. (2010) used *Bacillus pasteurii*, which are aerobic and urease production bacteria, because they are common and naturally occurring in soil. In addition, *Bacillus pasteurii* cells do not aggregate; this ensures a high cell surface to volume ratio, a condition that is essential for efficient cementation initiation. *Bacillus pasteurii* are particularly good candidates for bio-stabilization because they provide two sources of  $\text{CO}_2$ , respiration by the

cells and decomposition of urea (DeJong et al. 2006). This CO<sub>2</sub> reacts with water and calcium to form calcium carbonate –a bonding agent bond with particles.

## Methods

Ramakrishnan et al. (2005) presented the basic principle of MICP. They conducted a durability study of concrete beams that were treated with bacteria grown in three mediums: water, urea, and phosphate buffer. The beams were exposed to sulfate, alkaline, and freeze-thaw environments. The dimensions of the beams were established according to ASTM C666 standard test method for resistance of concrete to rapid freezing and thawing. Scanning electron microscope (SEM) and X-ray diffraction (XRD) were used to analyze the quantity and shape of MICP. They found the durability of concrete beams treated with bacteria was much higher than the control group. The authors concluded phosphate-buffer was the most effective bacteria medium and at the end of 28 curing days beams with bacterial concentration of  $1 \times 10^6$  cells/ml,  $1 \times 10^7$  cells/ml, and  $1 \times 10^8$  cells/ml had 13%, 20%, 34% less shrinkage deformations respectively than that of the control beams.

DeJong et al. (2006) recommended *Bacillus pasteurii* as the stabilization microorganism applied in soil improvement. These bacteria used urea as the nutrient and grow at  $30\pm2^\circ\text{C}$  with sufficient oxygen. To ensure the growing of bacteria and effective chemical reaction, nutrients and chemicals supplements were necessary. The initial biological treatment is primarily used for bacteria incubation, and the cementation treatments are the process of precipitating calcium carbonate and stabilizing the soil samples. The Ottawa 50-70 specimen used in this design was 72 mm in diameter with an aspect ratio 2:1. The experiment required a peristaltic pump to introduce the bacteria and urea medium into the specimen over a period of 20 minutes with a 20 mL/min flow rate. The specimens were set for 4 hours to allow the microbes to attach to the soil particles. The microbes bonded to the soil particles; the nutrient treatment was then initiated. The nutrient treatment process had a slower flow rate about 4 mL/min than the initial biological treatment. After few days, there will be some amounts of cementation between soil particles. This process is shown in Table 1.

**Table 1. Microbial induced cementation treatment and formula (DeJong et al. 2006)**

<b>Process</b>	<b>Constituents</b>
Urea medium (used in treatments below)	Contains per liter of double distilled water 3 g Bacto nutrient broth 20 g Urea $\text{NH}_2(\text{CO})\text{NH}_2$ 10 g $\text{NH}_4\text{Cl}$ 2.12 g $\text{NaHCO}_3$ Adjust pH of the medium to 6.0 with 5 N HCl prior to sterile filtration
Initial biological treatment	$2 \times 10^6$ cells/mL <i>Bacillus pasteurii</i> 400 mL Urea medium 8 mL of $\text{CaCl}_2$ stock solution (140g/L)
Cementation treatments	400 mL Urea medium 8 mL of $\text{CaCl}_2$ stock solution (140g/L)

Whiffin et al. (2007) used *Sporosarcina pasteurii*, a urease positive microorganism that must be cultivated under aerobic batch conditions. The cultivation medium contained 20 g/L yeast extract and 10 g/L  $\text{NH}_4\text{Cl}$  at a pH of 9, and the bacteria were stored at 4°C for 48 hours prior to use.

The experiment was conducted in a 5m PVC tube with an internal diameter of 66 mm. The soil sample is 125-250  $\mu\text{m}$  Itterbeck sand ( $D_{10} = 110 \mu\text{m}$ ,  $D_{50} = 165 \mu\text{m}$ ,  $D_{90} = 275 \mu\text{m}$ , dry density of 1.65 g/cm<sup>3</sup> and porosity of 37.8%). The PVC tube was positioned vertically with downward flow. A fluid reservoir containing the injected fluids is connected at the top of the PVC tube. The flow rate was kept constant at approximately 0.35 L/h and ambient temperature of  $18^\circ\text{C} \pm 2^\circ\text{C}$ . After this series of experiments, the soil samples in the PVC tube can be used for testing some soil properties.

### Characterization of untreated and treated materials

The microstructure and elements of untreated and bio-treated materials are characterized by scanning electron microscopy (SEM) and X-ray diffraction (XRD).

#### Scanning electron microscopy

Scanning electron microscopy (SEM) is used for observing the surface and void areas of bio-treated materials. It is the major tool to analyze the effect of bio-stabilization.

Scanning electron microscope (SEM) uses a focused beam of high-energy electrons to generate a variety at the surface of solid specimens. The signals are obtained from electron-sample interactions reveal information about the sample including external texture, chemical composition, and micro structure (Goldstein 1981).

DeJong et al (2010) conducted SEM analysis for bio-treated silica sand particles. There were some spaces between sand particles. After bio-treatment some calcite precipitations were produced and filled in the spaces. These precipitations can bond sand particles and stabilize them (Figure 1).

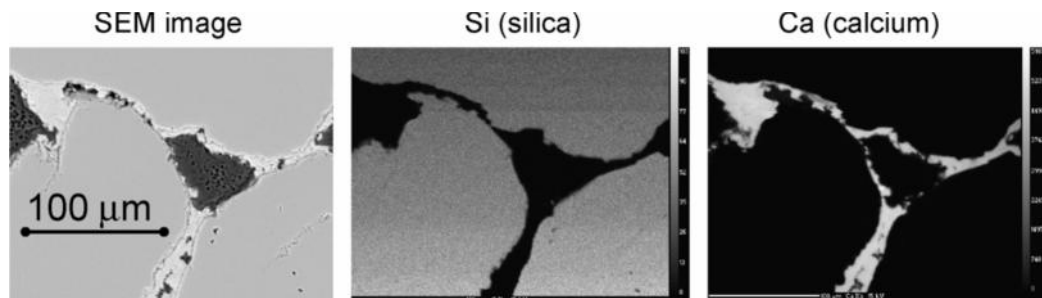


**Figure 1. SEM of treated silica sand particles (Reproduced from DeJong et al. 2010)**

#### X-ray diffraction

X-ray diffraction (XRD) is used to quantitatively analyze the mineral constituents of materials.

Bang and Ramakrishnan (2001) initiated and evaluated microbiologically enhanced crack remediation (MECR). They found that the microbially induced calcite precipitation produced a significant increase in compressive strength, which had good potential in concrete crack remediation. During their research, SEM and X-ray diffraction (XRD) analysis were used to identify the micro-structure and composition of MICP. The authors tested four groups: untreated sand sample, sand treated with liquid medium sample, sand treated with killed *Bacillus pasteurii* and liquid medium sample and sand treated with *Bacillus pasteurii* and liquid medium sample. The XRD quantitative analysis of the final weight fractions of sand samples was gathered (Table 2). Only the sample treated with *Bacillus pasteurii* had calcite precipitated detected by XRD quantitative analysis. For the untreated sand sample, XRD quantitative analysis verified that the untreated sands did not produce calcite. For the sand sample that was treated with liquid medium, and the sand sample treated with killed *Bacillus pasteurii*, there was no effect from bacteria and the indicated liquid medium.

**Table 2. XRD quantitative analysis of the final weight fractions of sand samples**

Sample	Quartz (SiO <sub>2</sub> )	Calcite (CaCO <sub>3</sub> )
1	0.96	ND
2	0.954	ND
3	0.892	ND
4	0.683	0.302

- a. Numbers represent an average of weight fraction values obtained from XRD quantitative analysis;
- b. Sample 1, untreated sand; sample 2, sand treated with medium; sample 3, sand treated with killed *Bacillus pasteurii* and medium; sample 4, sand treated with *Bacillus pasteurii* and medium.

### Benefits of bio-stabilization

*Bacillus pasteurii* has a level one bio-safety rating, which means it is not known to cause disease in healthy adult humans (America Type Culture Collection 2011). A biological process is more environmentally friendly than conventional chemical treatment methods, such as lime, cement, or fly ash. Such a natural process would use nonpathogenic organisms that are native to the subsurface environment (DeJong et al. 2006).

MICP is highly desirable because the calcite precipitation induced as a result of microbial activities is pollution free and natural (Ramakrishnan et al. 2005). Application of bio-based materials and processes can substantially contribute to a decreased need of limited non-renewable resources and energy (fossil fuels), a decrease in production of non-biodegradable waste materials, and thus a substantial decrease in environmental burden of geo- and civil engineering practices (Jonkers and van Loosdrecht 2010).

### **CHAPTER 3. METHODS**

The purpose of this chapter is to describe the methods used in the study. The main goal of this research was to develop and test a new stabilization technology. The research objectives were to:

- Develop a standard procedure for bacteria cultivation and bio-treatment for different soils;
- Compare the effects and functions of chemical and biological soil stabilizers;
- Introduce biological additives into soil and make specimens for testing the strength and other geotechnical properties of soil; and
- Analyze the micro-structure of bio-treated soil specimens and untreated soil specimens, and observe the changes after bio-treatment compared to untreated specimens.

This study was designed to test the effects of bio-stabilization on geomaterials as an alternative to chemical and mechanical stabilization. Companies, transportation agencies, and private road owners will benefit from this research because bio-stabilization has no or fewer environmental contamination, shorter treatment time requirements, and acceptable application costs based on the literature review (Ivanov and Chu 2008).

#### **Research design**

To address the objectives of this study, laboratory and field tests were conducted. Lab testing involved preparing bio-treated soil specimens and conducting these eight tests:

- Unconfined compression;
- Scanning electron microscope (SEM);
- Energy dispersive X-ray spectroscopy (EDS);
- Mercury porosimetry;
- Iowa pore index;
- Resistance of concrete to rapid freezing and thawing;
- Soil index test (soil classification, specific gravity, and absorption); and
- Resistance to degradation of aggregate by abrasion and impact in the Los Angeles machine.

### Bio-stabilization methods

The following section presents detailed laboratory process of preparing incubation medium, streaking out single colony, incubating microorganism, introducing microorganism to soil sample, and subsequent bio-treatment.

#### Laboratory processes

The *Bacillus pasteurii* for this study were procured from ATCC (America Type Culture Collection), and the ATCC manual provides the formula for culturing the bacteria for stabilizing soil samples (2011). The formula for making 1.0 L of the liquid culturing medium follows the recipe in the manual (Table 3)

**Table 3. Formula for making 1.0 L of the culture medium**

Constituents	Amount
Yeast extract	20.0 g
$(\text{NH}_4)_2\text{SO}_4$ or $\text{NH}_4\text{Cl}$	10.0 g
0.13 M Tris buffer (pH 9.0)	1.0 L

The step-by-step process for bio-stabilization is as follows:

#### Rehydrate freeze-dried *Bacillus pasteurii*

- A. Open vial of original freeze-dry bacteria (Figure 2).



**Figure 2. *Bacillus pasteurii* from ATCC**

- B. Introduce 5 to 6 ml of the culture medium into a test tube.

- C. Withdraw approximately 0.5 to 1.0 mL of the culture medium with a Pasteur pipette.
- D. Inject the culture medium in the vial to rehydrate the entire pellet.
- E. Transfer this rehydrated liquid back into the tube.
- F. Shake the tube gently to evenly mix the culture medium and the bacteria.
- G. Put the test tube into an incubator that is set at  $30^{\circ}\text{C} \pm 2^{\circ}\text{C}$  in aerobic conditions (ATCC 2011).

*Streak out lines to get a single colony in solid medium*

- A. Prepare agar solid medium in 100 mm x 15 mm Fishbrand plastic plates (Figure 3).

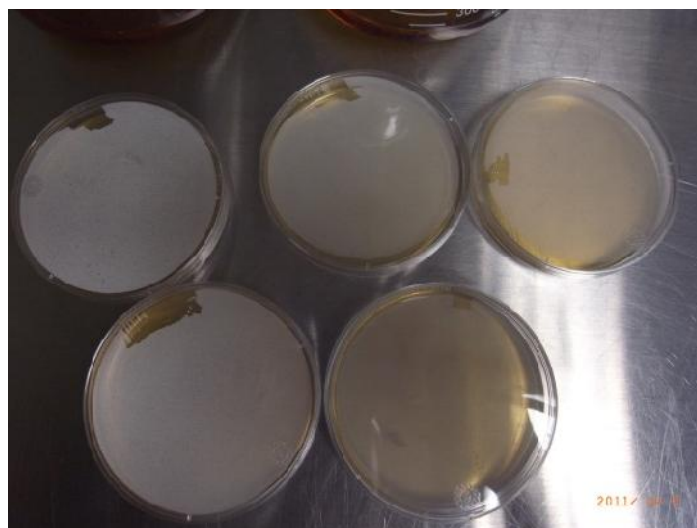


**Figure 3. Solid medium for *Bacillus pasteurii***

- B. Dip an inoculate loop into the test tube of the culture medium and bacteria suspension.
- C. Streak out lines with the loop on the surface of the solid medium.
- D. Incubate the plates at  $30^{\circ}\text{C}$ . After 48 to 72 hr, single colonies should propagate on each line. However, if there are only a few colonies on the lines, repeat steps B and C.

*Inoculate single colony into culture medium*

- A. Prepare recommended culture medium in flask or test tube (see Figure 4), the medium ingredients are listed in Table 3.

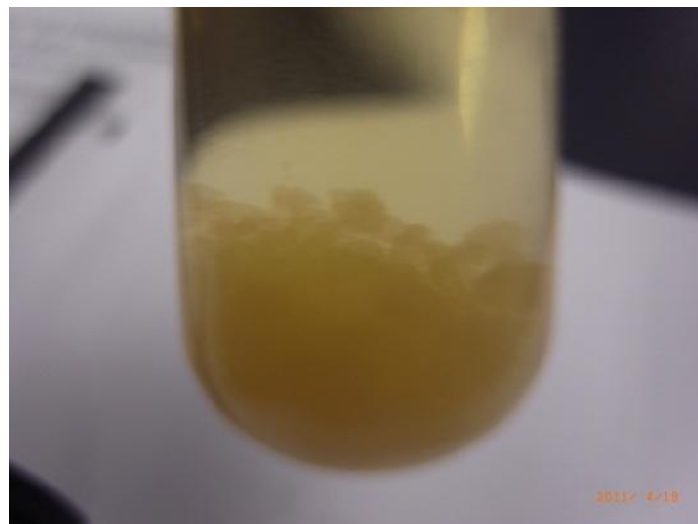


**Figure 4. Culture medium for *Bacillus pasteurii***

- B. Use sterile loop to transfer the bacteria colony into culture medium.
- C. Put the flask or test tube in incubator shaker: shaker will provide oxygen and temperature; generally it takes two days to culture enough bacteria for (see Figure 5).



**Figure 5. Flask with culture medium in incubator shaker**

*Dilute*

- A. Dilute the bacteria to achieve the target concentration
- B. Use spectrophotometer (UV-visible) to get the optical density (OD). For two days grow bacteria, the OD value is around 0.2 which means bacteria concentration is  $1.6 \times 10^8$  cells/mL.
- C. The OD can reflect the concentration of *Bacillus pasteurii*.

*Re-suspend in new culture medium*

- A. Introduce the target concentration of bacteria into new culture medium.

*Mix the culture medium and bacteria with soil (Figure 6)*

- A. The growth condition should be  $30^\circ\text{C} \pm 2^\circ\text{C}$  and aerobic.
- B. After 4 days (or less) growth, the treated soils are ready to make specimens.



**Figure 6. Introduce the culture medium into soil specimen**

**Sample preparation**

The first step in preparing the samples was to clean the PVC molds. Stainless steel clamps were used to join the tops of the two pieces of the molds and rubber bands were used to bind the bottoms of the mold pieces together. Aluminum foil was wrapped around the

bottom of the molds to reduce liquid leakage when the bio-treatment culture medium was introduced to the soil specimens. Aluminum film was also put inside of the mold to make remolding easier after bio-treatment. The molds were filled with the soil samples and put into a glass beaker to contain leakage. The glass beaker and mold were then placed into an autoclave for 25 minutes to sterilize the mold and the sample. The autoclave temperature was set at 121°C to sterilize the PVC mold.

### **Lab tests**

This section presents the tests that were conducted to verify the effects of bio-stabilization.

#### **Unconfined compression**

The objective of bio-stabilization is to bond soil particles, and unconfined compression tests verify the effects of bio-stabilization. Unconfined compression tests are a simple laboratory testing method to assess the mechanical properties of fine-grained soils and provide a measurement of the undrained strength and the stress-strain characteristics of soils. The tests were conducted according to ASTM D2166–06 Standard Test Method for Unconfined Compressive Strength of Cohesive Soil (2009). The compression equipment was a Geotest Instrument Corporation model S2010 device with a 2000 lbs. capacity was used in this study. The applied load was determined from reading the dial in increments of 10 lbs.

The compression stress for given applied loads is calculate by following equation,

$$\sigma_c = P/A \quad (1)$$

where:

$P$  = given applied load, lbs; and

$A$  = corresponding average cross-sectional area,  $\text{ft}^2$ .



**Figure 7. Unconfined compression test device**

#### **Scanning electron microscope (SEM)**

SEM analysis is expensive, complicated and time-consuming, but it is a non-destructive test. X-rays generated by electron interactions do not lead to sample volume loss, so samples can be analyzed repeatedly.

Accelerated electrons in a SEM carry considerable amounts of kinetic energy which is dissipated as a variety of signals produced by interactions between electrons and samples. These signals include secondary electrons, backscattered electrons, diffracted backscattered electrons, photons, visible light, and heat. SEM images are produced by secondary electrons and backscattered electrons (Goldstein et al. 1981). Diffracted backscattered electrons are used to determine micro structures and constituents of minerals. Photons are used for elemental analysis in a process referred to as EDS. Figure 8 shows the FEI Quanta FEG250 SEM equipment.



**Figure 8. FEI Quanta FEG250 SEM equipment (a. basic component, b. working stage)**

#### **Energy dispersive X-ray spectroscopy (EDS)**

Energy-dispersive X-ray spectroscopy (EDS) is an analytical technique used for the elemental analysis or chemical characterization of a sample. EDS investigates the interaction between some electrons of X-ray excitation and a sample. EDS characterizes the elements in each sample because each element has a unique atomic structure allowing unique set of peaks on its X-ray spectrum. To stimulate the emission of characteristic X-rays from a specimen, a high-energy beam of charged particles such as electrons or protons, or a beam of X-rays, is focused into the sample being studied. At rest, an atom within the sample contains ground state electrons in discrete energy levels or electron shells bound to the nucleus. The incident beam may excite an electron in an inner shell, ejecting it from the shell while creating an electron hole where the electron was. An electron from an outer, higher-energy shell then fills the hole, and the difference in energy between the higher-energy shell and the lower energy shell may be released in the form of an X-ray. The number and energy of the X-rays emitted from a specimen can be measured by an energy-dispersive spectrometer. As the energy of the X-rays is characteristic of the difference in energy between the two shells, and of the atomic structure of the element from which they were emitted, this allows the elemental composition of the specimen to be measured.

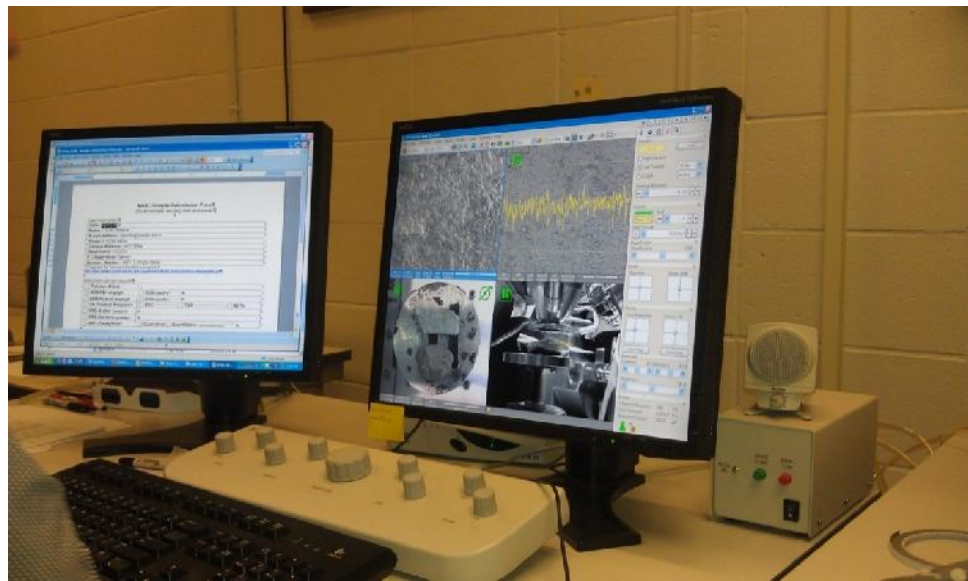


**Figure 9. Quantitatively determination of chemical compositions (right screen)**

### Mercury intrusion porosimetry

Mercury porosimetry is a technique used to determine pore size and pore volume. The pore size measurement range is 100 micrometers ( $\mu\text{m}$ ) down to 2.5 nm. Mercury is injected into the aggregates by high pressure and then extracted thoroughly. The total amount of intrusion mercury can derive the pore volume of aggregates.

The principle is converting absolute pressures to apparent intruded pore diameters. The relationship between pressure and pore size is calculated with equation 2:

$$d = \frac{4T(\cos\theta)}{P_{ABS}} \quad (2)$$

where:

$d$  = apparent pore diameter being intruded;

$T$  = surface tension of the mercury;

= contact angle between the mercury and the pore wall;

$P_L$  = absolute pressure causing the intrusion;

$P_G$  = pressure of gas, and

$P_{ABS} = P_G - P_L$ .

The mercury intrusion volume is read from the equipment directly, and then is converted to pore volume

Mercury porosimetry test refer to *ASTM D4404-10 Standard Test Method for Determination of Pore Volume and Pore Volume Distribution of Soil and Rock by Mercury Intrusion Porosimetry.*

### Iowa pore index

This test was developed by the Iowa DOT and used to characterize the freeze-thaw susceptible pore systems for coarse aggregates used in Portland cement concrete (Figure 10). This test method was verified by Iowa DOT as feasible for the aggregates that could absorb water at a slow rate. Water inside of aggregate in freezing will cause particle fracture when the pore system impedes the outward movement of water. This experiment tested the effect of bio-stabilization on resisting water to access into aggregate.



**Figure 10. Iowa pore index testing equipment**

From this test, two sets of data are generated: primary pore index and secondary pore index. The primary pore index is a calibration index which is used to verify if the equipment is working normally. The secondary pore index number represents the amount of water

injected into the capillary pore system of the aggregate. A secondary pore index of 27 or greater indicates an inability of aggregate to withstand saturated freeze-thaw pressures (Iowa DOT 219-D). The relationship between pore index and dial reading is given as follows:

$$\text{Primary pore index} = (\text{1 minute reading} - \text{pot expansion}) \times (9000 / \text{sample weight})$$

$$\text{Secondary pore index} = (\text{14 minutes reading}) \times (9000 / \text{sample weight})$$

### **Resistance of concrete to rapid freezing and thawing**

Freezing and thawing tests were conducted according to ASTM C666 Standard Test Method for Resistance of Concrete to Rapid Freezing and Thawing to determine the resistance of concrete specimens to rapidly repeated cycles of freezing and thawing. Procedure A, with rapid freezing and thawing in water, was used. A Humboldt H-3185 rapid freeze-thaw cabinet was utilized to perform the ASTM C666 test (Figure 11).



**Figure 11. Humboldt H-3185 rapid freeze-thaw cabinet**

The relative dynamic modulus of elasticity of concrete beam was measured during this experiment. The relative dynamic modulus of elasticity is calculated by following equation,

$$P_c = (n_f^2/n^2) \times 100 \quad (3)$$

where:

$P_c$  = relative dynamic modulus of elasticity, after c cycles of freezing and thawing, percent;

$n$  = fundamental transverse frequency at 0 cycles of freezing and thawing; and

$n_I$  = fundamental transverse frequency after c cycles of freezing and thawing.

### Soundness of aggregate by freezing and thawing

This test is conducted according to AASHTO T103-91 Standard Method of Test for Soundness of Aggregate by Freezing and Thawing to determine the resistance of aggregate to disintegration by freezing and thawing. Procedure A, total immersion with 50 cycles rapid freezing and thawing, was used (Figure 12). Before test, aggregates were separated and weighted according to the grading requirement (Table 4). After the completion of the final cycle, each sample was dried to constant mass at  $110^\circ \pm 5^\circ\text{C}$ , and sieved over the sieve shown for the appropriate size of particle in Table 5.



**Figure 12. Soundness of aggregate testing in freeze-thaw cabinet**

**Table 4. Grading requirement of aggregates**

<b>Size (Square-opening sieves)</b>	<b>Mass, g</b>
9.5 mm to 4.75 mm material	300 ± 5
12.5 mm to 9.5 mm material	330 ± 5
19.0 mm to 12.5 mm material	670 ± 10
25.0 mm to 19.0 mm material	500 ± 30
37.5 mm to 25.0 mm material	1000 ± 50
63.0 mm to 37.5 mm material	5000 ± 300

**Table 5. Sieve size for determination of weight loss**

<b>Size of aggregate</b>	<b>Sieve used to determine loss</b>
63.0 mm to 37.5 mm	31.5 mm
37.5 mm to 19.0 mm	16.0 mm
19.0 mm to 9.5 mm	8.0 mm
9.5 mm to 4.75 mm	4.0 mm

### **Soil index tests**

Three soil index properties were gathered in this research, soil classification, specific gravity, and absorption. The materials in this study were classified according to ASTM D2487-11 Standard Practice for Classification of Soils for Engineering Purposes (Unified Soil Classification System).

Specific gravity, the relative density of material as compared to the density of water at 23°C, is used to calculate the volume occupied by aggregate in mixtures containing aggregate, such as Portland cement concrete. Absorption reflects the quantity of water absorbed by aggregate that can influence concrete mix design. Tests for specific gravity and absorption were conducted according to ASTM C127-01 Standard Test Method for Density, Relative Density (Specific Gravity), and Absorption of Coarse Aggregate.

## CHAPTER 4. MATERIALS

This chapter describes the materials used in this research. Several materials were used in this study including: standard silica sand, low volume unpaved road surfacing materials from 160<sup>th</sup> avenue in Boone County and Vail Avenue in Hamilton County in Iowa, concrete pavement coarse aggregate, porous ceramic disks, microorganism *Bacillus pasteurii*, and liquid medium mixtures.

### Bio-stabilization materials

*Bacillus pasteurii* and liquid incubation medium are the bio-stabilization materials used in this project.

#### *Bacillus pasteurii*

*Bacillus pasteurii* occurs naturally in soils in small quantities. Instead of culturing the microorganism from soil, freeze-dried *Bacillus pasteurii* was purchased from the American Type Culture Collection (ATCC) (Figure 13). This microorganism (ATCC catalog number 6453) has a biosafety level 1 rating, and, according to the United States Centers for Disease Control and Prevention (CDC), is suitable for work involving well-characterized agents not known to consistently cause disease in healthy adult humans, and of minimal potential hazard to laboratory personnel and the environment.



**Figure 13. *Bacillus pasteurii* (ATCC catalog No. 6453)**

The microscopy view (Figure 14) shows that *Bacillus pasteurii* are rods that are usually 0.5–1.2  $\mu\text{m}$  in length. The optimum growth conditions for *Bacillus pasteurii* are 30°C, aerobic environment, and proper incubation medium (ATCC). Each of these factors is discussed in detail later in this chapter. *Bacillus pasteurii* prompt precipitation, so this microorganism is a good candidate for soil stabilization research.

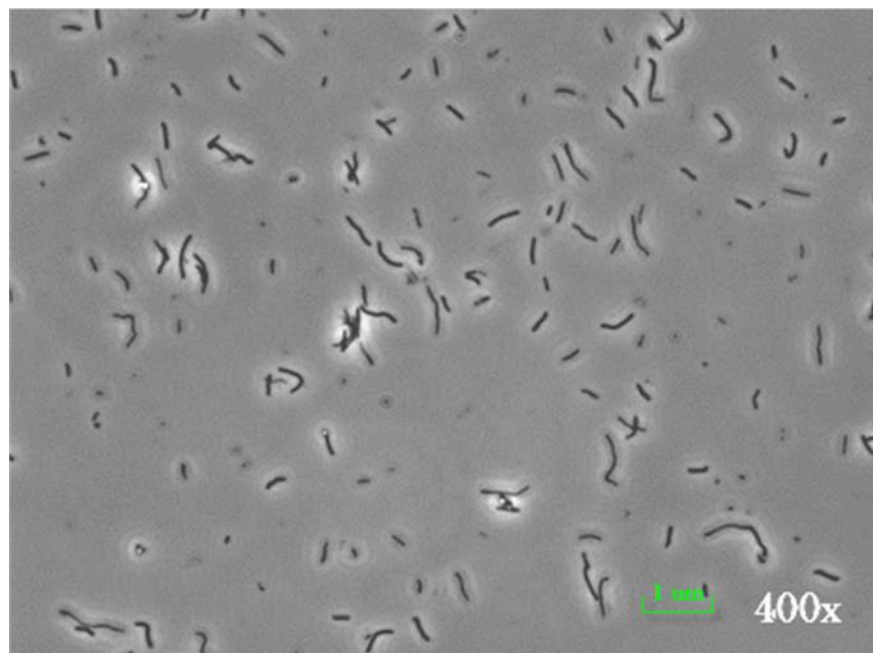


**Figure 14. Microscopy view of *Bacillus pasteurii***

### Liquid incubation medium

Agar is used to support nutrients when solid medium is needed.

Liquid medium was prepared to provide proper nutrients and catalysts. The liquid medium consists of four reagents. Yeast extract provides nutrients and Vitamin B for the bacteria to reproduce. Vitamin B is a growth factor that makes bacteria grows fast. Ammonium sulfate and ammonium chloride provide nitrogen that is used by bacteria amine groups, enzyme and other proteins. Tris buffer can stabilize pH value of medium. The reagents of liquid medium are listed in Table 6.

**Table 6. Formula for making 1.0 L of the incubation liquid medium**

<b>Reagent</b>	<b>Amount</b>
Yeast extract	20.0 g
(NH <sub>4</sub> ) <sub>2</sub> SO <sub>4</sub> or NH <sub>4</sub> Cl	10.0 g
0.13 M Tris buffer (pH 9.0)	1.0 L

After the completion of the bacteria culture, calcium chloride (CaCl<sub>2</sub>) was added to liquid medium to provide Ca<sup>2+</sup> that reacts with CO<sub>3</sub><sup>2-</sup> to precipitate calcium carbonate (CaCO<sub>3</sub>). CaCO<sub>3</sub> acts like glue to bond soil particles.

These constituents can be used to compare with energy dispersive x-ray spectroscopy (EDS) elemental analysis. EDS quantifies the component elements of target material. Then the element that takes effect on bio-stabilization can be identified. Details of the components of the constituents are provided in Table 7.

**Table 7. Quantity of ingredients for different reagents (as stated on bottle labels)**

<b>Calcium chloride (CaCl<sub>2</sub>)</b>			
Assay			100.10%
Ammonium			<0.005%
Barium (Ba)			<0.005%
Heavy metals (as Pb)			<5.0 ppm
Insoluble matter			<0.01%
Iron (Fe)			<0.001%
Magnesium			0.001%
Oxidizing substances			<0.003%
Potassium (K)			<0.001%
Sodium (Na)			<0.002%
Strontium (Sr)			<0.01%
Sulfate (SO <sub>4</sub> )			<0.01%
<b>Tris (C<sub>4</sub>H<sub>11</sub>NO<sub>3</sub>)</b>			
<b>Yeast extract</b>			
Copper (Cu)	1 ppm	The Lintner's average composition of the ash left on incinerating yeast	
Lead (Pb)	1 ppm	Potassium oxide (K <sub>2</sub> O)	33.5
<b>Ammonium chloride (NH<sub>4</sub>Cl)</b>		(including a little Na <sub>2</sub> O)	
Assay	99.90%	Magnesia (MgO)	6.1
Ca and Mg precipitate	0.001%	Lime (CaO)	5.5
Heavy metals (as Pb)	3 ppm	Iron oxide (Fe <sub>2</sub> O <sub>3</sub> )	0.5
Insoluble matter	0.004%	Phosphoric acid (P <sub>2</sub> O <sub>5</sub> )	50.6
Iron (Fe)	1 ppm	Sulphuric acid (SO <sub>3</sub> )	0.6
Phosphate (PO <sub>4</sub> )	1 ppm	Silica (SiO <sub>2</sub> )	1.3
Sulfate (SO <sub>4</sub> )	0.001%	Ingredients not determined	1.9

### Porous ceramic disks

To study the application of bio-coating for micro-porous material, hydrophilic porous ceramic disks were subjected to treatment (Figure 15). According to the disk manufacturer, these disks “meet demanding pressure and high temperature conditions with consistent pore structures and uniform hydraulic conductivity. The open pore structure provides a convoluted path of interconnecting networked channels, allowing complete flow through the material for migrating liquids” (Small Parts Inc. product description). The properties of these disks are as in the following Table 8.



**Figure 15. Ceramic hydrophilic porous disk after bio-treatment**

**Table 8. Specifications of porous ceramic disks**

Diameter (in.)	1.125
Thickness (in.)	0.281
Color	Pure white
Air entry value (bars)	0.5
Upper temperature range (°C)	805
Nominal pore size (µm)	6

### Geomaterials

Four types of geomaterials were tested in this study, standard silica sand, surface material from an unpaved road on 160<sup>th</sup> Street in Boone County in Iowa, surface material from unpaved road on Vail Avenue in Hamilton County in Iowa, and concrete coarse aggregate.

### Standard Silica Sand

The standard silica sand was clean, dry, and free-flowing uncemented sand that were used to test the effects of bio-stabilization (Figure 16). DeJong et al. (2006; 2010) verified that bio-stabilization works well for standard silica sand. The process used by DeJong et al. (2006, 2010) was revised in this study. To verify the new process, standard silica sand was purchased from AGSCO Corporation. The bulk density of the sand does not vary more than 1% which meets ASTM D1556-07 *Standard test method for density and unit weight of soil in place by the sand-cone method*. All of these data tested refer to ASTM D2487-11 *Standard test method for classification of soils for engineering purposes* (unified soil classification system).



**Figure 16. Standard silica sand without bio-treatment**

The data in Tables 1 and 2 were provided in a certification letter from AGSCO Corporation (June, 2010). Table 9 presents the soil index properties of silica sand and Table 10 shows the sieve analysis of the sand.

**Table 9. Silica sand index properties**

Soil index	Value
Porosity	40%
Specific gravity	2.65
Uniformity coefficient	1.4

**Table 10. Silica sand sieve analysis results**

Sieve size	Percent retained
#20	0.2%
#25	0.6%
#30	2.0%
#35	14.1%
#40	28.6%
#50	49.0%
#60	3.5%
Pan	2.0%
Total	100.0%

**Surface material from an unpaved road on 160<sup>th</sup> Street in Boone County, Iowa**

This soil came from 160<sup>th</sup> Street in Boone County in Iowa. The samples were taken about one kilometer west of the Boone and Story County line (Figure 17). Table 11 presents the soil index properties of the soil, and Table 12 shows the sieve analysis of the soil.

**Figure 17. Surface material from 160th Street in Boone County, Iowa**

**Table 11. 160<sup>th</sup> Street soil index properties**

<b>Soil index</b>	<b>Value</b>
<b>Atterberg limits</b>	PL = NP
	LL = NV
	PI = NP
<b>Classification</b>	USCS = SP-SM
	AASHTO = A-1-b
<b>Coefficients</b>	D <sub>85</sub> = 9.793
	D <sub>60</sub> = 2.416
	D <sub>50</sub> = 1.514
	D <sub>30</sub> = 0.611
	D <sub>15</sub> = 0.284
	D <sub>10</sub> = 0.179
	C <sub>u</sub> = 13.51
	C <sub>c</sub> = 0.87

**Table 12. 160<sup>th</sup> Street soil sieve analysis results**

<b>Sieve size</b>	<b>Percent finer (%)</b>
1.5	100.0
1	99.2
3/4	94.5
1/2	88.5%
3/8	84.6%
#4	73.4%
#10	56.0%
#20	37.3%
#40	22.3%
#60	13.2%
#100	8.9%
#200	6.8%

The soil was classified as SP-SM (poorly graded and silty sand) on the Unified Soil Classification System (USCS). The particle size distribution chart shows that the soil consists mostly of sands with few non-plastic fines. Figure 18 shows the particle size distribution of the 160<sup>th</sup> street soil.

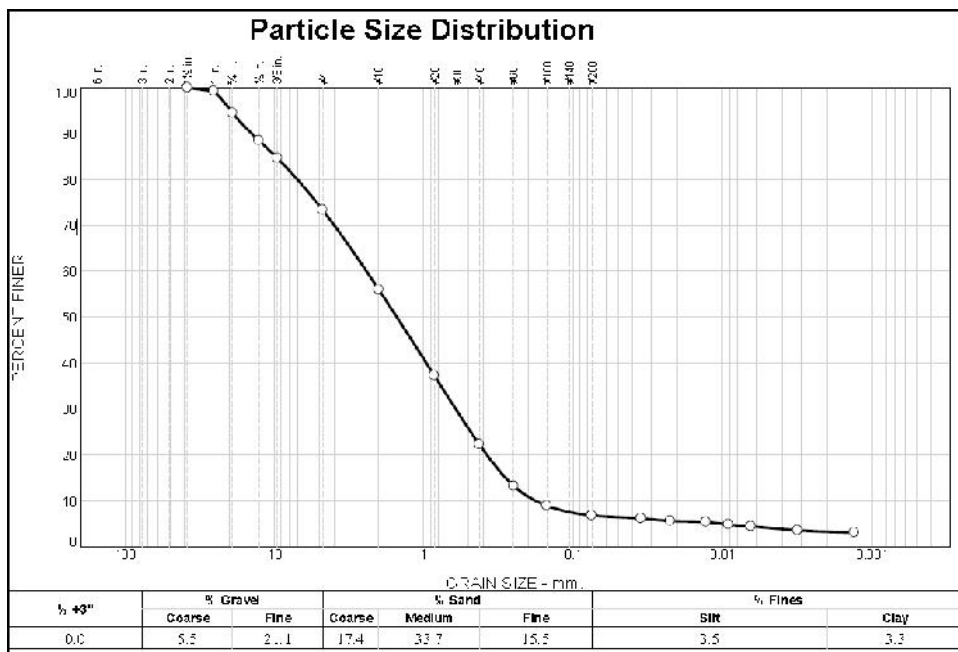


**Figure 18. 160<sup>th</sup> Street soil particle size distribution**

#### Surface material from an unpaved road on Vail Avenue in Hamilton County, Iowa

The soil came from a portion of Vail Avenue which is a north-south, low volume unpaved road located in Hamilton County in Iowa where freeze and thaw damage frequently occurs (Figure 19). Freezing and thawing action induces physical changes to granular surface roads that can negatively impact users and result in increased maintenance costs. Bio-stabilization could be used to mitigate the negative effects.



**Figure 19. Surface material from Vail Avenue in Hamilton County, Iowa**

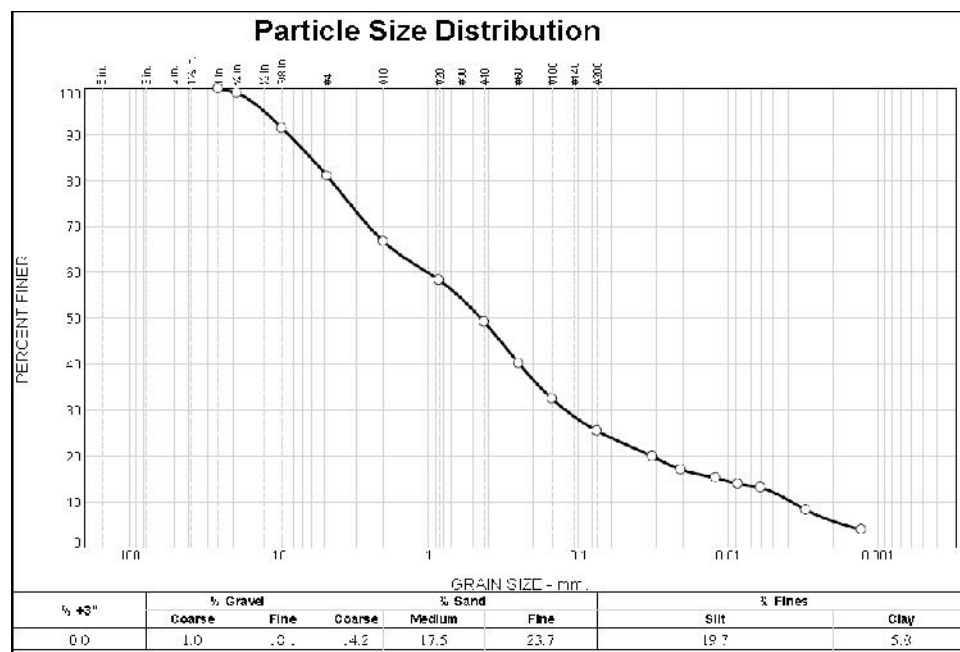
**Table 13. Vail Avenue soil index properties**

<b>Soil index</b>	<b>Value</b>
Atterberg limits	PL = NP
	LL = NV
	PI = NP
Classification	USCS = SM
	AASHTO = A-2-4(0)
Coefficients	D <sub>85</sub> = 6.125
	D <sub>60</sub> = 1.017
	D <sub>50</sub> = 0.447
	D <sub>30</sub> = 0.122
	D <sub>15</sub> = 0.011
	D <sub>10</sub> = 0.004
	C <sub>u</sub> = 269.12
	C <sub>c</sub> = 3.90

**Table 14. Vail Avenue soil sieve analysis results**

Sieve size	Percent finer
1	100.0%
3/4	99.0%
3/8	91.4%
#4	80.9%
#10	66.7%
#20	58.3%
#40	49.2%
#60	40.1%
#100	32.4%
#200	25.5%

The following is the particle size distribution of Vail Avenue soil. Based on the USCS, the soil is SM, silty sand. In the particle size distribution chart, fine gravel, sand, and silt are majority of this type of soil. More than 50% of the soils are sand, and 19.1% of the soil is composed by gravel. So the soil is non-plastic.

**Figure 20. Vail Avenue soil particle size distribution**

### **Concrete pavement coarse aggregate**

The concrete aggregates come from Winterset Ledge in southwest of Iowa. Martin Marietta Materials Company produced these materials (Figure 21).



**Figure 21. Concrete coarse aggregates without bio-treatment**

To ensure that this material is a candidate for research two tests we conducted, the Iowa pore index test and mercury intrusion porosimetry test. The pore index test showed that the aggregate had a secondary pore index of 28, so it is classified in the durability class 2 (Iowa DOT manual, 2010). We also conducted gradation for the aggregates (Table 15).

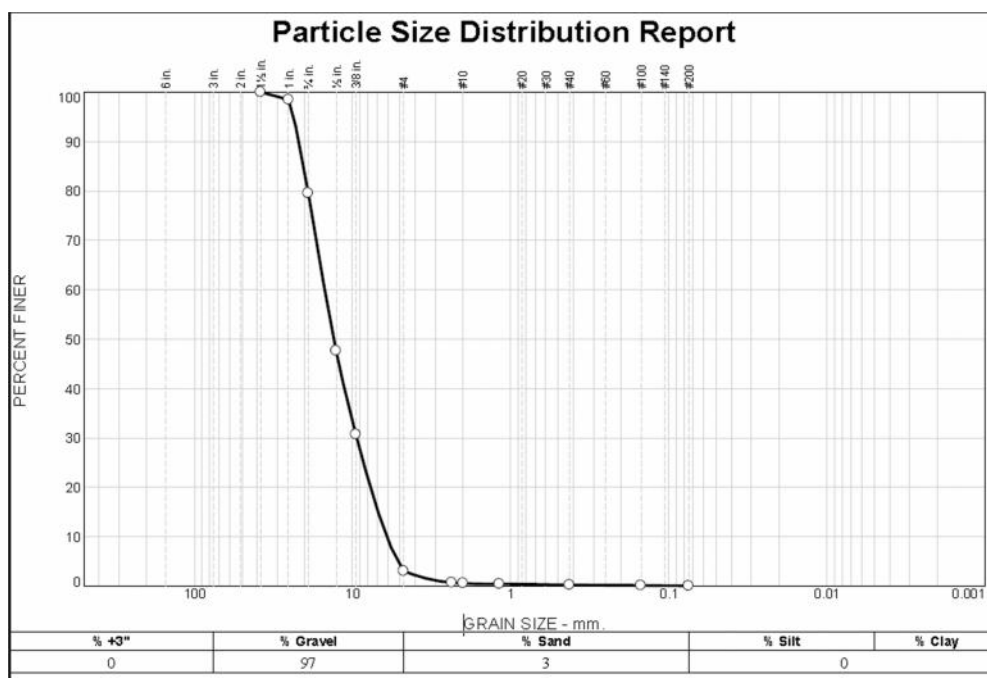
**Table 15. Concrete pavement coarse aggregate index properties**

<b>Index</b>	<b>Value</b>
Atterberg limits	PL = NP
	LL = NV
	PI = NP
Classification	USCS = GP
Coefficients	D <sub>85</sub> = 20.402
	D <sub>60</sub> = 14.996
	D <sub>50</sub> = 13.138
	D <sub>30</sub> = 9.394
	D <sub>15</sub> = 6.890
	D <sub>10</sub> = 6.073
	C <sub>u</sub> = 2.47
	C <sub>c</sub> = 0.97

**Table 16. Concrete pavement coarse aggregate sieve analysis results**

Sieve size	Percent finer
1.5	100
1	98
3/4	80
1/2	48
3/8	31
#4	3
#8	1
#10	1
#16	0
#40	0
#100	0
#200	0.1

The aggregate was classified as GP (poorly graded gravels) based on the USCS. The particle size distribution chart shows that the soil consists mostly of gravels. Figure 22 shows the particle size distribution of the concrete pavement coarse aggregate.

**Figure 22. Concrete pavement coarse aggregate particle size distribution**

The other index properties of the aggregates are in the following table.

**Table 17. Specific gravity and absorption of coarse aggregate**

	Mass 1(g)	Mass 2 (g)	Average
<b>Specific gravity (SSD)</b>	2.53	2.56	2.54
<b>Absorption (%)</b>	4.54%	3.61%	4.08%

## CHAPTER 5. RESULTS AND DISCUSSION

This chapter presents and discusses the results from two laboratory studies, increasing the strength of granular soil samples and plugging pores of coarse aggregate. For increasing strength of granular soil, unconfined compressive strength tests, scanning electron microscopy, and different bio-treatment cycle tests were performed using silica sand and a typical granular surface material for an Iowa unpaved road. For plugging pores of concrete aggregate tests, Iowa pore index tests, mercury intrusion porosimetry, scanning electron microscopy, X-ray diffraction, and different bio-treatment cycles were performed for using an Iowa concrete aggregate.

### **Increasing strength of granular soil**

Two cycles of bio-treatment of silica sands were studied to increase their unconfined compressive strength. After treatment, unconfined compression tests were performed to verify the effects of bio-treatment followed by scanning electron microscopy (SEM) to analyze the micro structure of the material. X-ray diffraction tests (XRD) were used to determine the constituents of the bio-precipitates.

### **Bio-treatment media and treatment cycles**

The untreated, loose silica sand has functional property but no cohesion and therefore no unconfined compressive strength. Bio-stabilization was performed for sand in using single cycle and double cycle treatments in two liquid media. American Type Culture Collection (ATCC) recommends a liquid medium for bacteria incubation that contains  $(\text{NH}_4)_2\text{SO}_4$ . However, because  $\text{SO}_4^{2-}$  can be harmful for some civil engineering materials and the environment. So cultured *Bacillus pasteurii* in an  $\text{NH}_4\text{Cl}$  liquid growth medium was studied. The bacteria grew well in both media after two days. Both the  $(\text{NH}_4)_2\text{SO}_4$  and  $\text{NH}_4\text{Cl}$  liquids are brown to yellow and there is no visual difference (Figure 23).



**Figure 23. Liquid medium with bacteria contains NH<sub>4</sub>Cl (left) and (NH<sub>4</sub>)<sub>2</sub>SO<sub>4</sub> (right)**

Nine samples were prepared for each of the two treatment cycle groups, single treatment and double treatment of samples treated with both the NH<sub>4</sub>Cl and (NH<sub>4</sub>)<sub>2</sub>SO<sub>4</sub>. The single treatment cycle lasted 5 days and the double treatment cycle lasted 10 days.

#### **Unconfined compression tests**

The 5-day (single treatment) and a 10-day (double treatment) bio-treatment cycle included three curing conditions: saturated, air dried, and oven dried. All of the samples were 0.115 ft in diameter because they were all prepared in the same sized molds (0.115 ft x 0.24 ft). The diameter is expressed in feet for ease of calculating force from the calibration certificate. Figure 24 shows a silica sand sample that failed after unconfined compression testing. We determined the corresponding force based on calibration certificate and used following equation to calculate the corresponding pressures

$$\sigma_c = P/A \quad (4)$$

where:

$P$  = given applied load, kPa; and

$A$  = corresponding average cross-sectional area, mm<sup>2</sup>.



**Figure 24. Failed silica sand sample after unconfined compression**

The following sections provide the compressive strength results. The next section shows the results of bio-stabilization using the  $\text{NH}_4\text{Cl}$  medium, and the following section shows the results using the  $(\text{NH}_4)_2\text{SO}_4$ . To verify the effects of bacteria on silica sands, we conducted experiments on samples treated with each liquid medium that did not contain any bacteria. For each group of experiments, we divided each group into three sub-groups: saturated, air-dried, and oven-dried. Saturated means after bio-treatment the samples were fully saturated with water. Air-dried means after bio-treatment we put the samples outdoors to dry. Oven-dried means after bio-treatment we put the samples into oven which supply a constant  $110^\circ\text{C}$  temperature to dry the samples.

#### *Compressive strengths from the $\text{NH}_4\text{Cl}$ liquid medium*

We ran a 5-day and a 10-day bio-treatment cycle of three samples in three conditions, saturated, air dried, and oven dried. From these strength data, we can easily find that bio-treatment has remarkable effect on increasing strength of material.

The oven-dried samples had 3–6 times greater strength than air-dried samples. The saturated samples did not perform any strength. It is worth noting that double bio-treatment

with  $\text{NH}_4\text{Cl}$  liquid medium and oven-dried samples performed a huge increase of strength. So we picked some pieces of that sample to conduct X-ray diffraction test in order to analyze the constituents of the material.

The gauge reading sheet only provides corresponding force values when reading values are 50 or greater so any gauge reading below 50 means almost no compressive strength.

Bio-stabilization is best fit for silica sands, especially after two cycles bio-treatment. In Figure 25, silica sand samples have higher UC strength compared to SM soil and SP-SM soil samples. Double bio-treatment can significantly improve the UC strength of silica sand samples, especially after oven-dried treatment. For SM soil and SP-SM soil, bio-treatment also increased the UC strength from 0 to around 1000 psf, and even to around 2000 psf after oven-dried treatment.

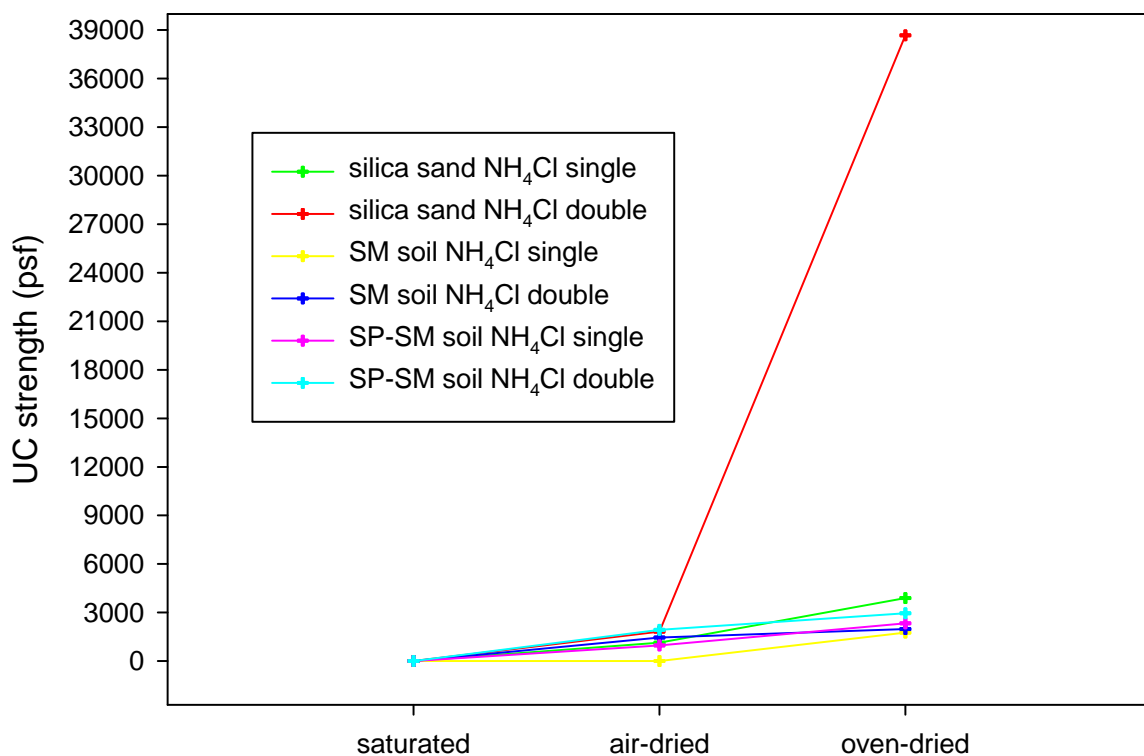


**Figure 25. UC strength of samples with  $\text{NH}_4\text{Cl}$  medium treatment**

*Compressive strengths from the  $(\text{NH}_4)_2\text{SO}_4$  liquid medium*

From these data (Figure 26), we can see the similar effect when we used  $(\text{NH}_4)_2\text{SO}_4$  in liquid medium. The oven-dried samples performed higher strength than air-dried samples.

The gauge readings for the samples saturated were too small to convert to force and strength values. Also oven-dried can help bio-treatment to improve UC strength of samples. And silica sand samples performed higher strength than SM soil and SP-SM soil samples.

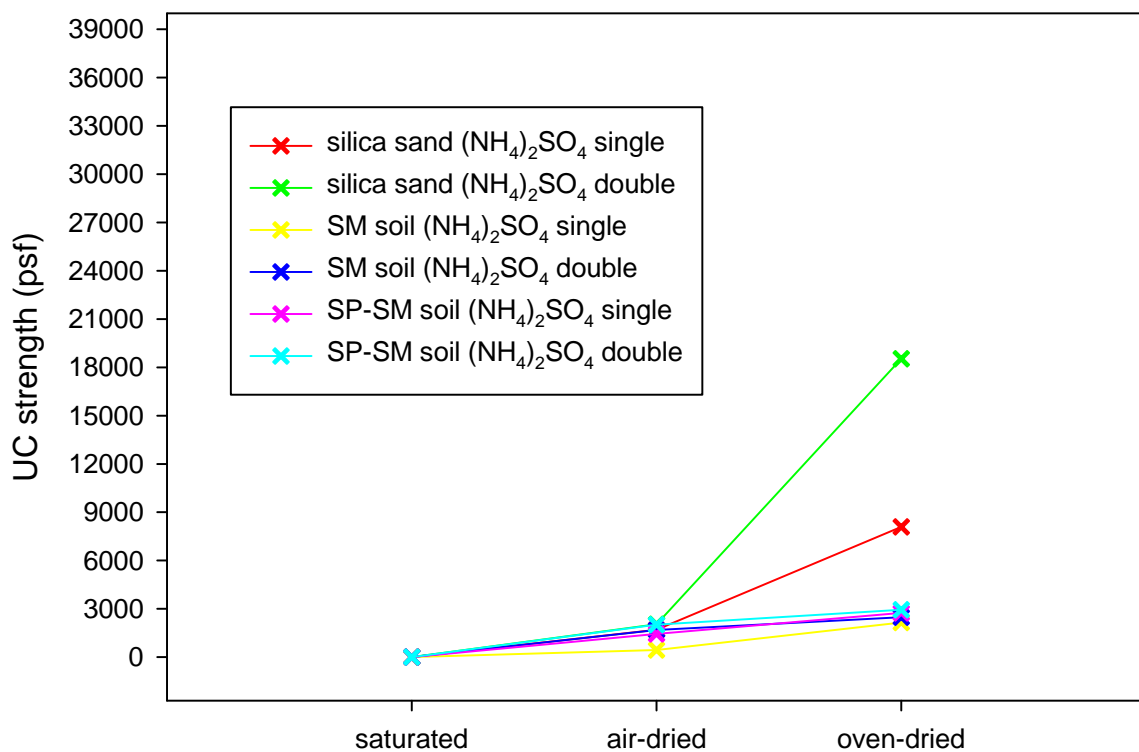


**Figure 26. UC strength of samples with  $(\text{NH}_4)_2\text{SO}_4$  medium treatment**

We also prepared double bio-treated SM soil samples with  $\text{NH}_4\text{Cl}$  in order to examine the effect of lower temperatures oven-dried (Figure 27). SM soil samples have highest UC strength under  $110^\circ\text{C}$  oven-dried condition. Lower oven-dried temperature, lower UC strength.

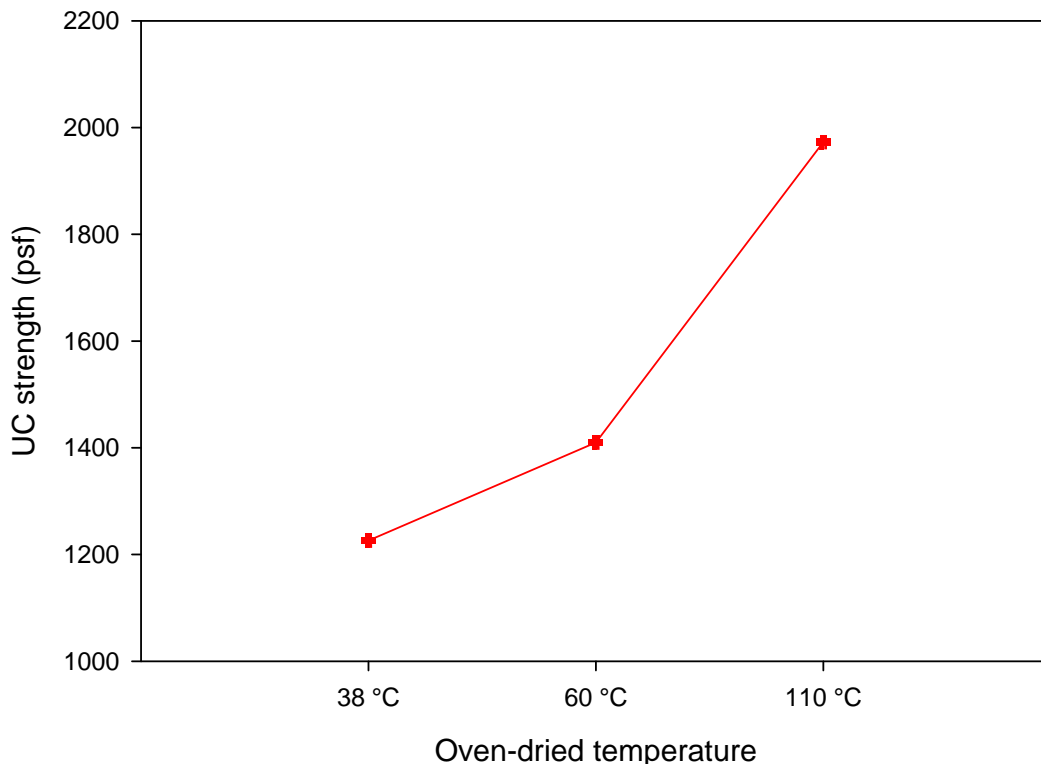


**Figure 27. UC strength of SM soil samples at different oven-dried temperature**

#### *Summary of unconfined compression tests*

Bio-treatment increases the strength of silica sands, SM soil, and SP-SM soil. The strength of silica sand increased much more than the other materials. Double bio-treatment has more improvement on soil samples. In addition, the strength increasing is greater for oven-dried samples after bio-treatment. Thus we suppose more bio-treatments can increase the strength continuously.

The bio-treatment effects and strength improvements are similar for  $\text{NH}_4\text{Cl}$  or  $(\text{NH}_4)_2\text{SO}_4$  liquid media. However, sulfates promote the formation of sulfuric acid that will damage concrete so  $\text{NH}_4\text{Cl}$  would be a better choice as a medium for incubating microorganism for bio-stabilization.

Higher oven-dried temperature helps improve the strength and may prompt mineral forming reactions (Figure 27).

In addition, silt and clay decrease bio-stabilization effects (Table 18). The higher the silt and clay content, the lower the unconfined compressive strength. So this is the reason why

average compressive strengths of soils for SM soil and SP-SM soil samples are lower than silica sand samples. This opinion is also verified by DeJong 2010.

**Table 18. Silt and clay content of granular soil**

Materials	Silt and clay content
SP	0.0%
SP-SM	6.8%
SM	25.5%

#### Scanning electron microscopy (SEM)

We used SEM to show the detailed structure of bio-treated samples. We first examined untreated silica sand at three magnification, 50x (Figure 28), 300x (Figure 29), and 3000x (Figure 30). Figure 28 shows the regular shapes of the particles and that there are voids between the particles. Figure 29 shows the surface of one particle that is relatively smooth with no other substances. At 3000x magnification some cracks, embossing, and cavities are evident (Figure 30).

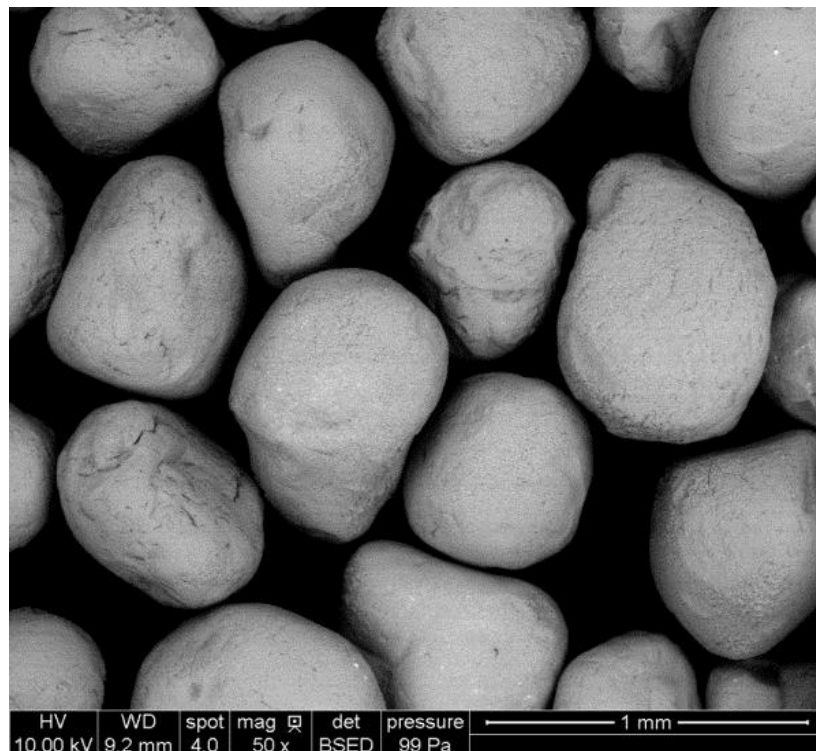


**Figure 28. 50x magnification of untreated silica sand**

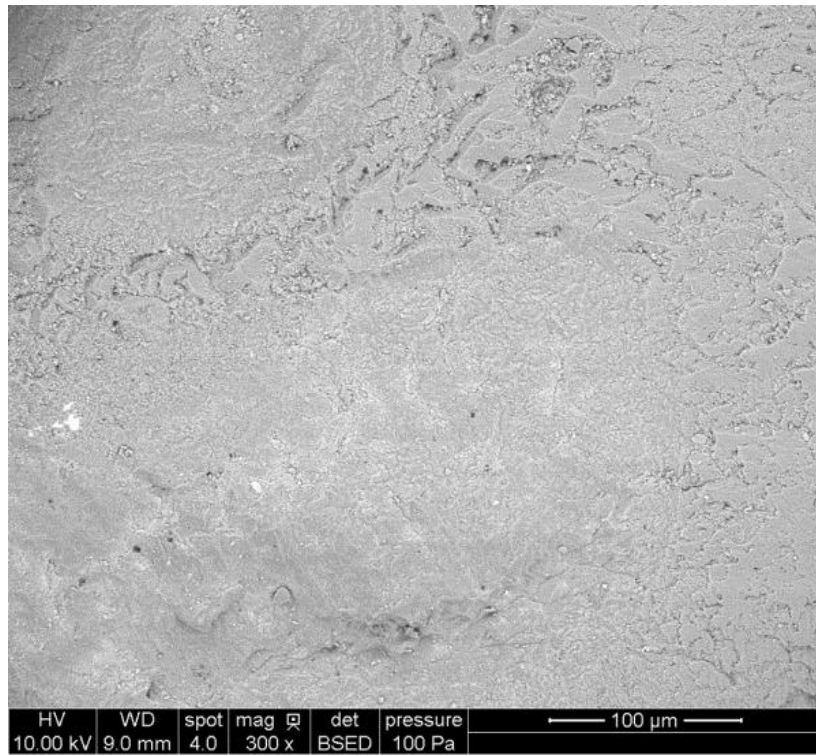


**Figure 29. 300x magnification of untreated silica sand**

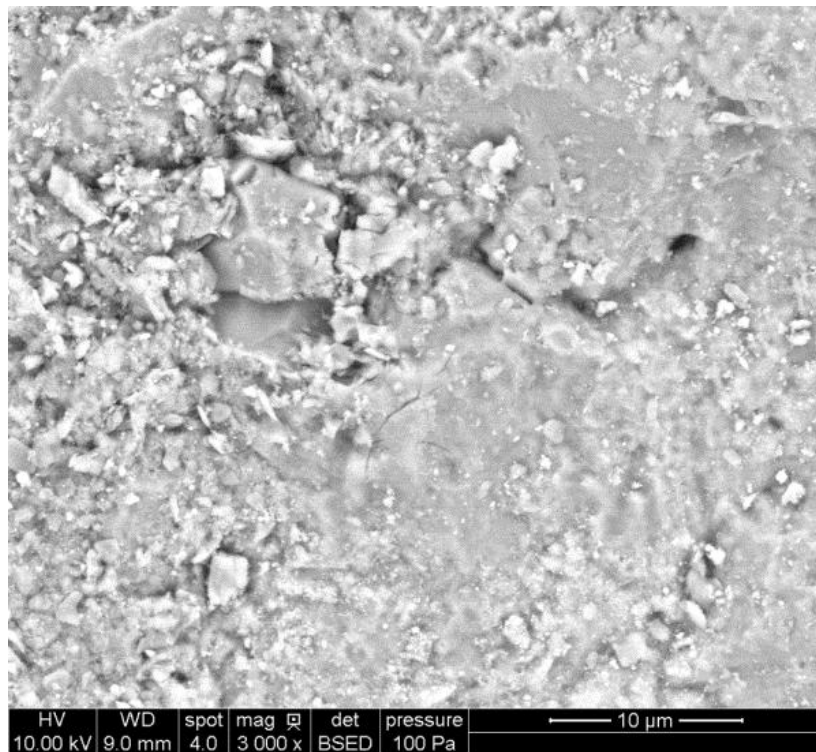


**Figure 30. Silica sands without bio-treatment (3000x)**

After examining the untreated silica sand, we then examined the bio-treated silica sand at 10 magnification, 50x (Figure 31), 100x (Figure 7), 200x (Figure 33), 300x (Figure 34), 350x (Figure 35), 600x (Figure 36), 1000x (Figure 37), 1400x (Figure 38), 1500x (Figure 39), and 3000x (Figure 40). Figure 31 shows some voids between sand particles were filled or semi-filled and the surfaces of sands were rough. Figure 7 shows there were some small particles attached on the surfaces of sands. Figure 33 presents there are some produced layers on the surfaces. Figure 34 shows a silica sand particle was covered by bio-precipitates and there are some lumps exist. Figure 35 and Figure 36 show the voids between particles were not filled totally, but there are some substances exist in the void. In Figure 37, Figure 38, Figure 39 and Figure 40, the magnification is large enough to examine the shape and texture of bio-precipitates. The bio-precipitates are consisting of some bar-like, lumpy, squamous and irregular substances. They attached together and glued the silica sand particles.

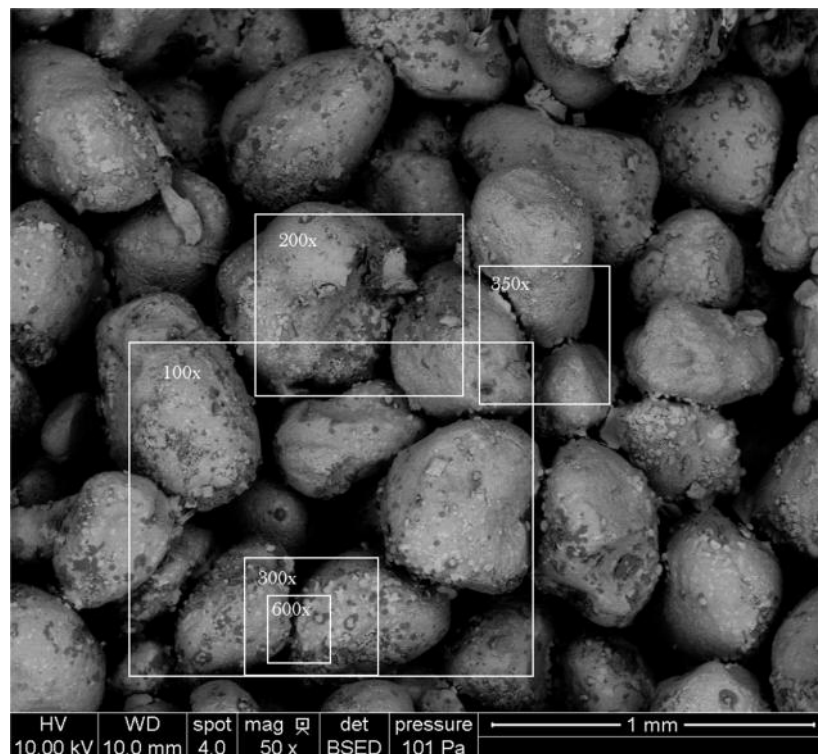


**Figure 31. Silica sands with bio-treatment (50x)**

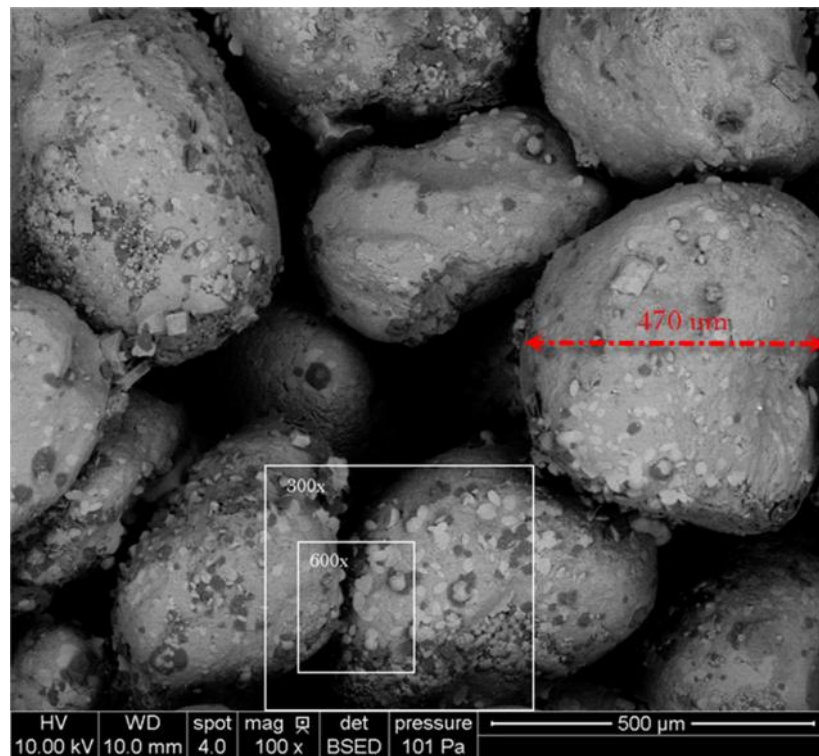


Figure 32. Silica sands with bio-treatment (100x)

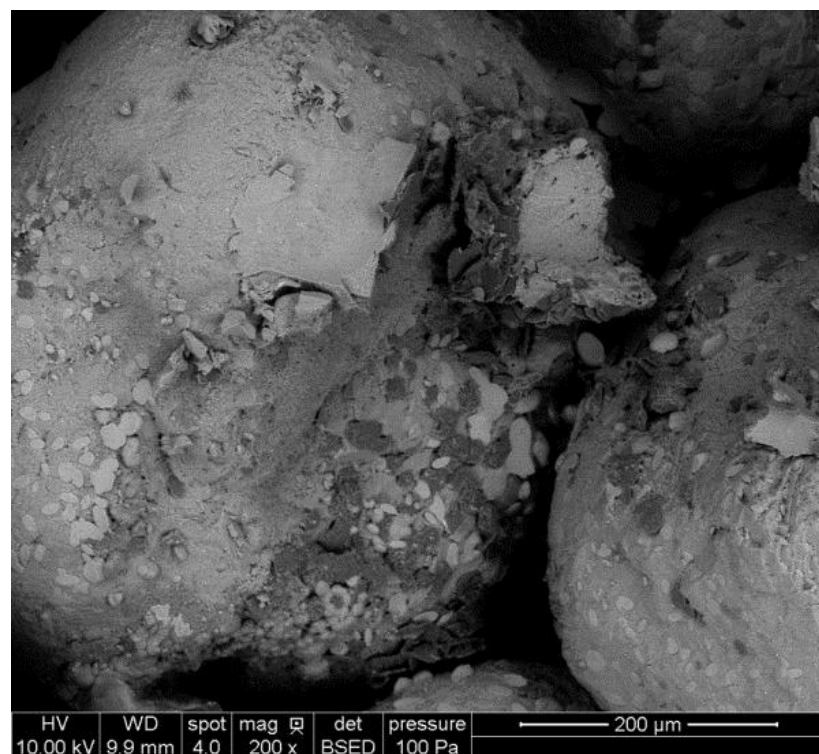
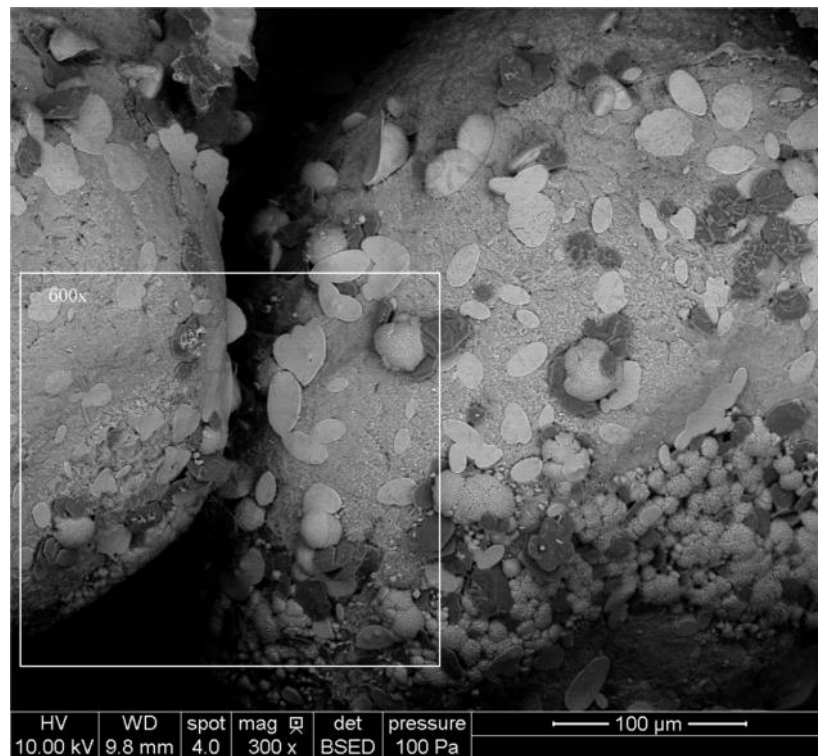


Figure 33. Silica sands with bio-treatment (200x)



**Figure 34. Silica sands with bio-treatment (300x)**

In Figure 35, there are some bio-precipitates attached on the boarder of particles. And between particles, these bio-precipitates formed joints to bond particles together, although the precipitates were disturbed or broken.



**Figure 35.** Silica sands with bio-treatment (350x)

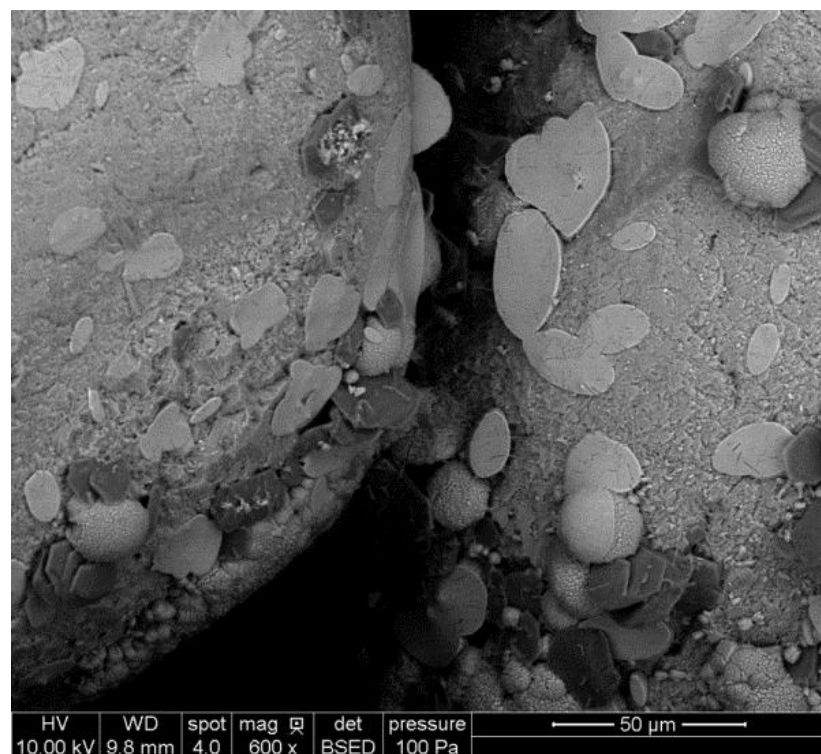


**Figure 36.** Silica sands with bio-treatment (600x)

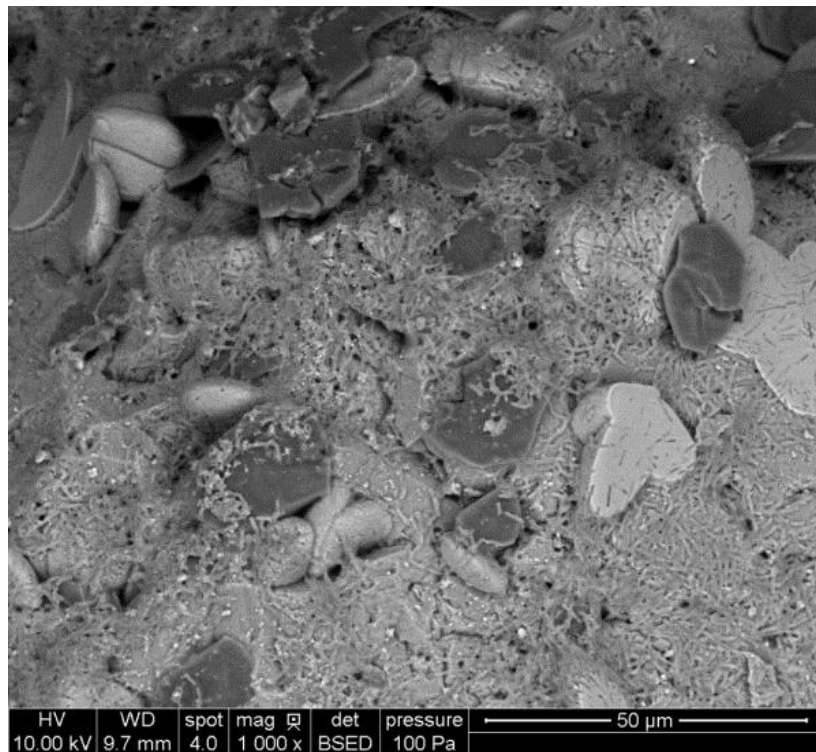
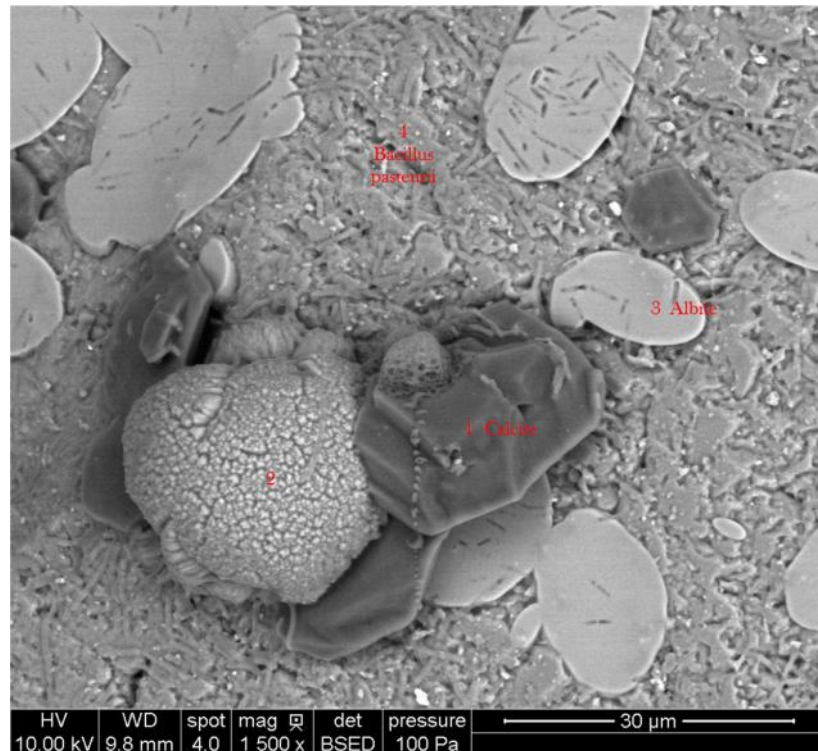


Figure 37. Silica sands with bio-treatment (1000x)



Figure 38. Silica sands with bio-treatment (1400x)

In Figure 39, there are four points that indicate different substances from SEM view. Then we ran energy dispersive x-ray spectroscopy (EDS) to analyze the element of these substances. The EDS results are in Table 19 and Table 20.



**Figure 39. Silica sands with bio-treatment (1500x)**

Table 19 shows there are three elements detected by EDS for untreated silica sands. So the silica sand consists of oxygen, aluminum, and silica. Compared to untreated silica sand, bio-treated silica sand has some more elements exist. For point 3 and point 4, the elemental analyses show there are large amount of calcium and sodium. And based on the result of XRD, the minerals produced by bio-treatment consist of these elements. So we believe point 1 indicates mineral Calcite, and point 3 indicates mineral Albite.

**Table 19. Elemental analysis of untreated silica sand**

<b>Element</b>	<b>Atomic %</b>	<b>Weight %</b>
O	57.391	43.427
Al	0.469	0.598
Si	42.140	55.975
Total	100.000	100.000

**Table 20. Elemental analysis for bio-treated silica sand**

<b>1500x, point 1</b>			<b>1500x, point 2</b>		
<b>Element</b>	<b>Atomic %</b>	<b>Weight %</b>	<b>Element</b>	<b>Atomic %</b>	<b>Weight %</b>
O	53.191	35.351	O	57.264	37.724
Na	0.428	0.409	Na	0.202	0.192
Al	0.177	0.199	Al	0.076	0.085
Si	15.981	18.645	Si	11.917	13.781
P	0.041	0.053	P	0.085	0.109
S	1.493	1.989	S	2.561	3.381
Cl	22.844	33.642	Cl	6.767	9.878
K	0.417	0.677	K	0.336	0.541
Ca	5.428	9.036	Ca	20.791	34.309
Total	100	100	Total	100	100
<b>1500x, point 3</b>			<b>1500x, point 4</b>		
<b>Element</b>	<b>Atomic %</b>	<b>Weight %</b>	<b>Element</b>	<b>Atomic %</b>	<b>Weight %</b>
O	52.685	35.195	O	52.13	36.856
Na	0.748	0.718	Na	0.091	0.092
Al	0.269	0.303	Al	0.191	0.227
Si	18.949	22.221	Si	37.949	47.097
P	0.008	0.011	P	0	0
S	10.317	13.813	S	1.584	2.245
Cl	3.649	5.401	Cl	3.752	5.877
K	1.037	1.694	K	0.388	0.671
Ca	12.337	20.645	Ca	3.915	6.934
Total	100	100	Total	100	100

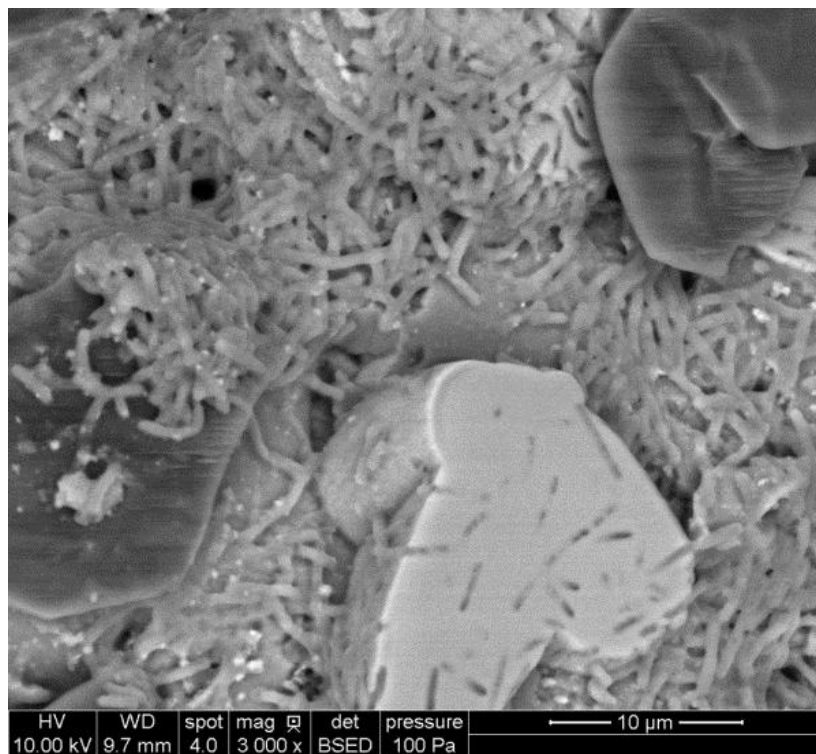


**Figure 40. Silica sands with bio-treatment (3000x)**

From above figures, we can easily find the huge difference between bio-treated silica sands and untreated silica sands. Some substances tried to fill out the void between particle and particle. The shapes of these substances are various, including round, flat, clubbed, irregular. These substances are assumed to be bio-precipitates produced by bacteria we used. These precipitates assembled together and almost covered the surface of the silica sands. The bio-precipitation bonded particle to particle together like glue. This is the reason why bio-treatment is capable to increase the strength of samples.

#### X-ray diffraction (XRD) test

In order to examine the constituents of bio-precipitates, XRD tests were conducted. There are 4 main constituents were found (Figure 42): calcite– $\text{CaCO}_3$ , dolomite– $\text{CaMg}(\text{CO}_3)_2$ , quartz– $\text{SiO}_2$ , and albite– $(\text{Na}, \text{Ca})(\text{Si}, \text{Al})_4\text{O}_8$ . Based on the Mohs' scale of hardness (Table 21), calcite has a 3-scale hardness, dolomite has a 3.5-scale hardness, quartz has a 7-scale hardness, and albite has a 6.5-scale hardness. Only quartz and albite have large hardness. From XRD result for untreated silica sands (Figure 41), the constituent was quartz, so the

calcite, dolomite, and albite came from bio-stabilization process. And Albite is assumed to be the reason why bio-stabilization can increase the strength of silica sand samples.

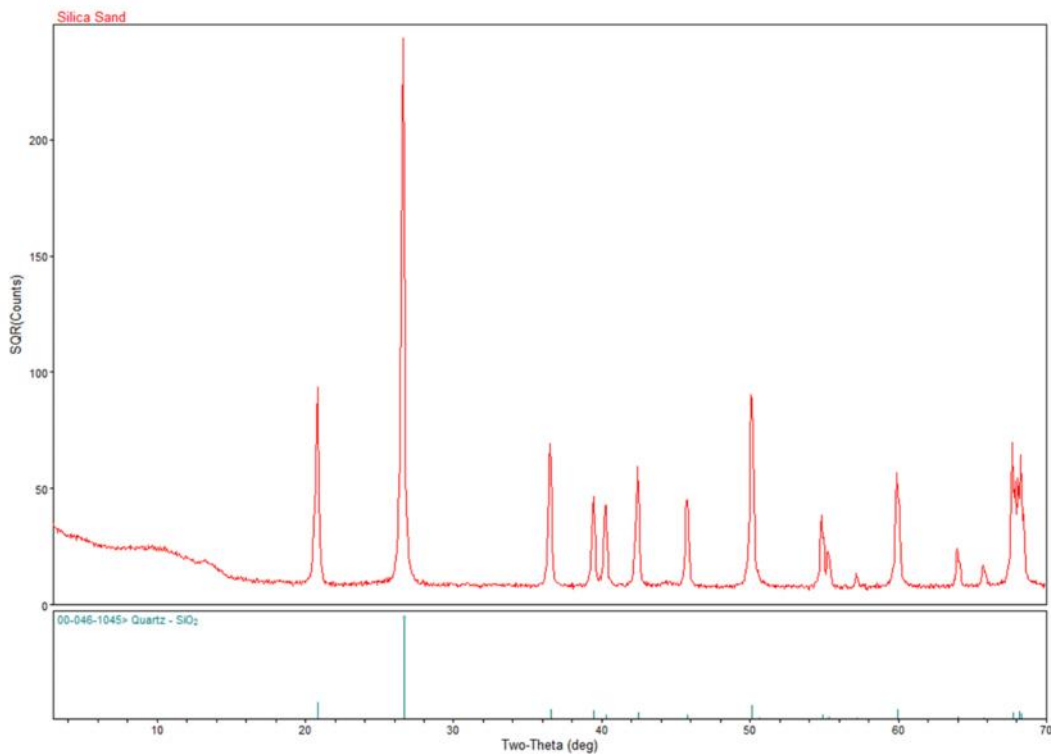


**Figure 41. XRD results for untreated silica sand**

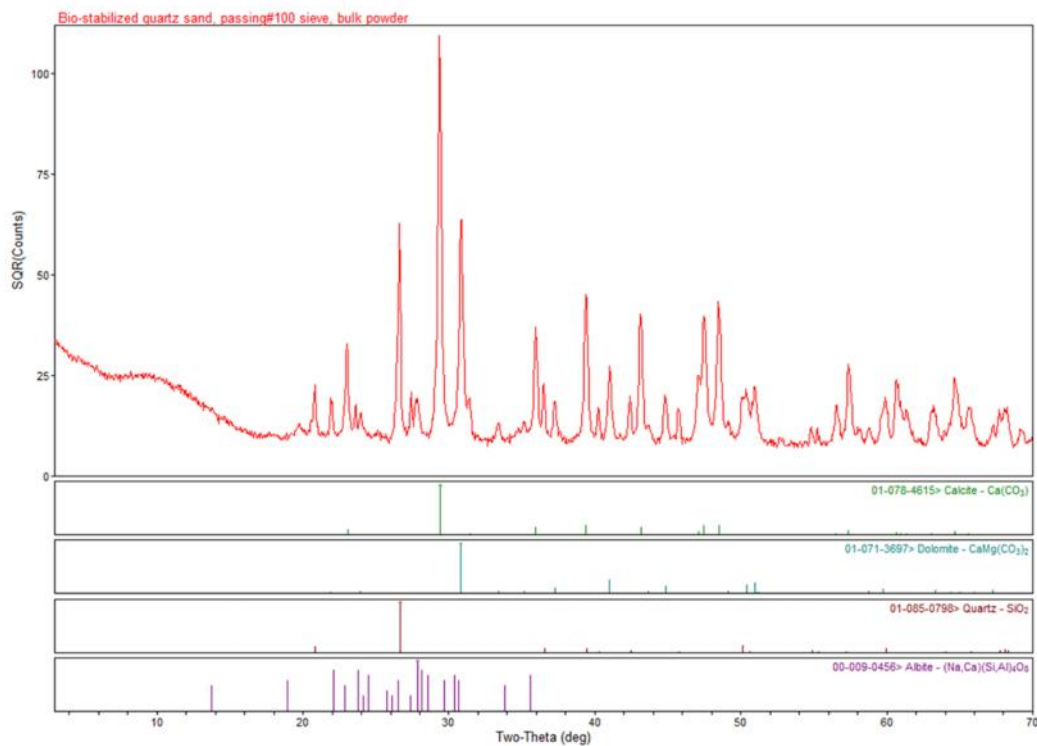


**Figure 42.** XRD results for bio-stabilized silica sand

**Table 21.** Mohs' scale of hardness (Mohs, 1773–1839)

Hardness scale	Mineral
1	Talc
2	Gypsum
3	Calcite
4	Fluorite
5	Apatite
6	Feldspar
7	Quartz
8	Topaz
9	Corundum
10	Diamond
1 is softest, 10 is hardest	

### **Plugging pores in concrete aggregate**

We used bio-stabilization to plug the pores in concrete aggregate. The original concrete aggregates were low quality and had relatively large pores that are susceptible to D-cracking so we bio-treated the aggregate in ten cycles. After treatment, we ran Iowa pore index and mercury intrusion porosimetry tests to determine the quality and size distribution of pores inside the aggregates. Freezing and thawing tests were conducted to evaluate the durability of bio-treated concrete. Then we used scanning electron microscopy and X-ray diffraction to detect and analyze the micro-structure and material constituents of the aggregate.

#### **Bio-treatment cycles**

The properties of concrete aggregates have already been discussed in the previous chapter. The bio-treatment method is similar with silica sands and described in the method chapter. We designed 11 groups of experiments corresponding with number of bio-treatment cycles. So we divided them into 0-cycle bio-treatment to 10-cycle bio-treatment. ATCC recommends a liquid medium which contains  $(\text{NH}_4)_2\text{SO}_4$  used for bacteria incubation. However,  $\text{SO}_4^{2-}$  is harmful for civil engineering material and environment. So we used  $\text{NH}_4\text{Cl}$  to replace  $(\text{NH}_4)_2\text{SO}_4$  for preparing liquid medium.

There is no difference between  $(\text{NH}_4)_2\text{SO}_4$  and  $\text{NH}_4\text{Cl}$  liquid medium when we detect them by naked eyes. The color of liquid medium is brown to yellow. We cultured same bacteria and put them in a same incubator shaker. After two days, the bacteria grew well in both of them.

#### **Iowa pore index test**

This test is used to determine the pore volume of concrete aggregates. All data were gathered from Iowa DOT material research center.

**Table 22. Iowa pore index of concrete aggregates**

Sample	Primary pore index	Secondary pore index
Aggregates from Fort Calhoun	16	30
Aggregates from Winterset Ledge	88	28
Bio-treated aggregates	16	25

Note: original aggregate are relative good quality and come from Iowa DOT; new aggregate come from Winterset Ledge in southwest of Iowa and are relative bad quality.

The primary pore index represents the water volume that comes into pores of aggregates at the first one minute. During the first one minute of running equipment, relative large pores will be filled by water. This index is usually a control value that indicates whether the equipment is leaking or not. The secondary pore index represents the amount of water injected into the aggregate capillary pore system 0.1 to 0.01 micrometer radius (Iowa 219C, 2000).

The original and new aggregates both are untreated. From above results, the primary pore index of new aggregates is much larger than the original aggregates. So the new aggregates have more amount and larger size pores than original aggregates.

**Table 23. Quality of aggregates refer to secondary pore index (Iowa DOT manual, 2010)**

Durability class	Quality	Test limits	Test method
<b>Class 2</b>	Secondary pore index	Max. 30	Iowa 223
<b>Class 3</b>	Secondary pore index	Max. 25	Iowa 223
<b>Class 3i</b>	Secondary pore index	Max. 20	Iowa 223

Note: Class 3i is the best quality level, then class 3, and then class 2.

Comparing the secondary pore index of our aggregates to Iowa DOT durability class, we can see our aggregates are in class 2 level. It means the aggregates have a relative low quality to withstand saturated freeze-thaw pressures. But after bio-treatment, the aggregate durability class changed to class 3, which is better quality than class 2.

For the bio-treated aggregates in Table 22, the secondary pore index decreased a little. Theoretically, after bio-treatment the pores of aggregates should be plugged and the volume of pores should decrease apparently. After discussion and analysis, we think the bio-precipitates are sensitive to water. This is a primary reason why bio-treatment increased secondary index a little. During UC tests, the saturated soil samples cannot perform strength.

### **Mercury intrusion porosimetry**

In this testing, we have 11 groups of experiment. They are different from the bio-treatment cycles. 0-treatment means no treatment applied on aggregates, 2-treatment means two bio-treatment cycles (10 days) applied on aggregates, and 5-treatment means 5 bio-

treatment cycles (25 days) applied on aggregates. All raw data are attached in the Appendix. Table 24 is a summary of intrusion data.

**Table 24. Mercury intrusion porosimetry data summary**

Bio-treatment cycle	Total intrusion volume (mL/g)
<b>0-treatment</b>	0.0697
<b>1-treatment</b>	0.0435
<b>2-treatment</b>	0.0371
<b>3-treatment</b>	0.0385
<b>4-treatment</b>	0.0599
<b>5-treatment</b>	0.0255
<b>6-treatment</b>	0.0199
<b>7-treatment</b>	0.028
<b>8-treatment</b>	0.0267
<b>9-treatment</b>	0.0529
<b>10-treatment</b>	0.0528

After bio-treatment, the total intrusion volume is decreased in order of treatment cycles increasing until 6-treatment. It means the pores of aggregates are plugged by bio-precipitates and pore volume decreased. There are still some pores exist, and these pores come from bio-precipitates and some inner pores were not plugged.

We used the mercury intrusion porosimetry raw data to plot some figures for analysis, cumulative intrusion vs. pore size (Figure 43), incremental intrusion vs. pore size (Figure 44), differential intrusion vs. pore size (Figure 45), log differential intrusion vs. pore size (Figure 46), and pore size distribution (Figure 47). Both of these figures can present the pore size data at different treatment cycles. Figure 43 clearly shows the cumulative volume of mercury intrusion at different treatment cycles. The cumulative intrusion volume began to increase from pore size 0.5–0.9 µm, and at pore size 0.002 µm, the volume is tend to constant. The bio-treatment effect is obvious, the cumulative intrusion volume summarized in Table 24. The cumulative intrusion volume of 0-treatment is 3.5 times more than 6-treatment. The decrease of pore volume reflects the pores of aggregates were plugged by bio-precipitates.

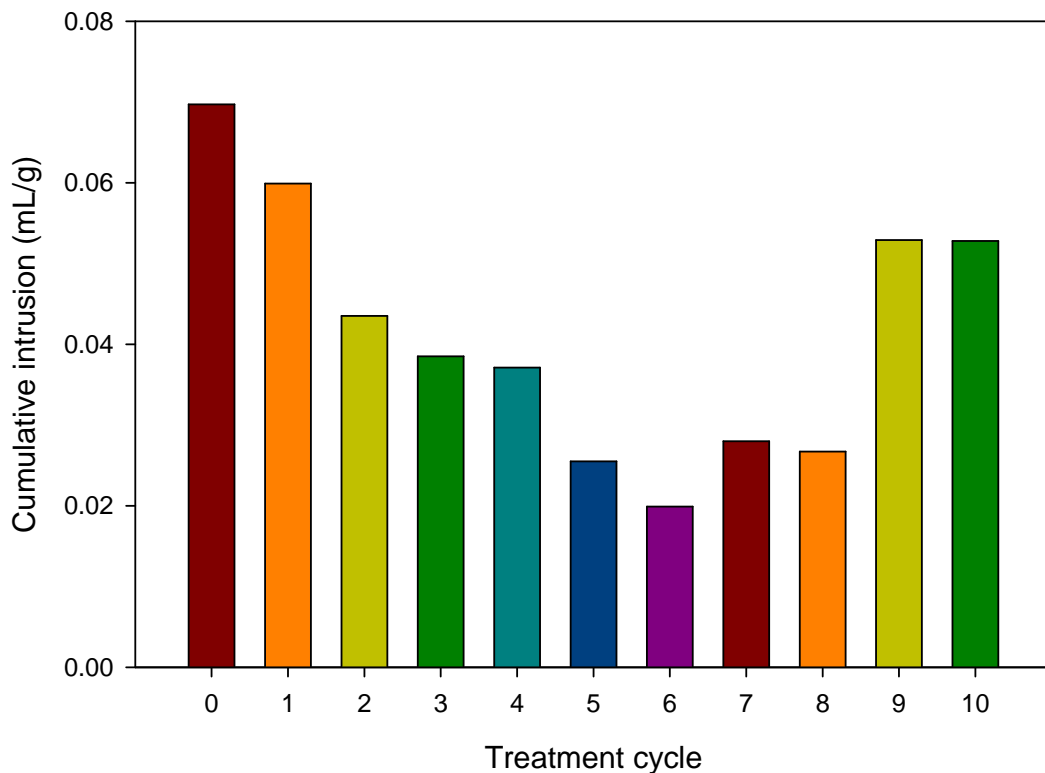


**Figure 43. Cumulative intrusion versus pore size at different treatment cycles**

Incremental intrusion vs. pore size (Figure 44) presents the pores of aggregates distributed from 0.03  $\mu\text{m}$  to 1  $\mu\text{m}$ . The raw aggregates have two peak values; one is from 0.28  $\mu\text{m}$  to 0.5  $\mu\text{m}$ , another one is from 0.07  $\mu\text{m}$  to 0.28  $\mu\text{m}$ . And the incremental intrusion volume reached to 0.012 mL/g and 0.0056 mL/g, respectively. This means the pores of aggregates mostly consist of these two pore size ranges. Vernon and Wendell (1982) proved nondurable aggregates associated with D-cracking pavements exhibited a predominance of 0.04  $\mu\text{m}$  to 0.2  $\mu\text{m}$  diameter pore sizes. If the pore size is in this size range, the aggregates are most susceptible to freeze and thaw effect. After 5 bio-treatment cycles, the size of aggregates pores were decreased to 0.28  $\mu\text{m}$ –0.4  $\mu\text{m}$  and 0.1  $\mu\text{m}$ –0.28  $\mu\text{m}$ . More remarkable, the incremental intrusion volumes were decreased to 0.004 mL/g, and 0.0028 mL/g, respectively. Even after six cycles of bio-treatment, the aggregate pore size was decreased to 0.11  $\mu\text{m}$  0.18  $\mu\text{m}$ . the incremental intrusion volume was decreased to 0.0199 mL/g. The pores occurred in original material were plugged effectively. Six cycles of bio-treatment changed the pore size around three times smaller than untreated material.

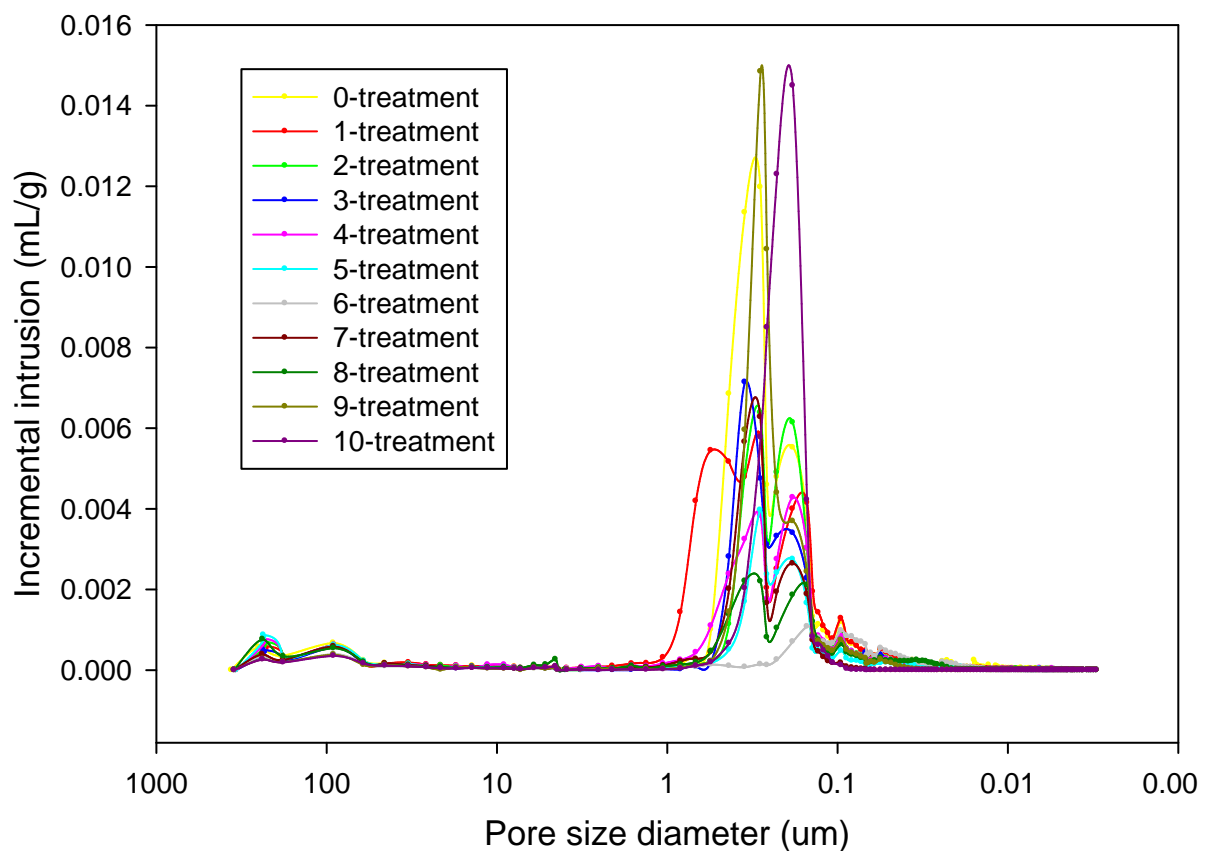


**Figure 44. Incremental intrusion versus pore size at different treatment cycles**

Differential intrusion and log differential intrusion are another two expression method for mercury intrusion porosimetry. They could reflect the pore size distribution changes more intuition. In Figure 45, the differential intrusion value rose and fell apparently, and there are some peaks we can detect. These peaks represent intrusion volume and the corresponding pore size ranges which take most of mercury. In mathematics, the differential is a liner description of local change rate of function. The derivative plot has the virtue of clearly identifying points of inflection, which in this case shows us where clusters of pores of a particular diameter occur.

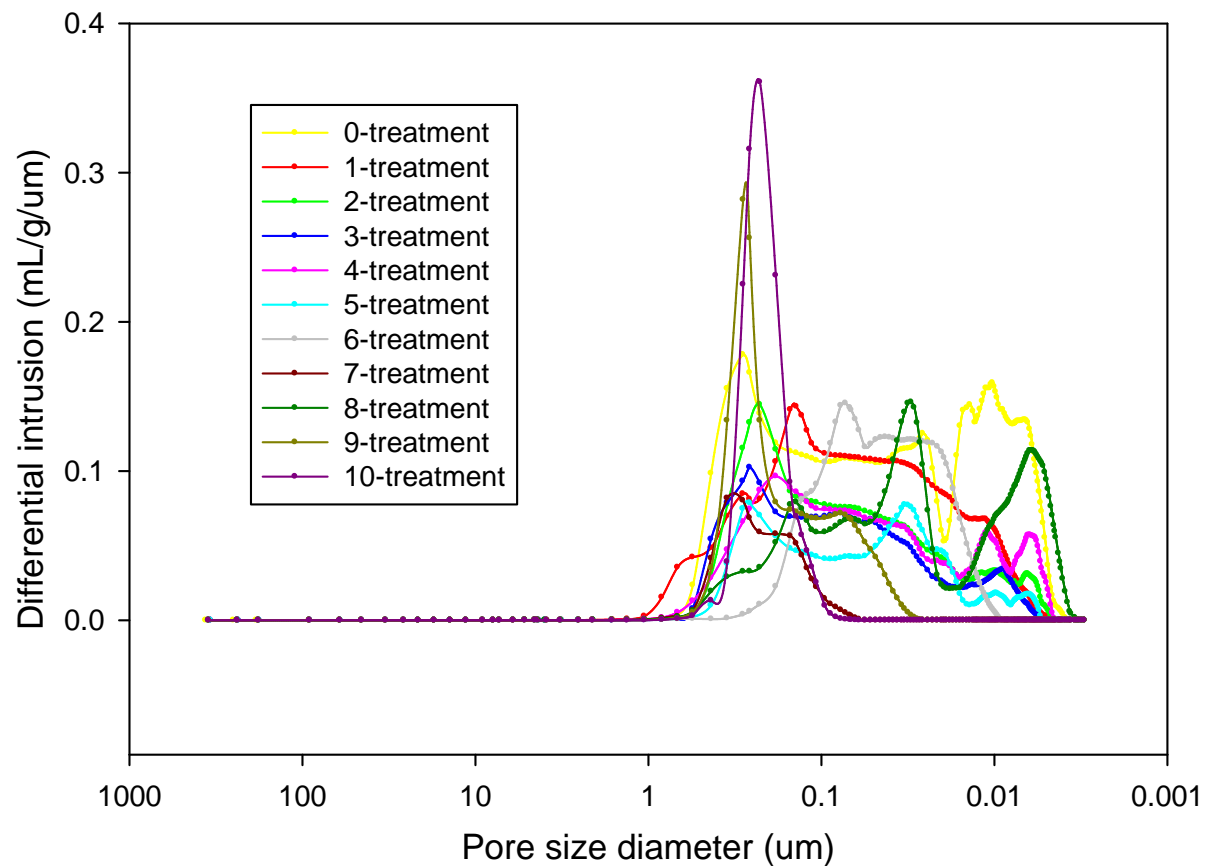


**Figure 45. Differential intrusion versus pore size at different cycles**

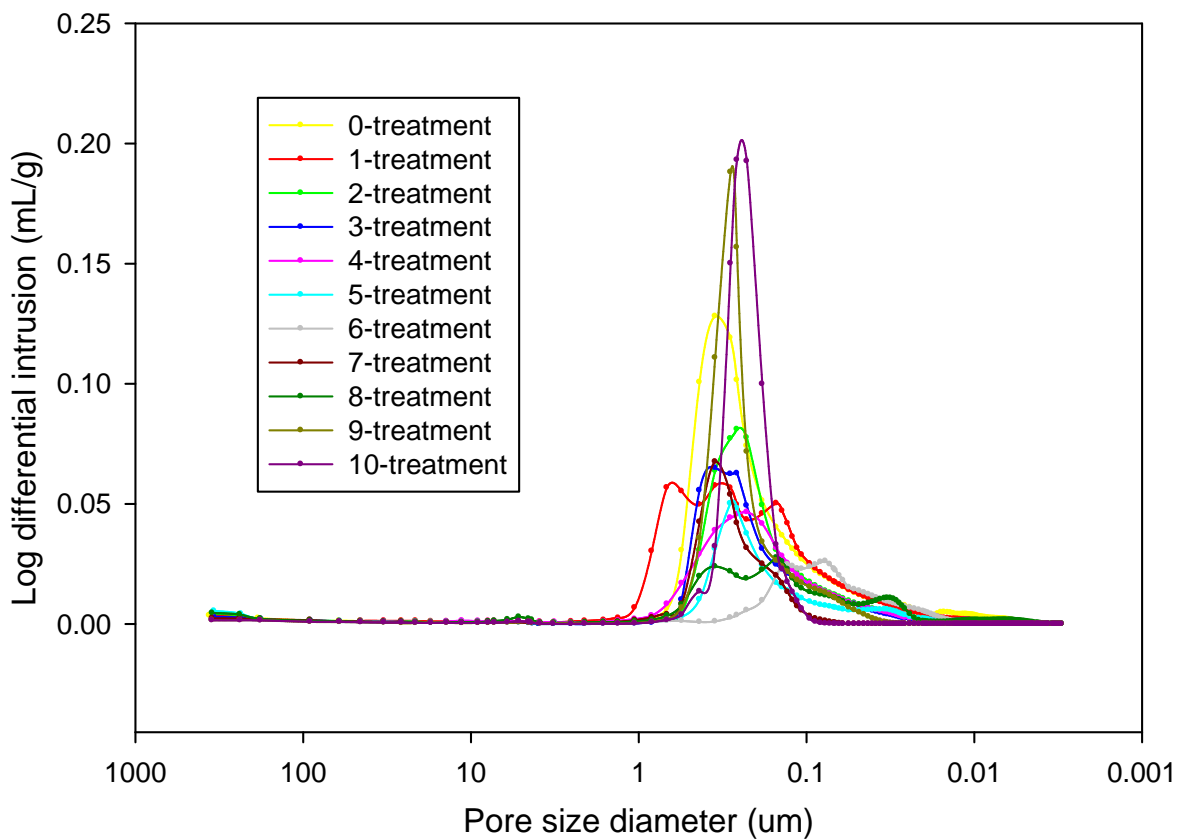


**Figure 46. Log differential intrusion versus pore size at different cycles**

From the following bar chart of pore size distribution (Figure 47), we can easily find the pores of aggregates are mostly consisting of  $0.04\text{ }\mu\text{m}$ – $2\text{ }\mu\text{m}$  size pores. The pores of 6-cycle bio-treated aggregate are concentrated on  $0.04\text{ }\mu\text{m}$ – $0.2\text{ }\mu\text{m}$  that most susceptible for D-cracking. So the optimum cycles of bio-treatment need to be evaluated in the future. In addition, the mercury intrusion volumes are almost decreased in order of bio-treatment cycles increasing except after 6-cycles. Few exceptions probably are caused by experiment errors. Further bio-treatment after 6-cycle looks increasing the pores between  $0.04\text{ }\mu\text{m}$ – $0.4\text{ }\mu\text{m}$ . We suppose the reason is bio-precipitates themselves contain a lot of pores.

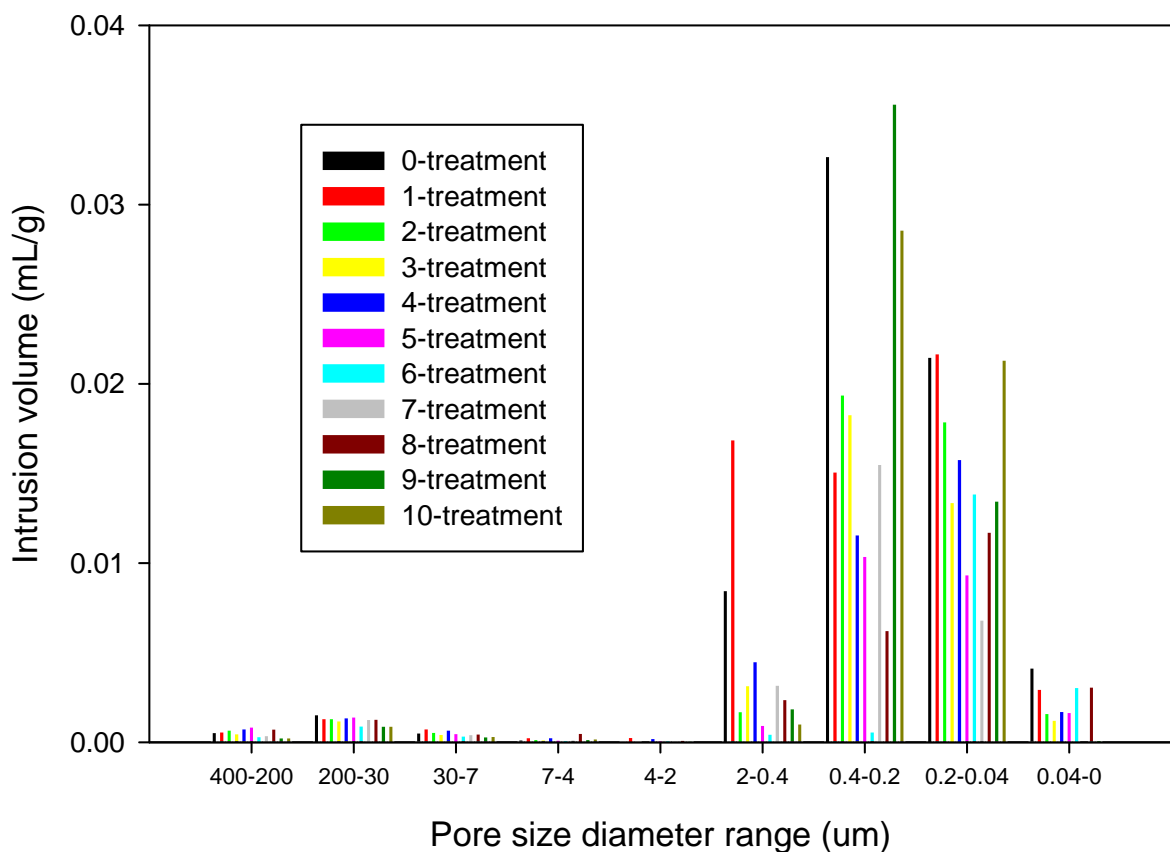


**Figure 47. Pore size distribution at different treatment cycles**

Consequently, based on these results, we believe bio-stabilization is capable to reduce porosity of coarse aggregate to achieve mitigation of freezing and thawing impact and increased durability of concrete pavement.

### Freezing and thawing test

To evaluate the durability of bio-treated aggregate concrete and untreated concrete, we mixed fresh concrete and conducted compression and freezing thawing test. The coarse aggregates were bio-treated and mixed with cement, sands and water. The control group used untreated coarse aggregates mixed with cement, sands and water. During concrete mixing, some ammonia smell-like gas was emitted and lower water absorption was obvious compared to control group. We gathered three main data during test, compressive strength, weight loss and relative dynamic modulus of elasticity. The untreated concrete beams were failed after 90 freezing thawing cycles, the average dynamic modulus is 57.98%. ASTM

C666 suggests no to continue testing if dynamic modulus less than 60% of original. However, after 90 freezing thawing cycles, bio-treated aggregate concrete beams have 76.18% for average dynamic modulus. Even after 120 freezing thawing cycles, the dynamic modulus of bio-treated aggregate concrete beams is still higher than untreated concrete beams at 90 freezing thawing cycles (Figure 48). The relative dynamic modulus of untreated concrete is sharply decreased after 60 freezing and thawing cycles. This indicates bio-treatment for coarse aggregate is capable for improving concrete durability. One possible influence for bio-treated aggregate concrete is salts. Because the liquid medium used to incubate microorganism contains  $\text{NH}_4\text{Cl}$  and  $\text{CaCl}_2$  that very bad for concrete durability. These two types of salt will damage concrete heavily. This evidence further indicates bio-treatment considerably prevents freezing and thawing damage to concrete.

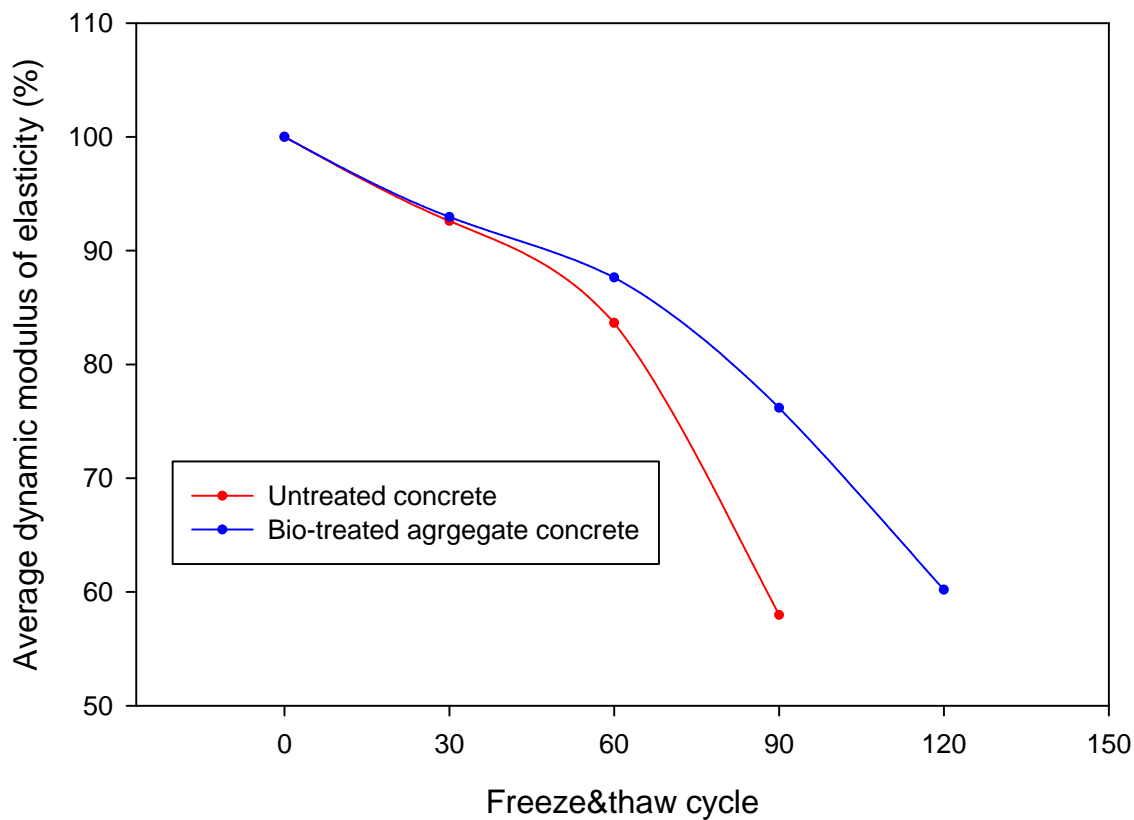


**Figure 48. Variation of relative dynamic modulus after freeze and thaw**

In addition, we weighed the beams every 30 freezing thawing cycles (Figure 49). Although untreated concrete lost less weight than bio-treated aggregate concrete at the first

90 cycles, rapidly decreasing of weight indicates freezing and thawing effect damaged untreated concrete very heavily. The weight loss of bio-treated aggregate concrete is relative stable, after 150 cycles the weight loss is less than 7%. In addition, soundness of aggregates by freezing and thawing test (AASHTO T103-91) was conducted. The weight loss of untreated aggregate after 50 freezing and thawing cycles is 26.3%, and it is 20.9% for bio-treated aggregate. There is 5.4% difference, in terms of improvement, it is 20.5%. This results reinforced that bio-treatment is capable to increase the durability of porous aggregate.

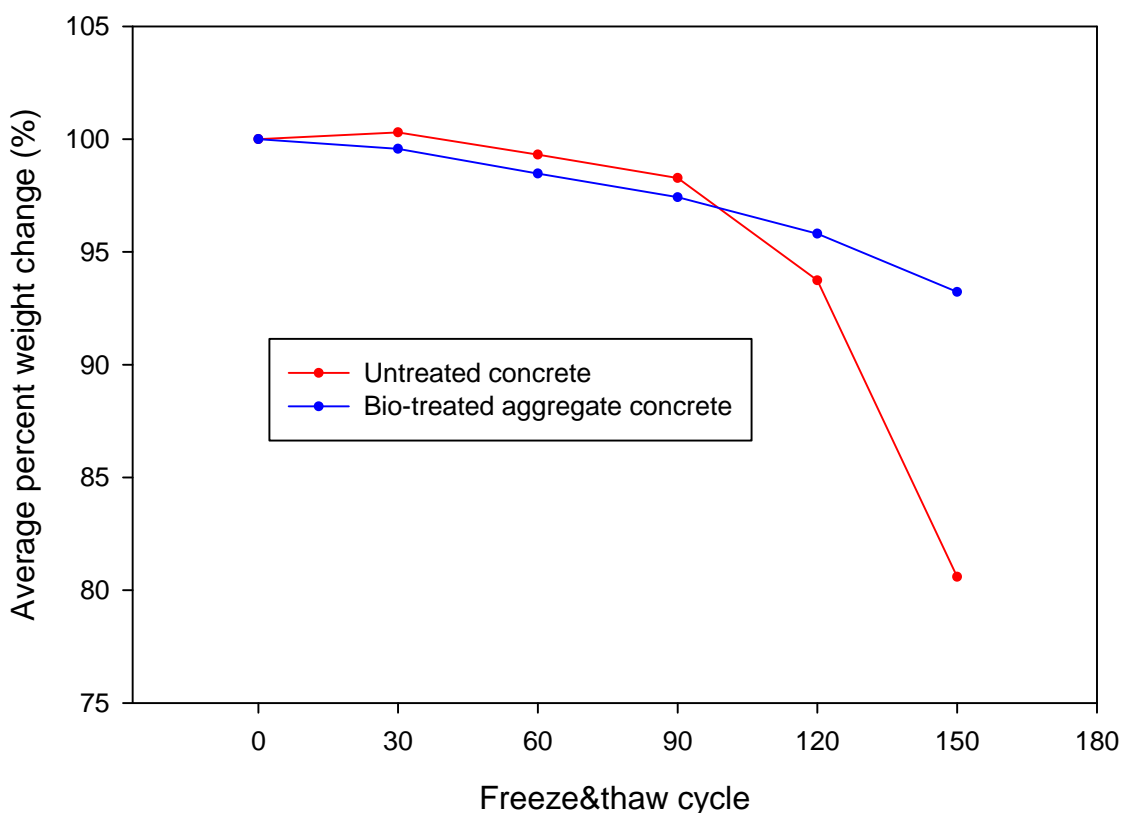


**Figure 49. Variation of weight change after freeze and thaw**

The following photos showed damages of concrete after each 30 freezing thawing cycles. From these two photos, it is obvious that untreated concrete beam was damage heavier than bio-treated aggregate concrete.

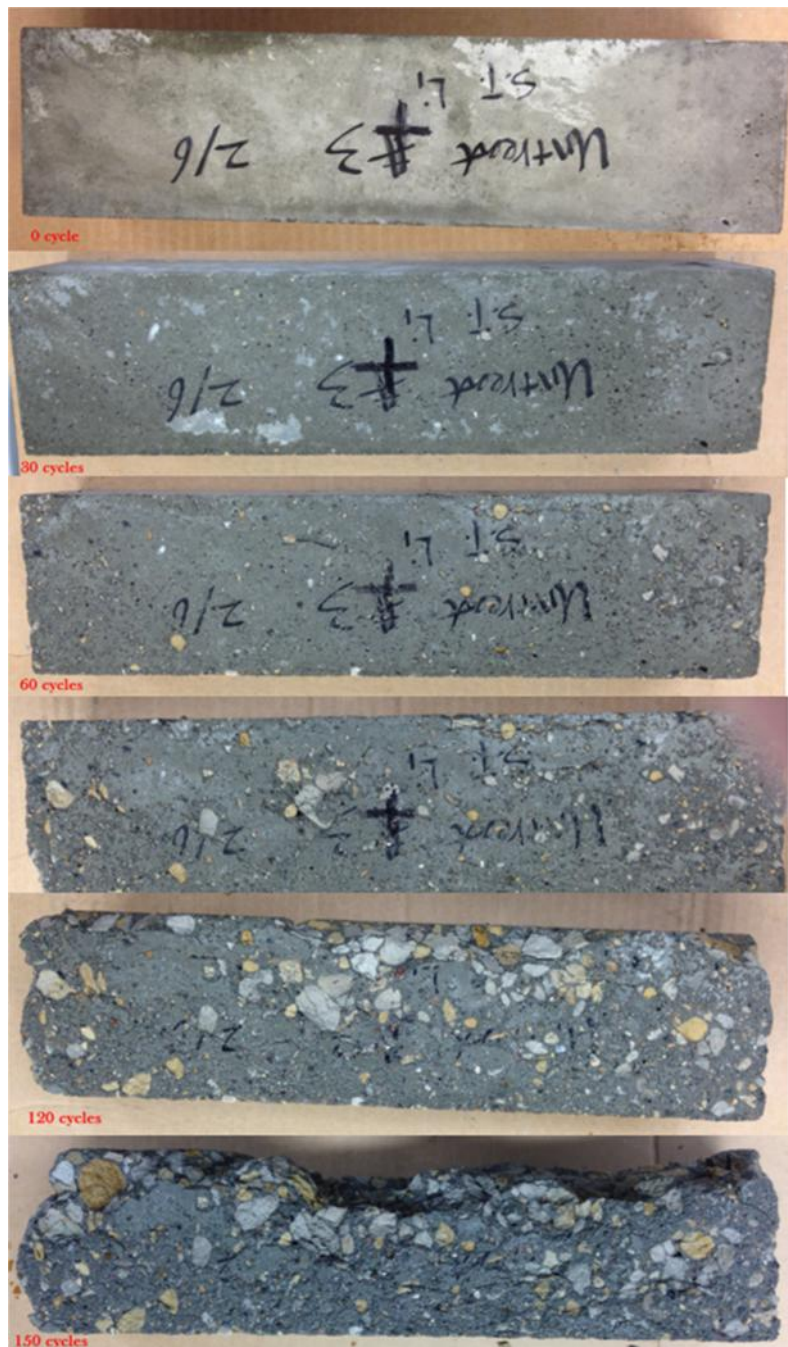


**Figure 50.** Untreated concrete beam at different freezing thawing cycles



**Figure 51. Bio-treated aggregate concrete beam at different freezing and thawing cycles**

#### Compression test

The compressive strength of untreated concrete is larger than bio-treated aggregate concrete after first 7 days wet curing. Because the slump of bio-treated aggregate concrete is 6 in., untreated concrete had 2 in. In addition, the air content of freshly mixed concrete is 5%,

and bio-treated aggregate concrete had 6.7%. Higher air content and slump caused lower compressive strength of bio-treated aggregate concrete. However, after 28 days wet curing, the air content of untreated concrete and bio-treated aggregate concrete is similar, 5.3% and 4.8%, respectively. So the compressive strength of untreated and bio-treated aggregate concrete is similar (Figure 52). The air content of freshly mixed concrete is measured by pressure method (ASTM C231), and the air content of 28-day concrete is measured by microscopical determination of air-void system (ASTM C457). So the variation of air content value is acceptable.

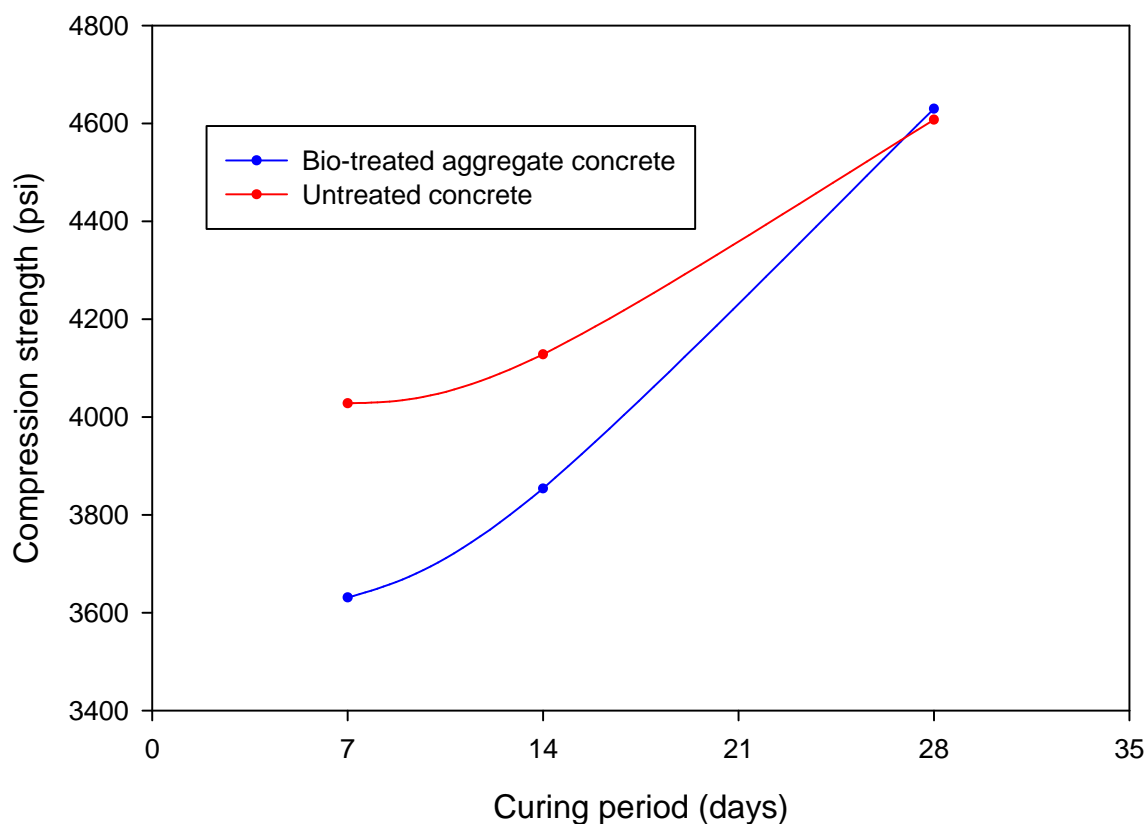


**Figure 52. Compressive strength of concrete**

#### Scanning electron microscopy (SEM) test

Before treating concrete aggregates, we used some ceramic plates to prove whether bio-stabilization is capable to plug in the pores. These ceramic plates have 5 micron pores inside of them. We examined these plates by SEM at 5 different magnification, 100x (Figure 53), 300x (Figure 54), 1000x (Figure 55), 3000x (Figure 56), and 10000x (Figure 57). Figure 16–

20 show the untreated ceramic plates. In Figure 53 there are many black dots filled in some white dots. Figure 54 shows the ceramic plate consists of some small pieces, and these small pieces are not tightly aggregated. Figure 55 presents the surface of ceramic plate is rough, and between these small pieces there are some voids. Figure 56 reflects the voids more clearly. Figure 57 shows these small pieces are angular and there are considerable voids between them.

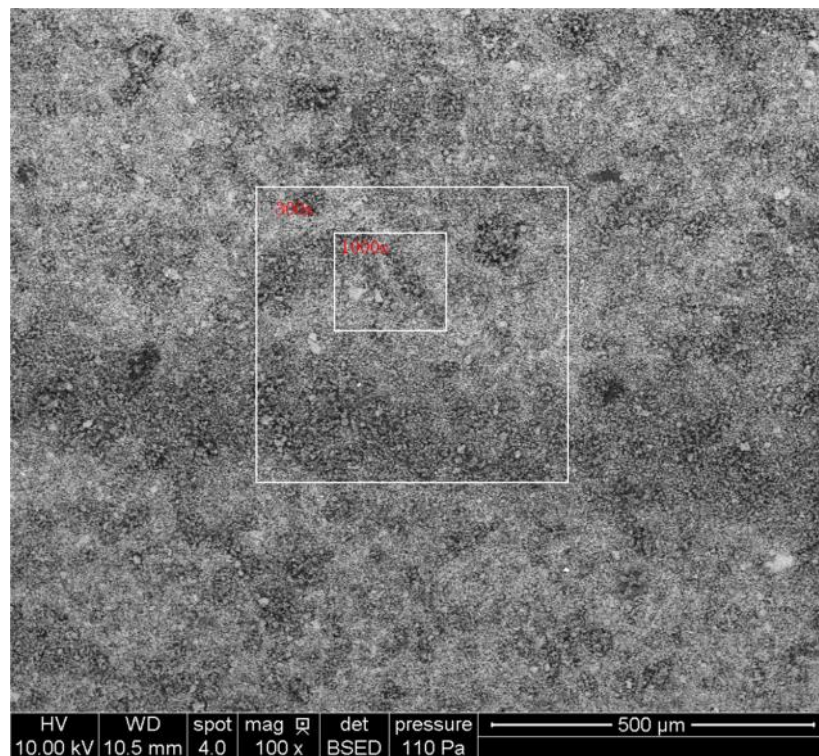


**Figure 53. Ceramic plate without bio-treatment, 100x**

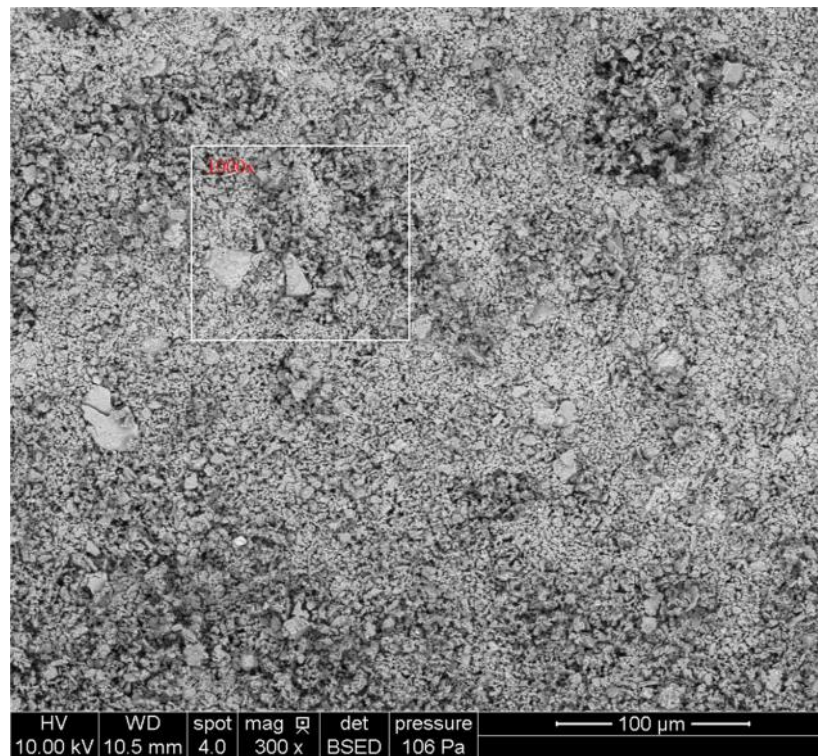


**Figure 54.** Ceramic plate without bio-treatment, 300x

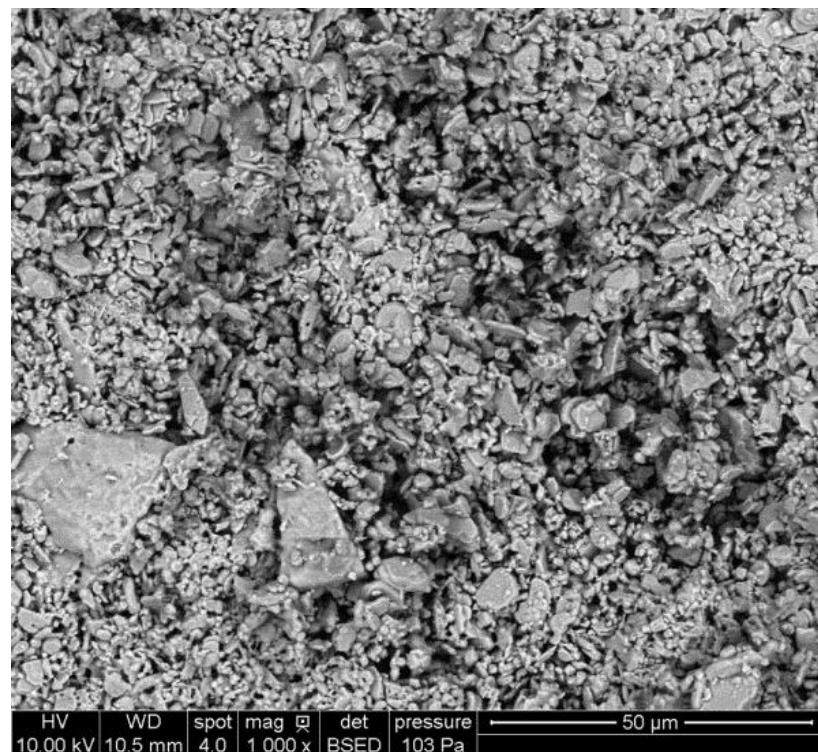


**Figure 55.** Ceramic plate without bio-treatment, 1000x

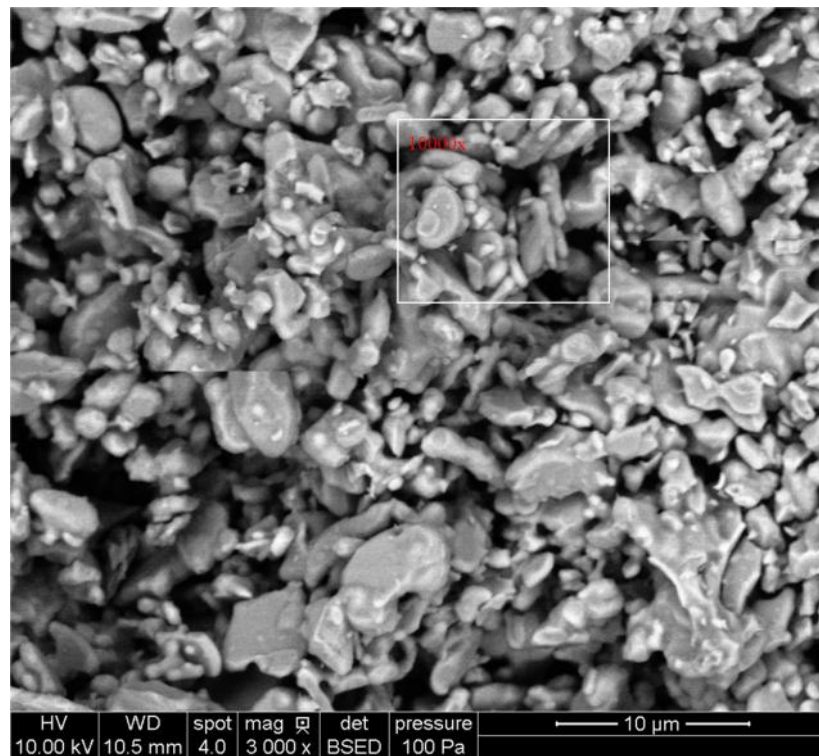


Figure 56. Ceramic plate without bio-treatment, 3000x

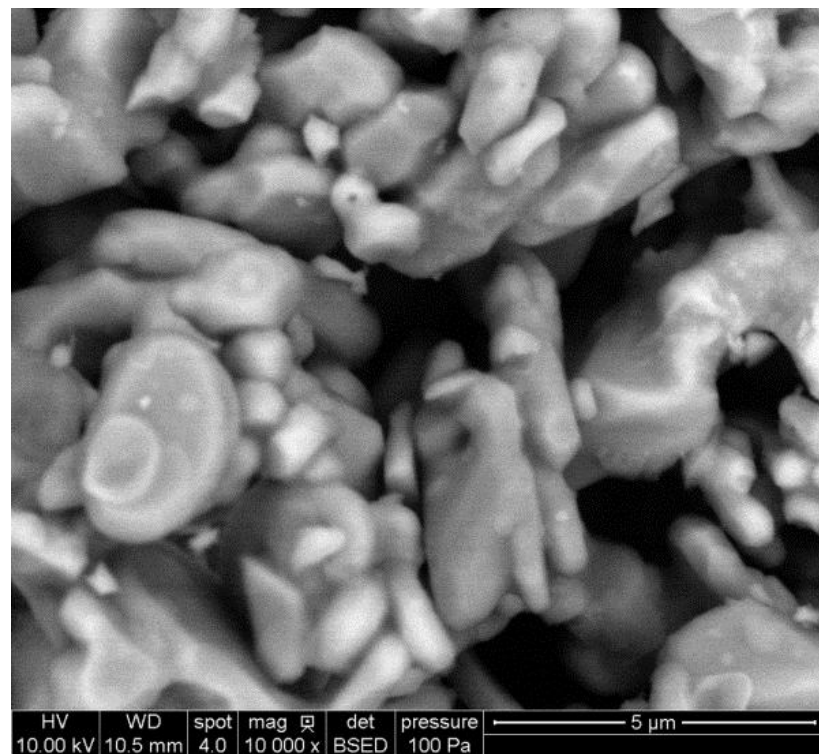
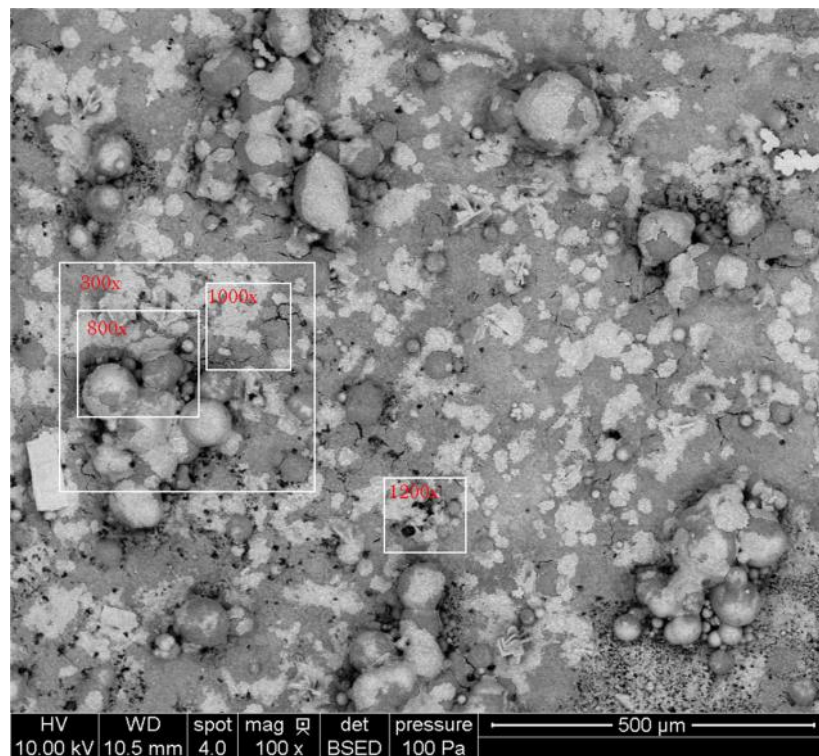
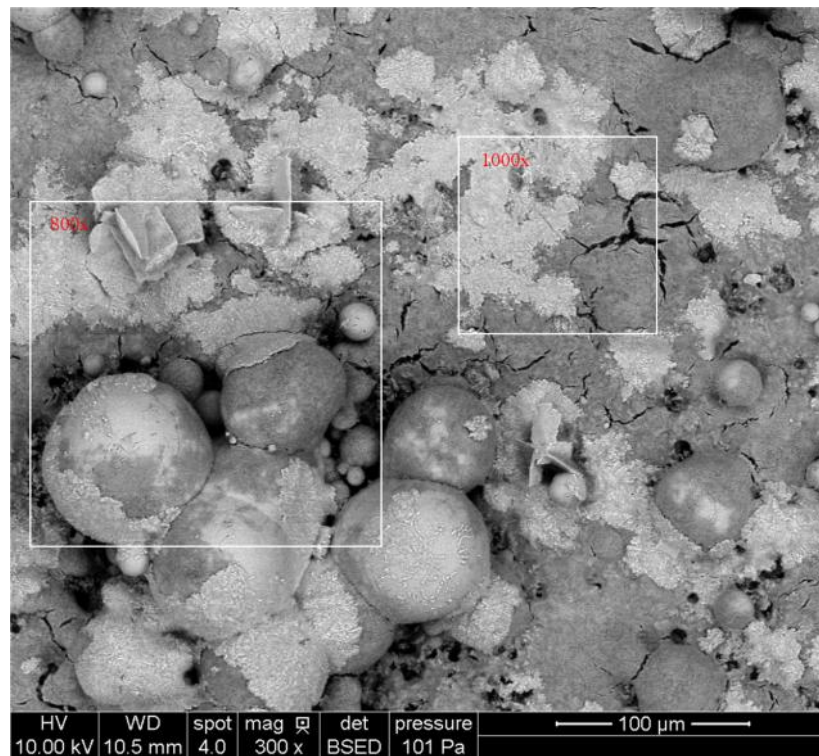


Figure 57. Ceramic plate without bio-treatment, 10000x

We also examined the bio-treated ceramic plates. Figure 58 shows there are some white sheets attached on the surface. Figure 59 and Figure 60 show the voids were plugged (white stuff) and there are some humps. Figure 61 shows the bio-precipitates are flat and at same level as original ceramic pieces. There are some cracks and concaves that occurred in the bio-precipitates (Figure 62). In Figure 63, we can see the bio-precipitates plugged the voids edge by edge.



**Figure 58. Ceramic plate with bio-treatment, 100x**



**Figure 59.** Ceramic plate with bio-treatment, 300x

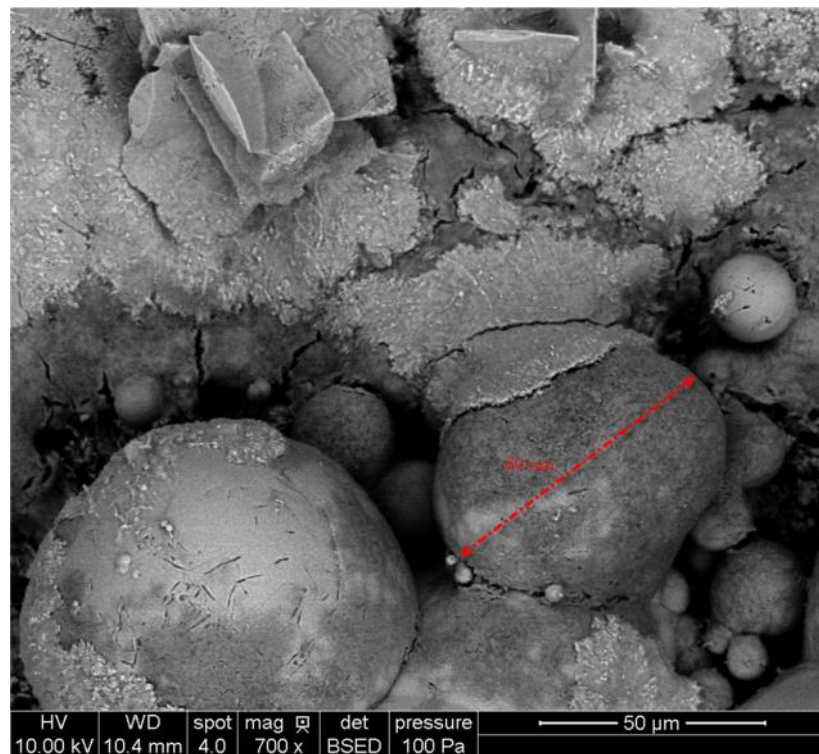


**Figure 60.** Ceramic plate with bio-treatment, 700x

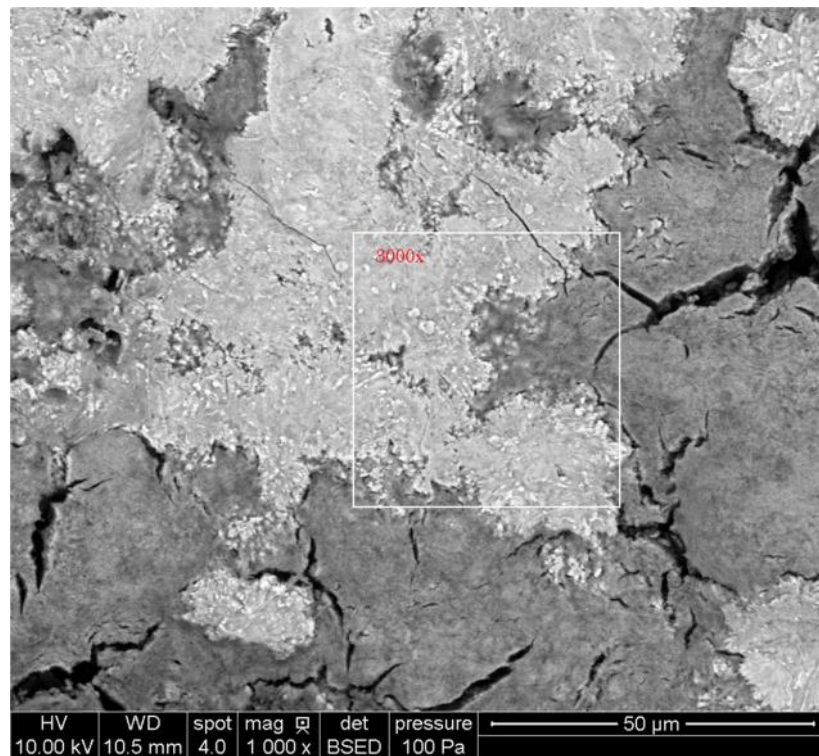


**Figure 61. Ceramic plate with bio-treatment, 1000x**

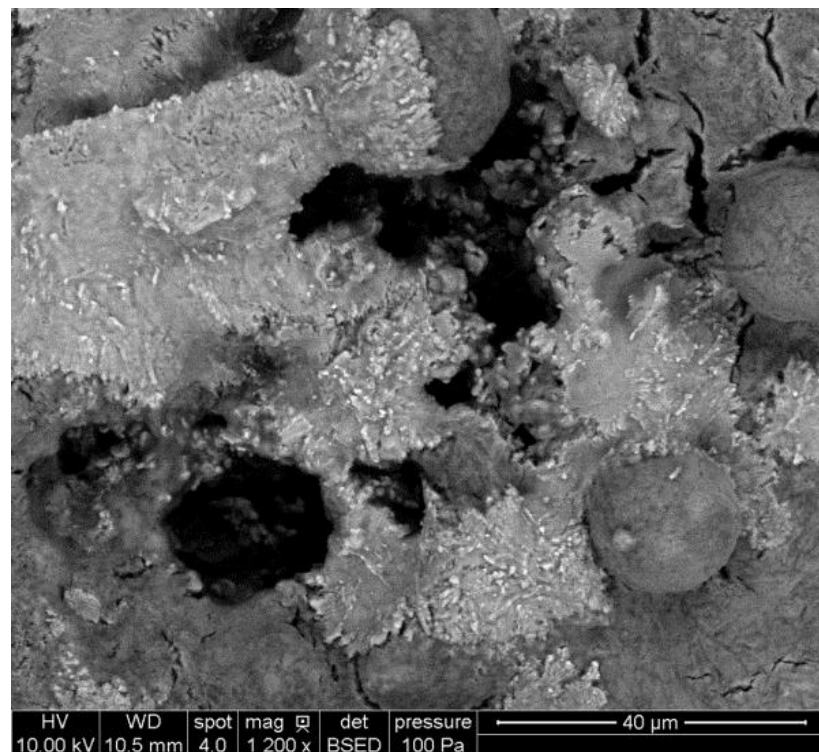


**Figure 62. Ceramic plate with bio-treatment, 1200x**

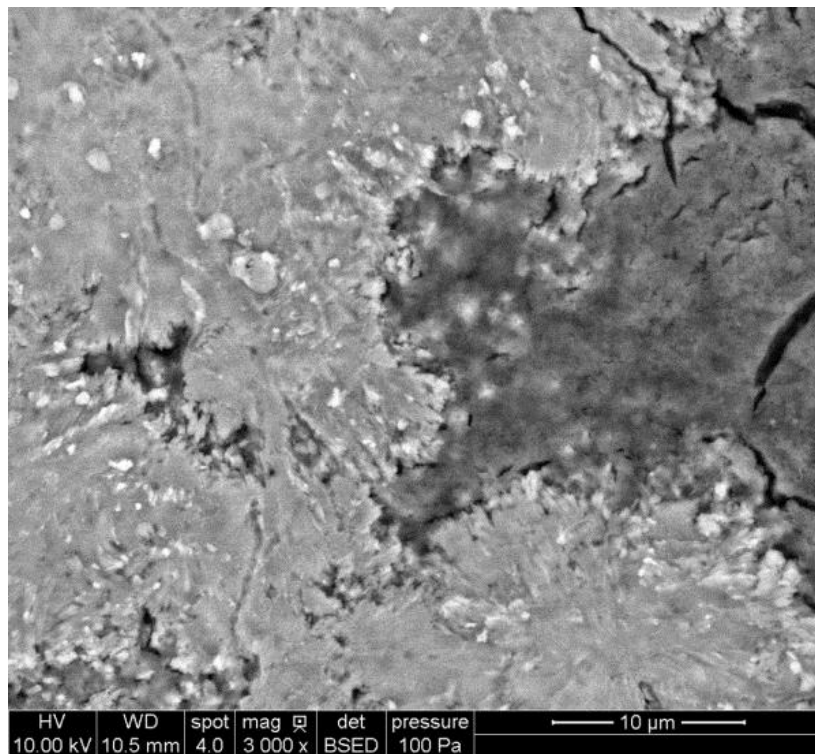


**Figure 63. Ceramic plate with bio-treatment, 3000x**

After verifying the effect of bio-stabilization on surface of material, we also want to know if bio-stabilization is capable to penetrate the material then plug pores inside of materials. So we broke and split the porous ceramic disc into two pieces, and we used SEM to detect the fracture surface. Figure 64 shows the bio-precipitates formed a layer on the surface of ceramic disc. We can see clearly that beneath the layer there were still some pores in Figure 65 and Figure 66. After magnifying the view to 3000 times, the pores still existed in ceramic disc. However, compared to Figure 56, the small particles of disc were not angular in Figure 66. There are some rounded substances around the small pieces. In addition, the area of black background was less than showing of Figure 56. It means the bio-stabilization can penetrate into pores inside of materials. Because the bio-precipitates on the surface plugged the pores, so the following produced bio-precipitates cannot go into the material.

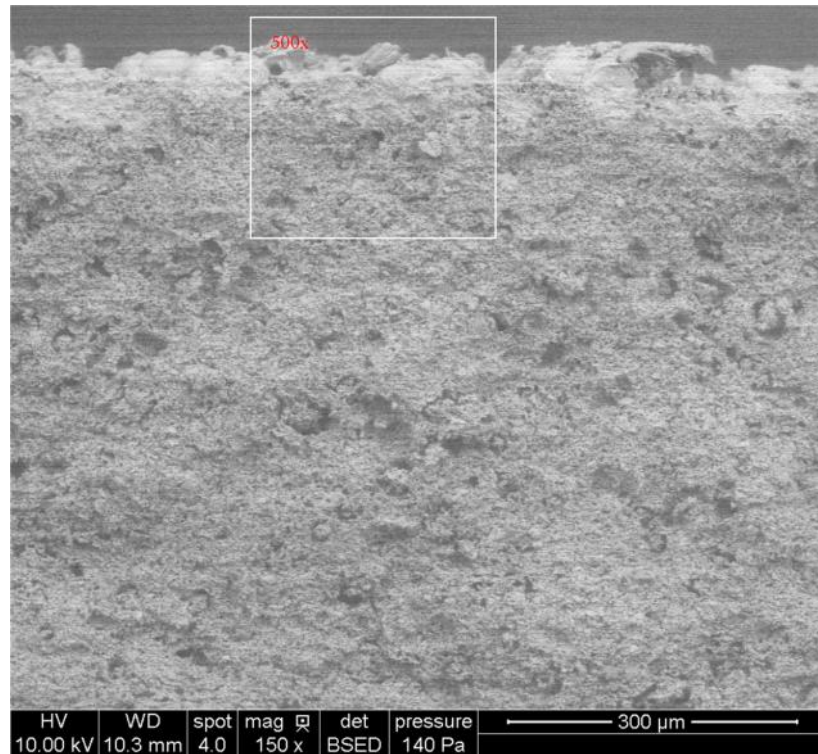


Figure 64. Section of ceramic plate with bio-treatment, 150x

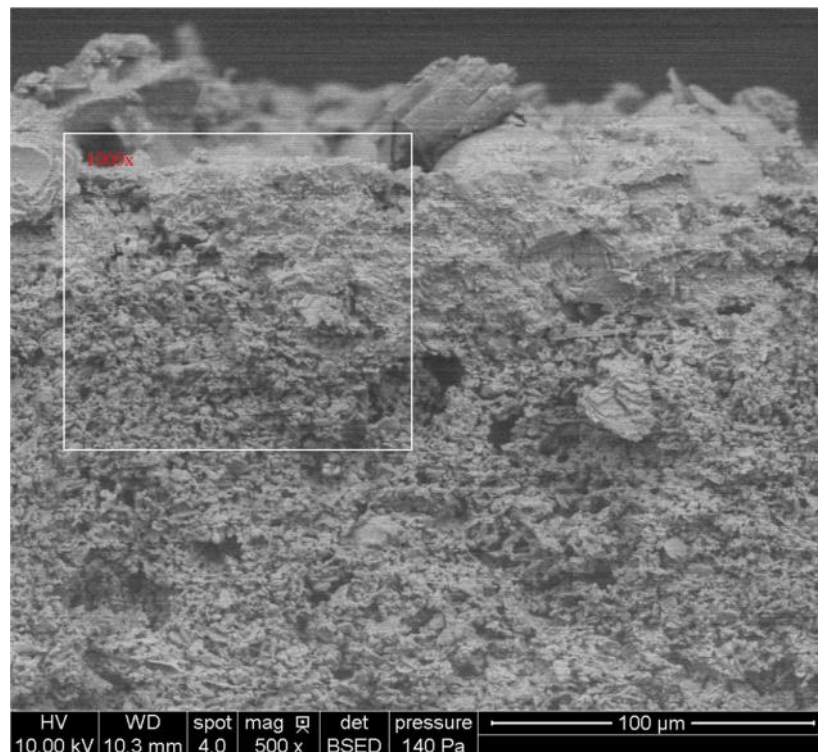
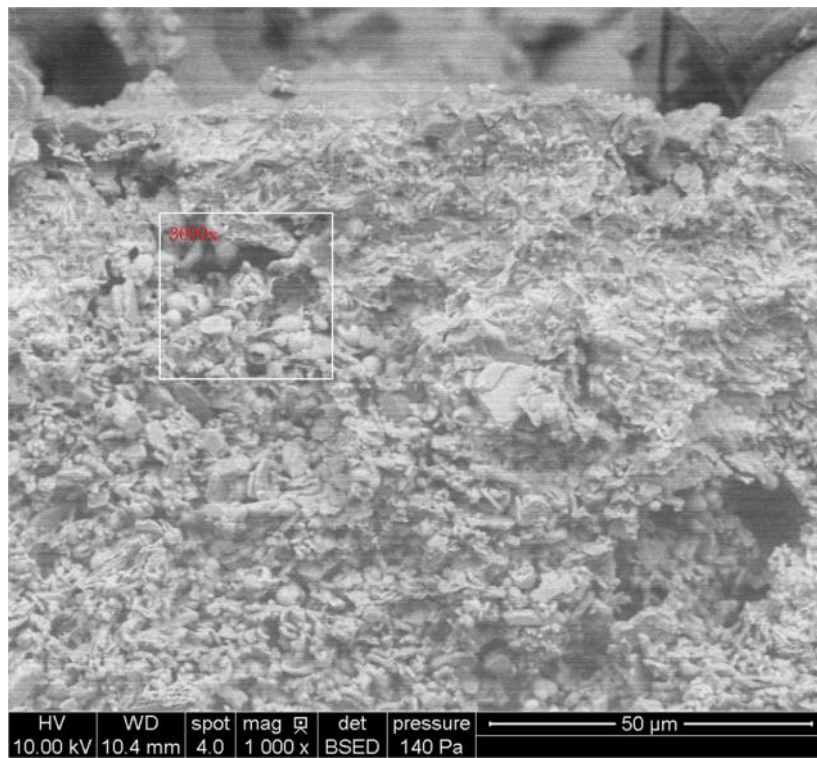
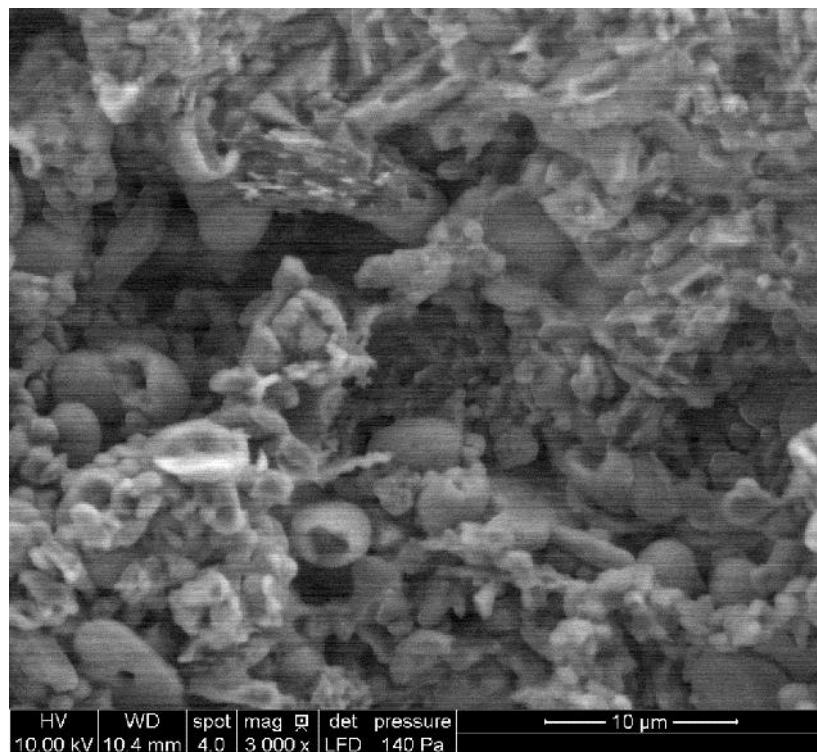


Figure 65. Section of ceramic plate with bio-treatment, 500x



**Figure 66.** Section of ceramic plate with bio-treatment, 1000x



**Figure 67.** Section of ceramic plate with bio-treatment, 3000x

After verifying bio-stabilization is capable to plug inner pores, then we used SEM to examine untreated concrete aggregates from Fort Calhoun, Washington. We examined aggregates at 5 different magnification, 150x (Figure 68), 500x (Figure 69), 1500x (Figure 70), 5000x (Figure 71), 15000x (Figure 72). In Figure 68 the surface of aggregate is not smooth. Figure 69 and Figure 70 show the surface sags and crests, and the aggregate consists of many small particles. Figure 71 shows there are some voids (black shadow) that exist. Figure 72 shows the voids are irregular between particles. These voids are susceptible for freeze and thaw effect. So they will decrease the durability of concrete.

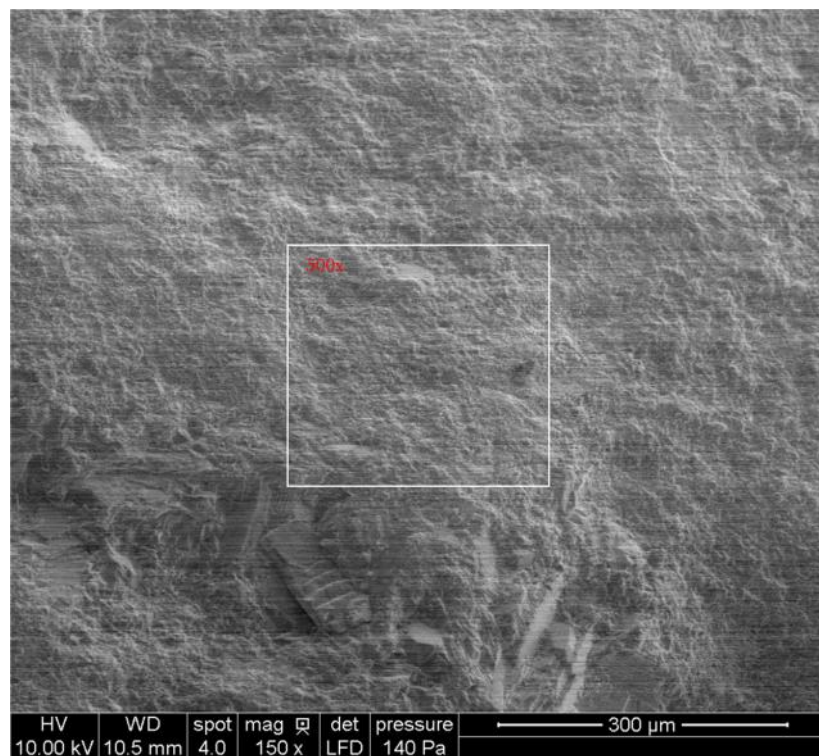


**Figure 68. Fort Calhoun aggregates without bio-treatment, 150x**

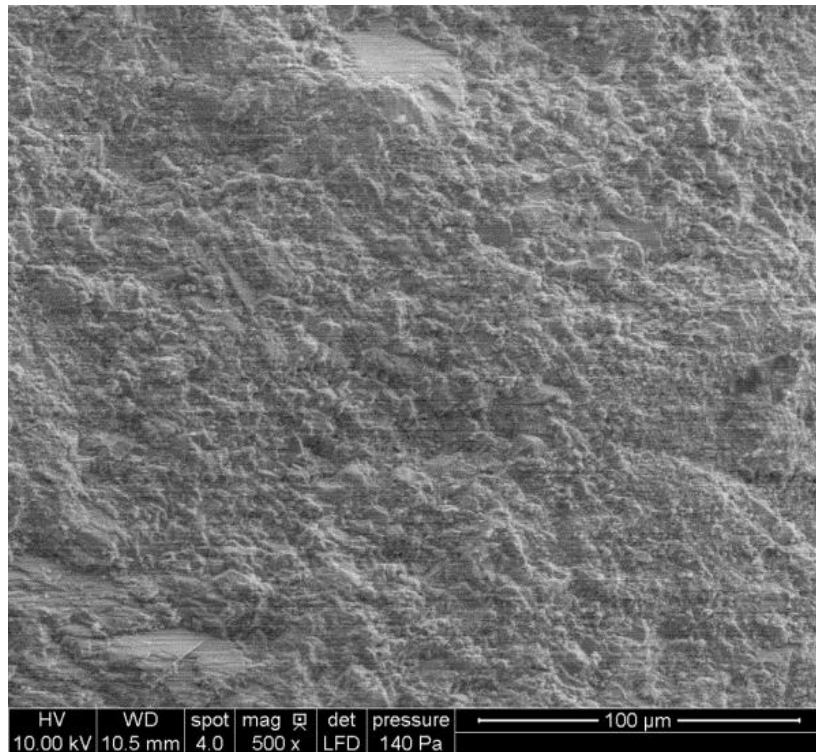


Figure 69. Fort Calhoun aggregates without bio-treatment, 500x

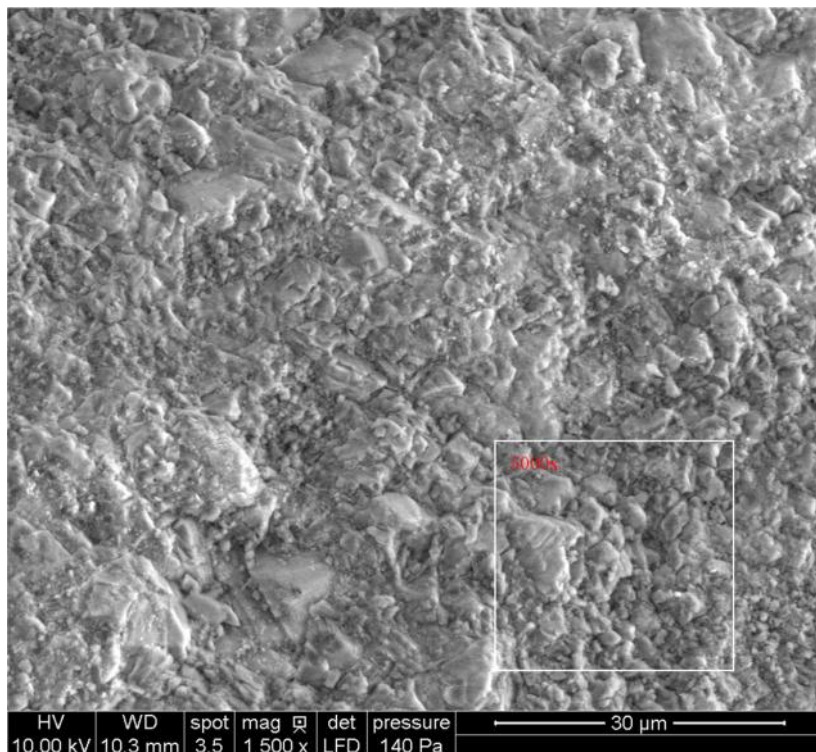
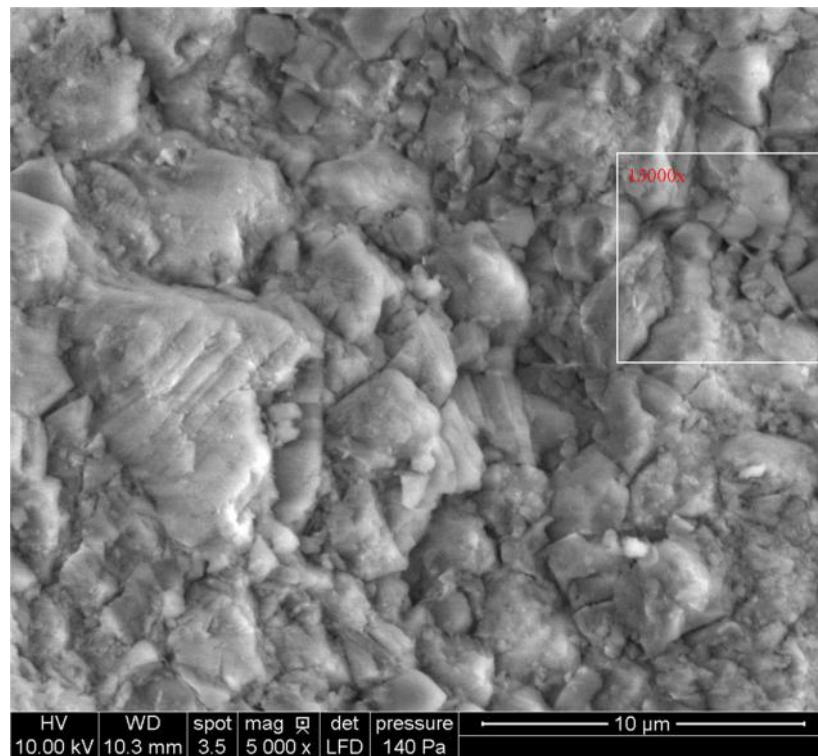
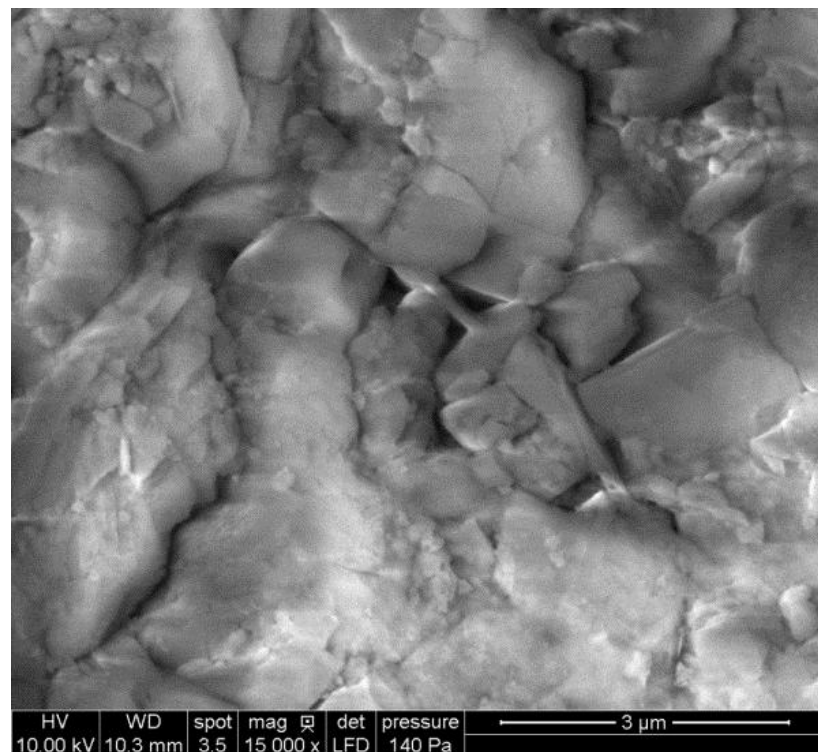


Figure 70. Fort Calhoun aggregates without bio-treatment, 1500x



**Figure 71.** Fort Calhoun aggregates without bio-treatment, 5000x



**Figure 72.** Fort Calhoun aggregates without bio-treatment, 15000x

To verifying whether bio-stabilization is capable to plug in the pores of aggregate, we bio-treated the aggregates and use SEM to examine the differences between raw aggregates and bio-treated aggregates at 5 magnification, 150x (Figure 73), 500x (Figure 74), 1500x (Figure 75), 5000x (Figure 76), 15000x (Figure 77). In Figure 73, we found the surface texture of aggregate are totally different to untreated aggregate. It seems some substances covered the surface. Figure 74 shows there are some irregular humps attached on the surface. Figure 75 shows the surface is not smooth, but the texture is not angular. Figure 76 shows what the bio-precipitates look like. Figure 77 shows the pores of aggregate were plugged, and there are no obvious voids compared to Figure 72. Based on SEM examination, we believe bio-stabilization is capable to plug the pores of aggregates. In order to gather accurate effect and data of bio-stabilization on aggregates, we conducted mercury intrusion porosimetry tests to get the accurate pore volume and pore size distribution of aggregates.

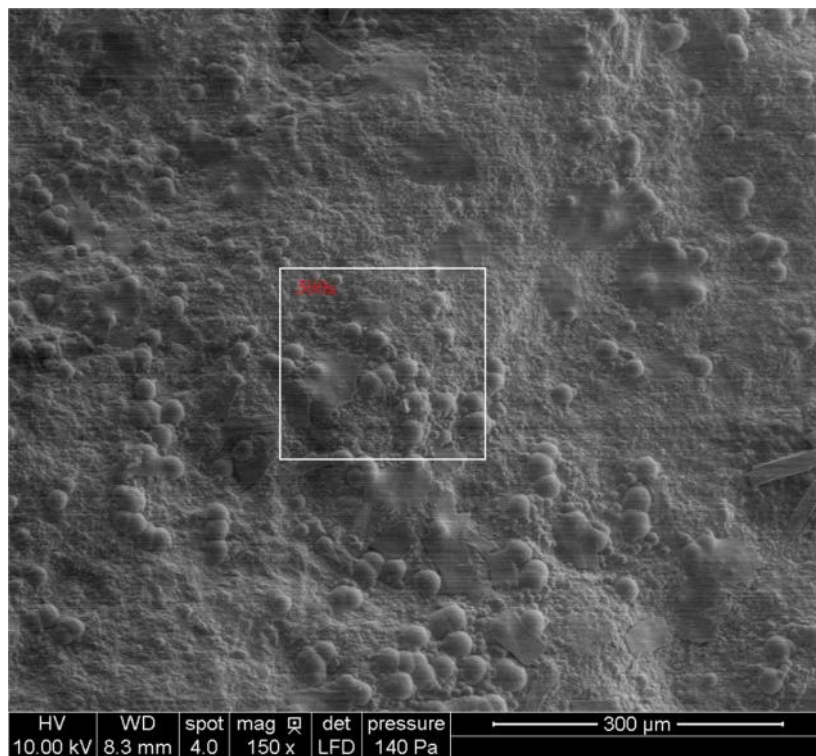


**Figure 73. Fort Calhoun aggregates with 1 cycle bio-treatment, 150x**

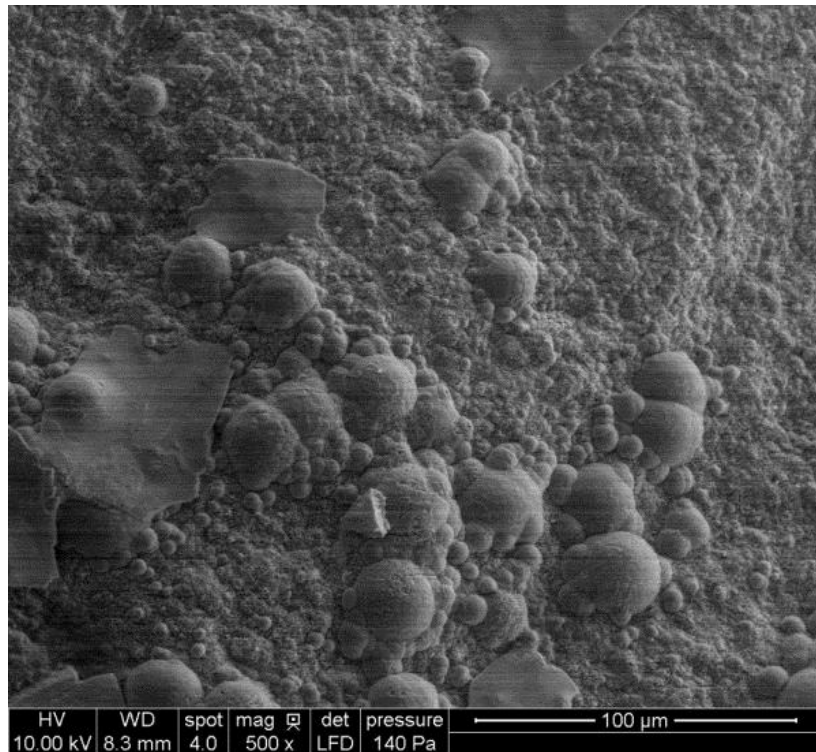


**Figure 74. Fort Calhoun aggregates with 1 cycle bio-treatment, 500x**

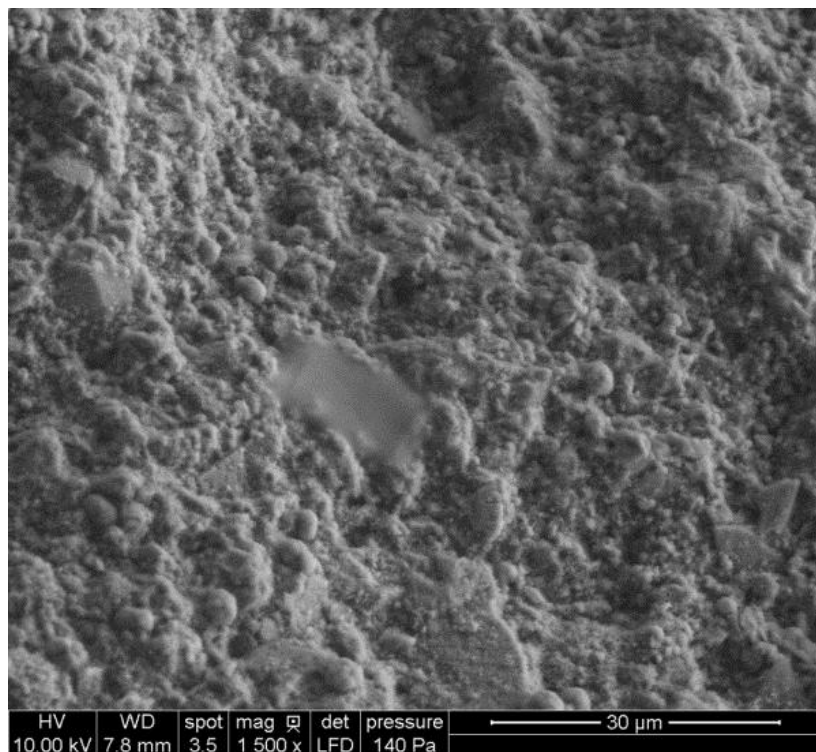


**Figure 75. Fort Calhoun aggregates with 1 cycle bio-treatment, 1500x**

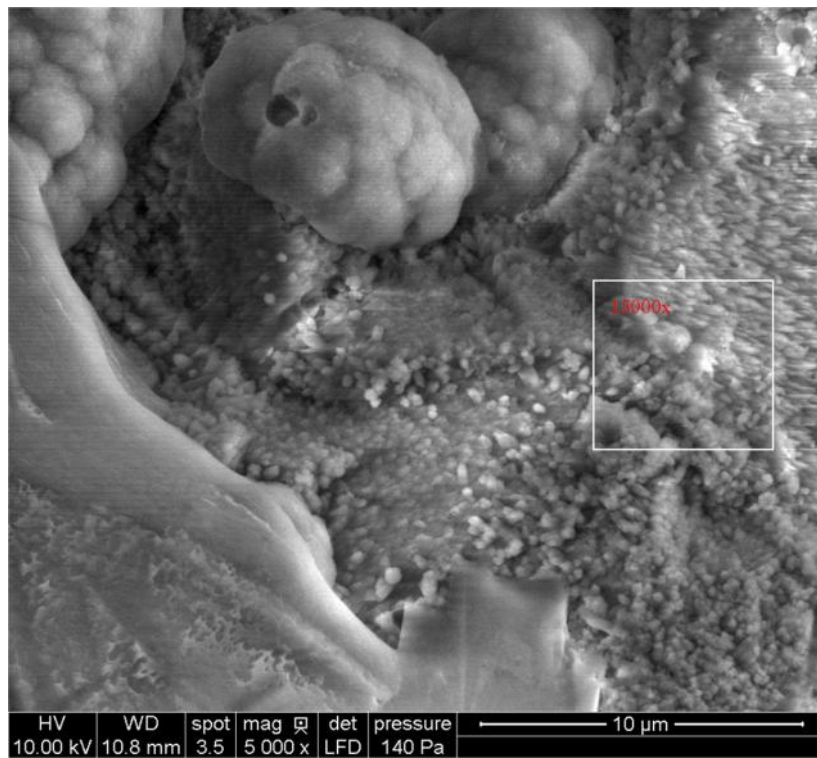


Figure 76. Fort Calhoun aggregates with 1 cycle bio-treatment, 5000x

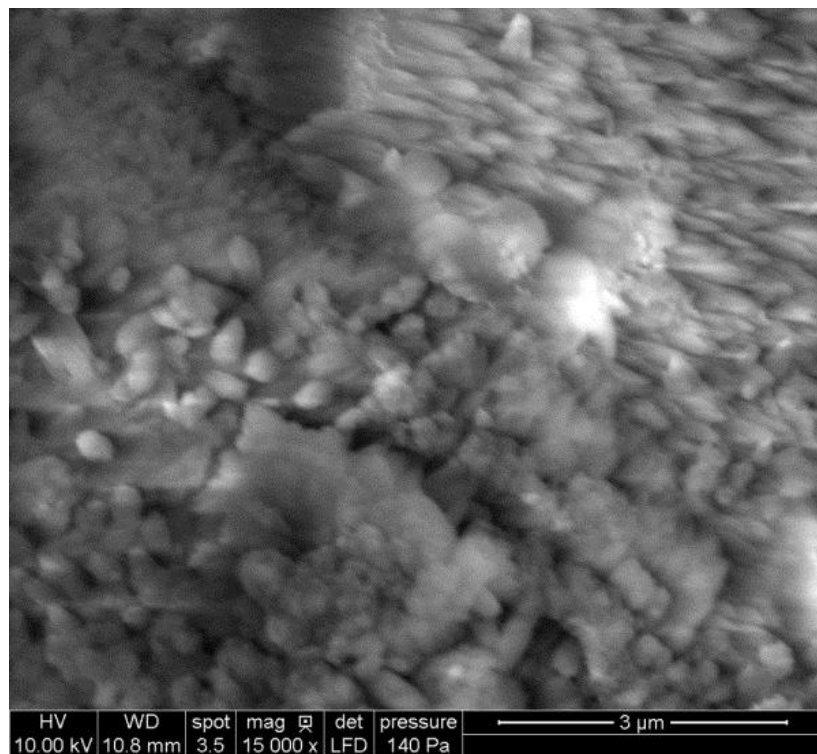
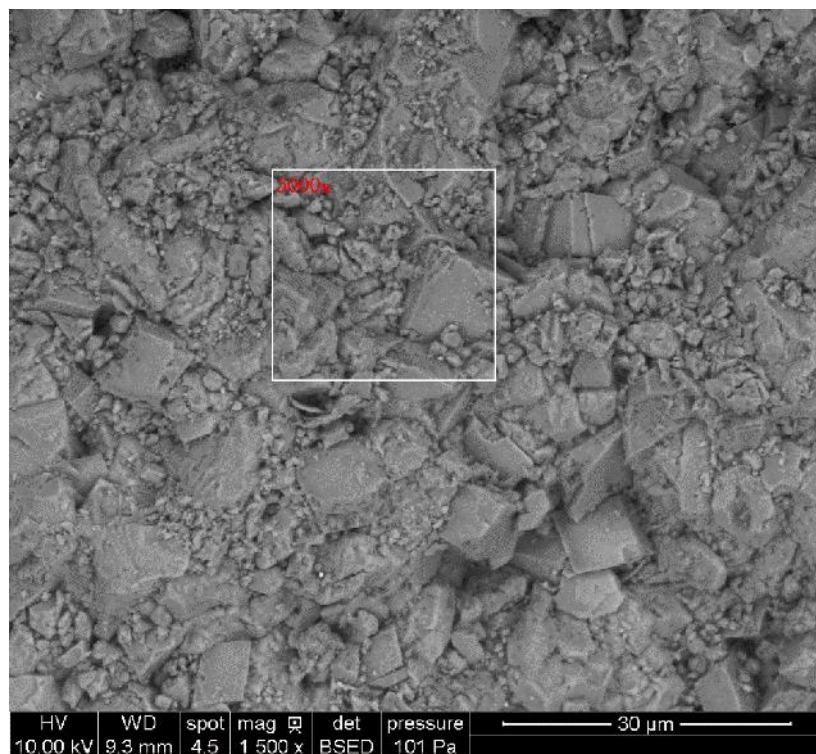
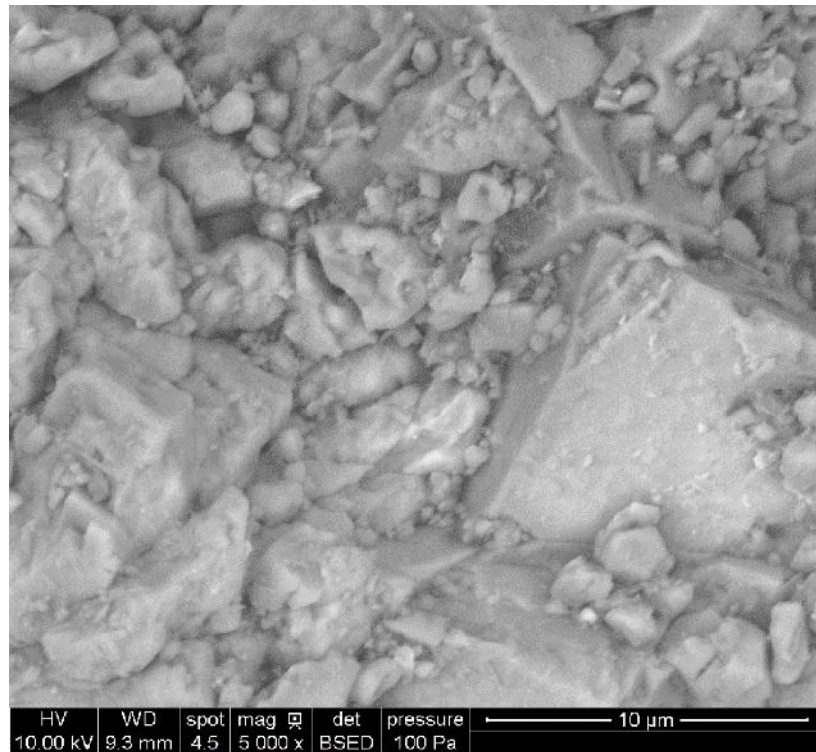


Figure 77. Fort Calhoun aggregates with 1 cycle bio-treatment, 15000x

To examine the bio-stabilization effects on lower quality aggregates and difference of micro structure between different cycle's bio-treated aggregates, SEM was conducted on raw aggregates, 1-treatment aggregates, and 10-treatment aggregates. The tested aggregates were from Winsterset Ledge in southwest of Iowa. Iowa pore index test and mercury intrusion porosimetry indicated that the aggregates are porous and low quality. In the following figures, Figure 78 and Figure 79 showed untreated aggregates, Figure 80 and Figure 81 showed 1-treatment aggregates, Figure 82 and Figure 83 and showed 10-treatment aggregates. The surface texture of untreated aggregates was flaky and rough. In Figure 79, there were many pores presented between flaky particles.



**Figure 78. Winsterset Ledge aggregates without bio-treatment, 1500x**



**Figure 79. Winterset Ledge aggregates without bio-treatment, 5000x**

After 1 cycle bio-treatment, the surface texture was totally different from untreated aggregates. In Figure 80, there were some rounded and smooth stuff attached on aggregate surface. In Figure 81, there were some strip shape matters attached on the sphere. The diameter of these matters is about  $1 \mu\text{m}$ , so it is indicated those are *Bacillus pasteurii*. The elemental analysis of these micro structures is in detail in later section.

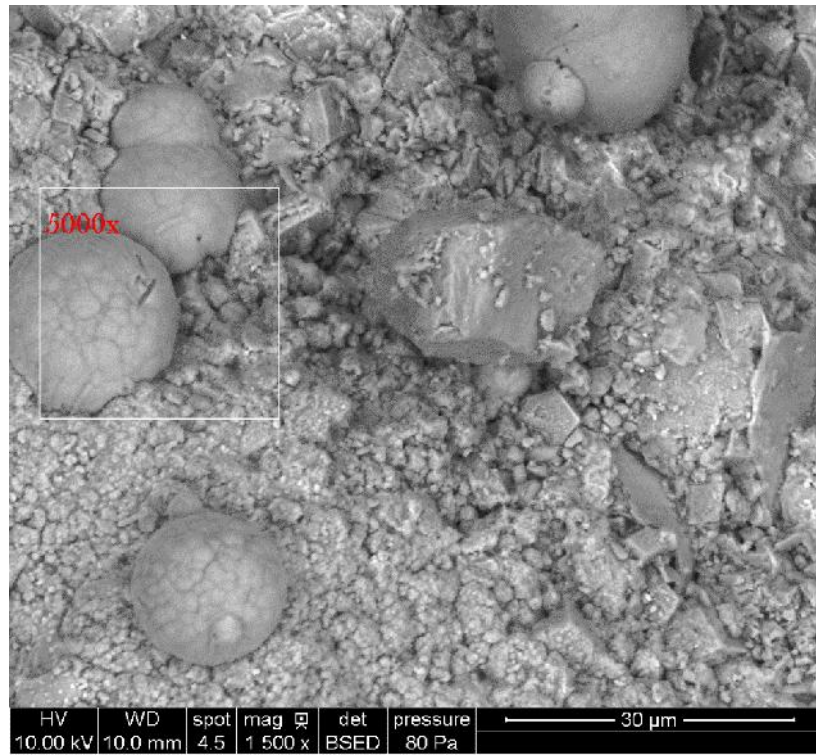


**Figure 80.** Winterset Ledge aggregates with 1 cycle bio-treatment, 1500x

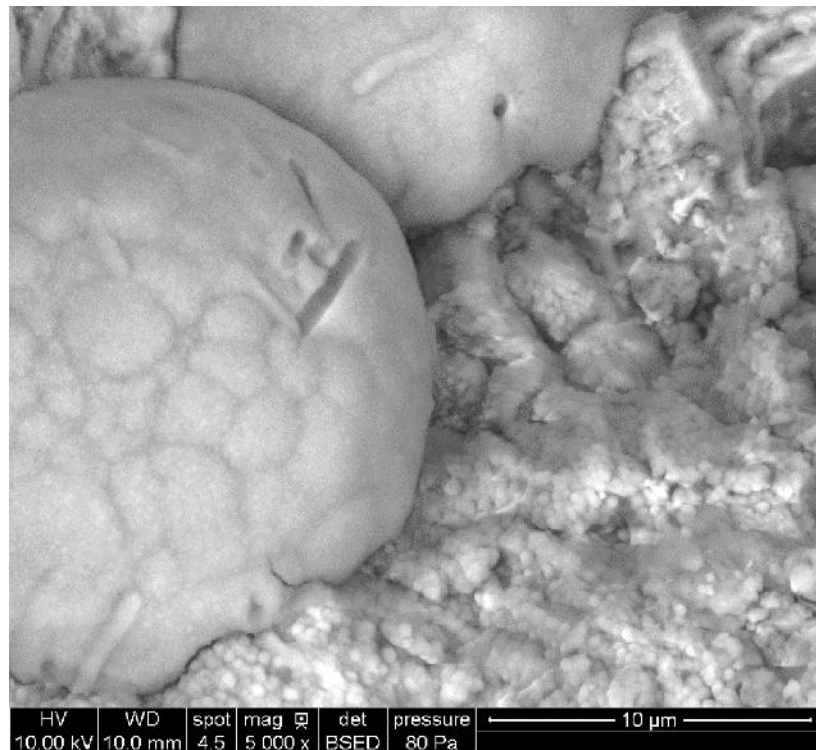


**Figure 81.** Winterset Ledge aggregates with 1 cycle bio-treatment, 5000x

Mercury intrusion porosimetry indicated that after 6 cycles' bio-treatment the pore size was increased. It does not mean bio-treatment is invalid for decreasing pore size of aggregates. In Figure 82 and Figure 83, there were many 1 $\mu\text{m}$  diameter rounded particles present. Between these small particles there were many pores, and the structure is relative loose. This is the reason why 10 cycles' bio-treatment increased the mercury intrusion volume.

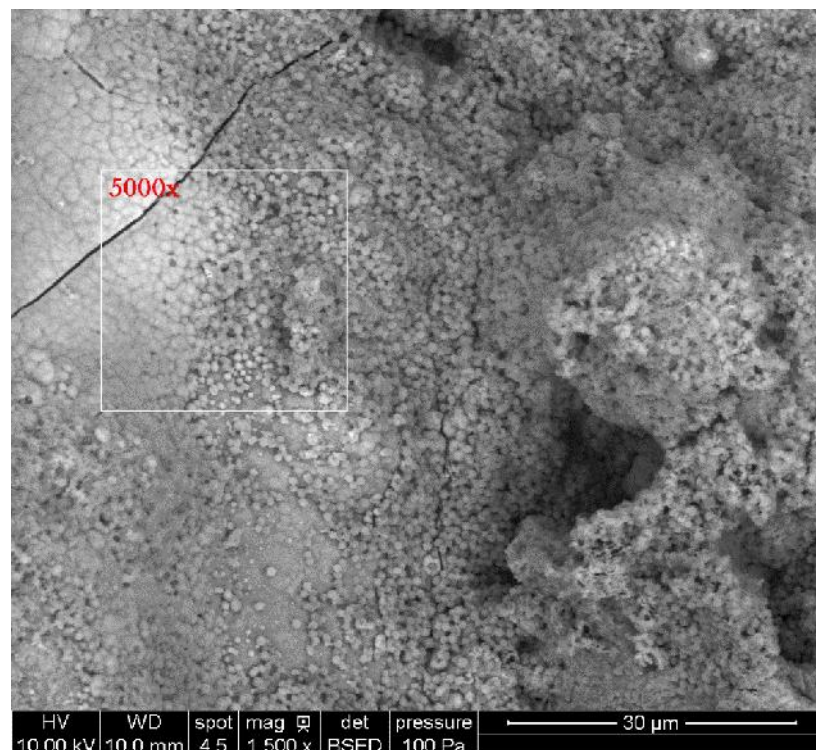


**Figure 82. Winterset Ledge aggregates with 10 cycles' bio-treatment, 1500x**

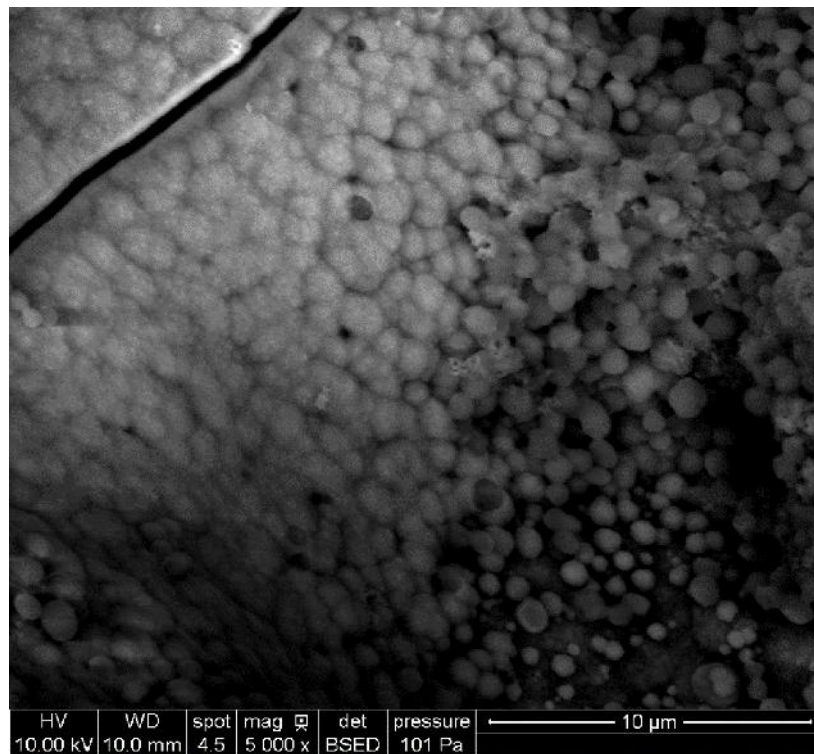


**Figure 83. Winterset Ledge aggregates with 10 cycles' bio-treatment, 5000x**

After analyzing aggregates, bio-treated and untreated hardened concrete were examined by SEM. Figure 84 showed that the aggregate and paste tightly connected together. It seems that there was no stuff between aggregate and paste. Figure 85 showed that there was crack along the contact surface of the aggregate and paste. This could be evidence that the durability of untreated concrete is low.

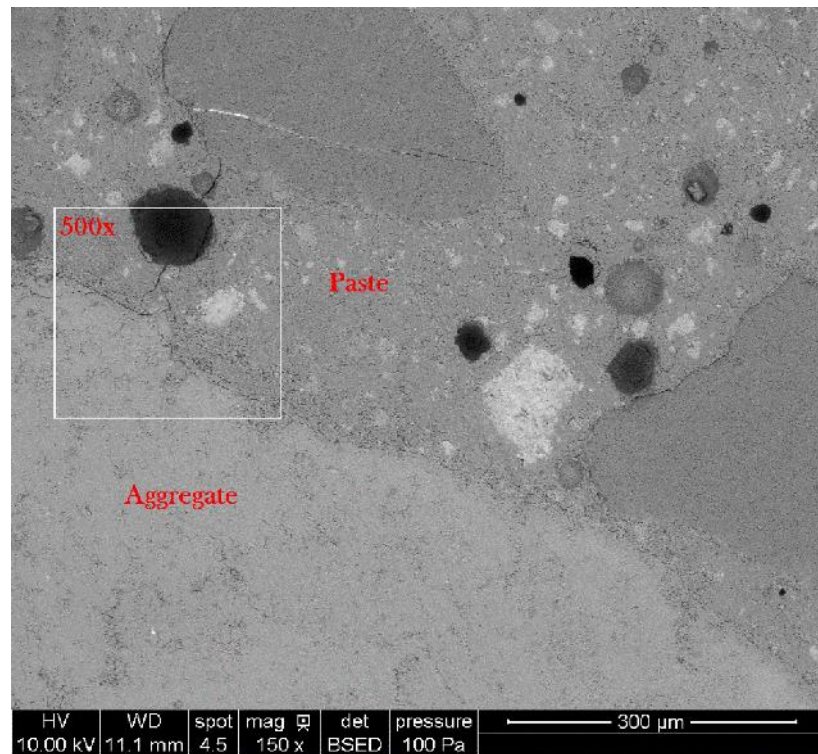


**Figure 84. Hardened concrete without bio-treatment, 150x**

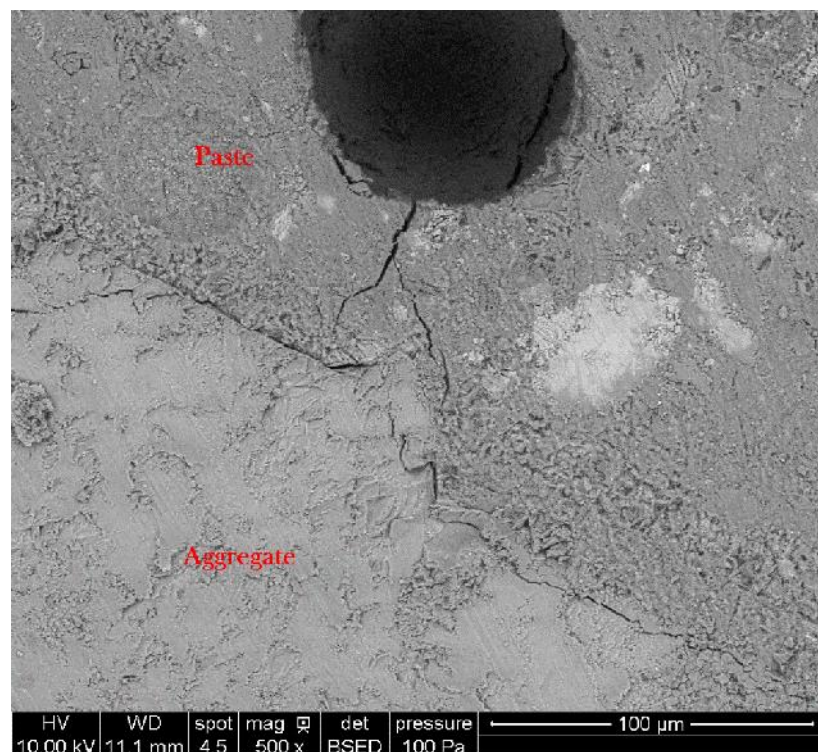


**Figure 85. Hardened concrete without bio-treatment, 500x**

We cut a 2 in. x 2 in. slab from a hardened concrete cylinder. And the concrete slab was polished with 70  $\mu\text{m}$ , 15  $\mu\text{m}$  and 6  $\mu\text{m}$  polishing grid, successively. In the following figures, the aggregate did not contact with paste directly. There was a thin and loose layer about 15  $\mu\text{m}$  in thickness. In Figure 89, between two red lines, it is the bio-treatment zone. The particle shape in this zone is similar with the structure in Figure 80. So this evidence explained that bio-treated concrete is more durable than untreated concrete.

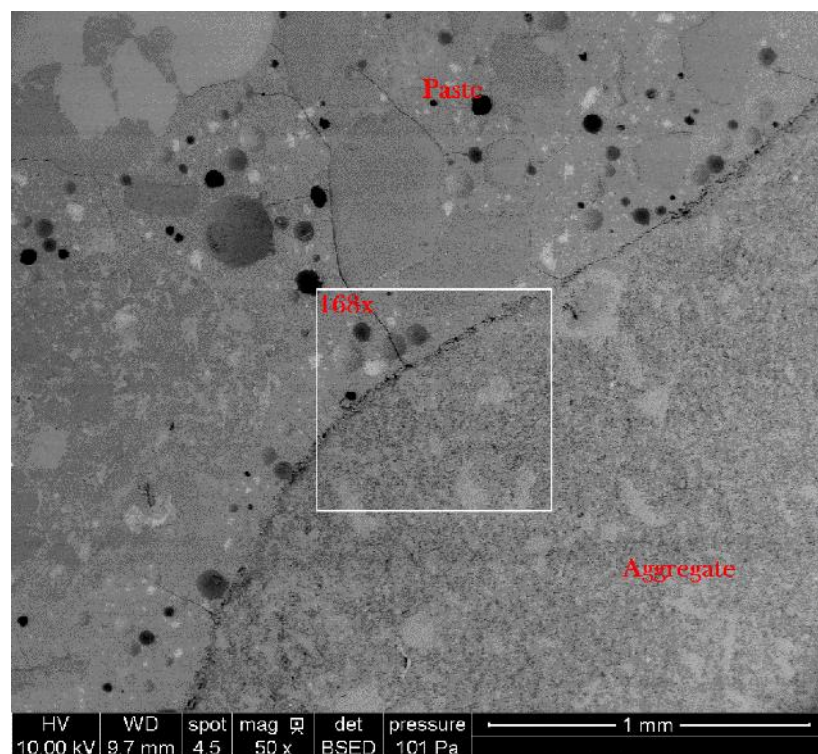


**Figure 86. Hardened concrete with bio-treatment, 50x**

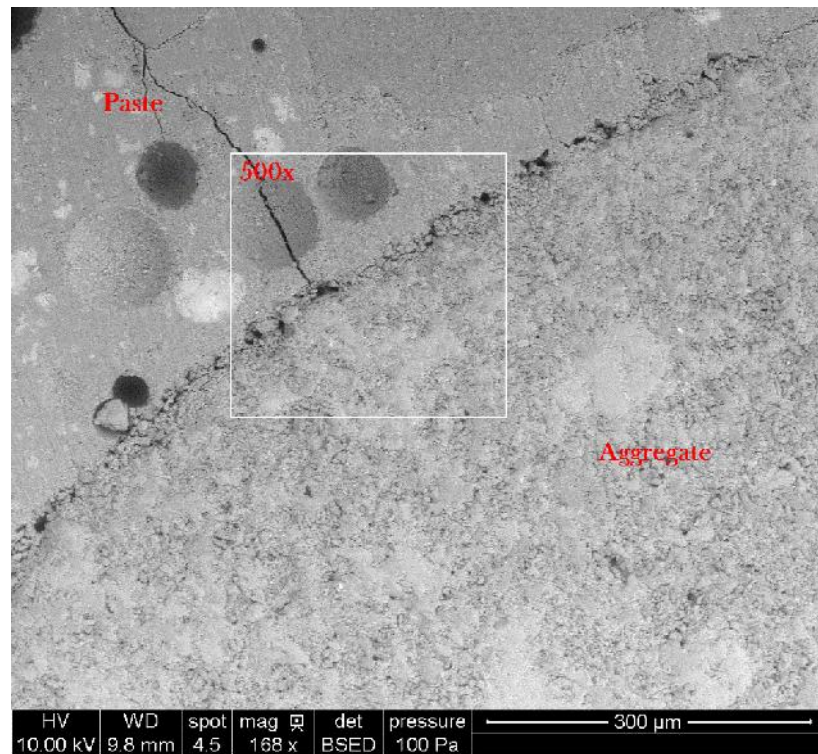


**Figure 87.** Hardened concrete with bio-treatment, 168x

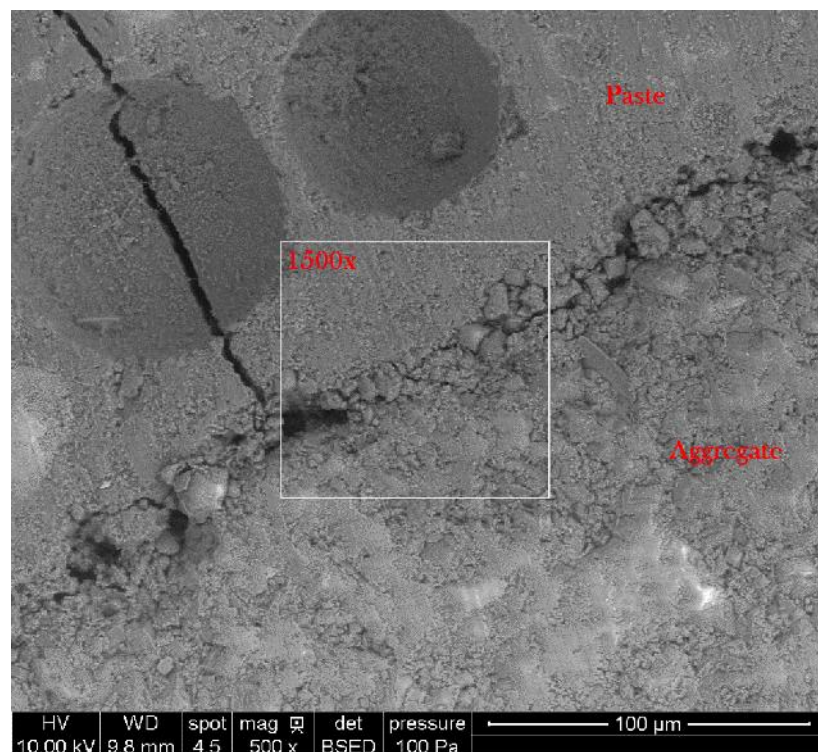


**Figure 88.** Hardened concrete with bio-treatment, 500x

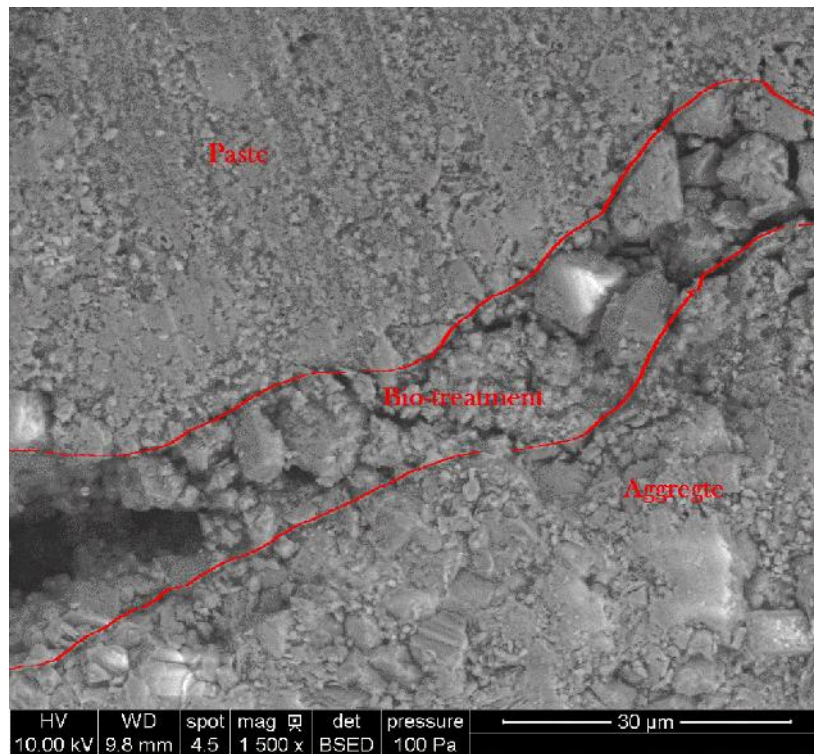


**Figure 89.** Hardened concrete with bio-treatment, 1500x

#### Energy dispersive X-ray spectroscopy (EDS) test

SEM is used to detect the micro structure of aggregate and concrete. EDS analyzes the elemental composition of aggregate and concrete. We conducted EDS for untreated aggregates, 1 cycle bio-treated aggregates, 10 cycles' bio-treated aggregates, untreated concrete, and 5 cycles' bio-treated concrete. C, O, Mg, Al, Si, and Ca are the major constituents of untreated aggregate (Figure 90). The untreated aggregate was high in Ca, C, and O (calcite), and it also contained Mg (with Ca, C, and O) from dolomite, and Al, Si, K, Fe (with O) from feldspar.

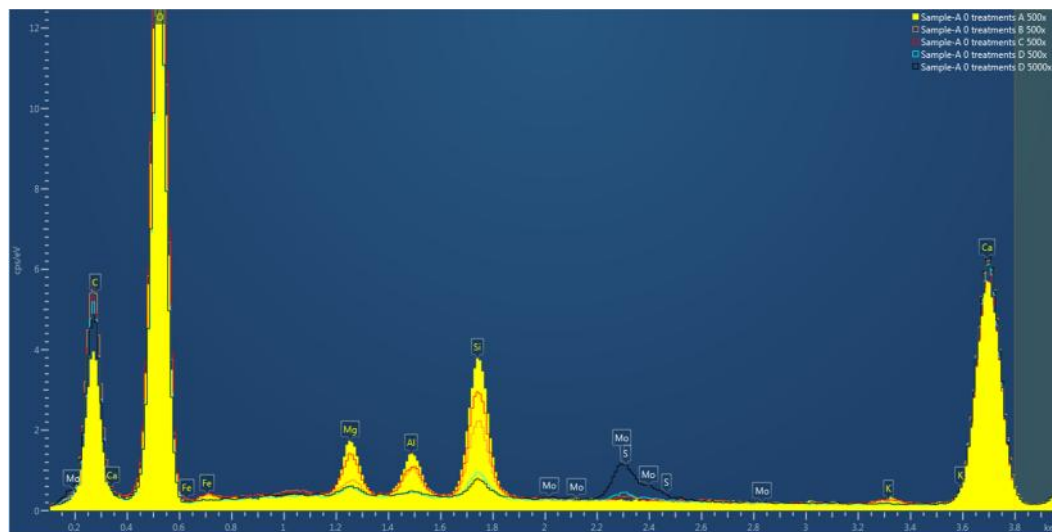


**Figure 90. Elemental composition of untreated aggregates**

In Figure 91, Cl and P were detected. Cl came from  $\text{CaCl}_2$  treatment medium, and P came from yeast that provide energy for microorganism. In addition, the quantities of Ca and C are higher than untreated aggregate. This indicated that more calcite was detected. Calcite is a production of bio-treatment.

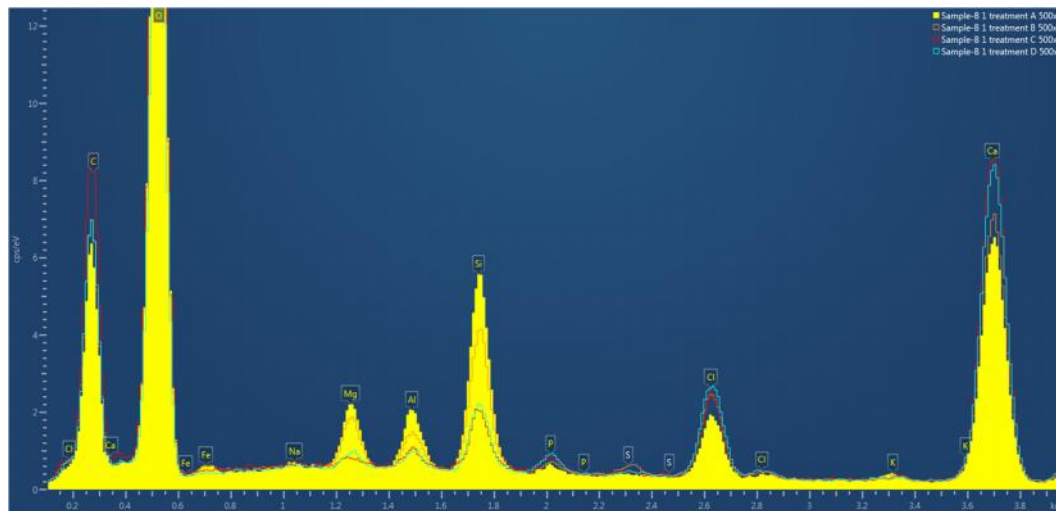


**Figure 91. Elemental composition of 1 cycle bio-treated aggregate**

Elemental mapping was plotted to locate and analyze the bio-treatment. Three positions were examined, round blob, fine texture, and thin rough layer (Figure 92). In Figure 93, Ca and O are widespread, they come both from the original aggregate and the coating. Cl, and P are increased in the round blobs and fine textured area. Al and K are correlated with Si as

part of the underlying feldspar grains. Si is sometimes found by itself in quartz grains. Mg is found with Ca in dolomite grains. So we confirmed that bio-treatment coating consist of calcite correlated with P and Cl.

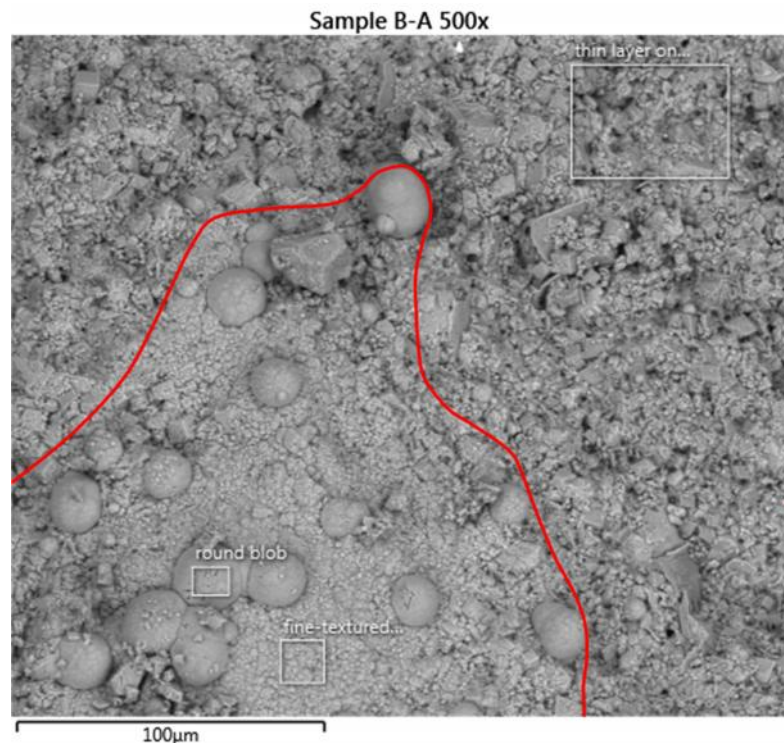


**Figure 92. SEM of 1 cycle bio-treated aggregate**

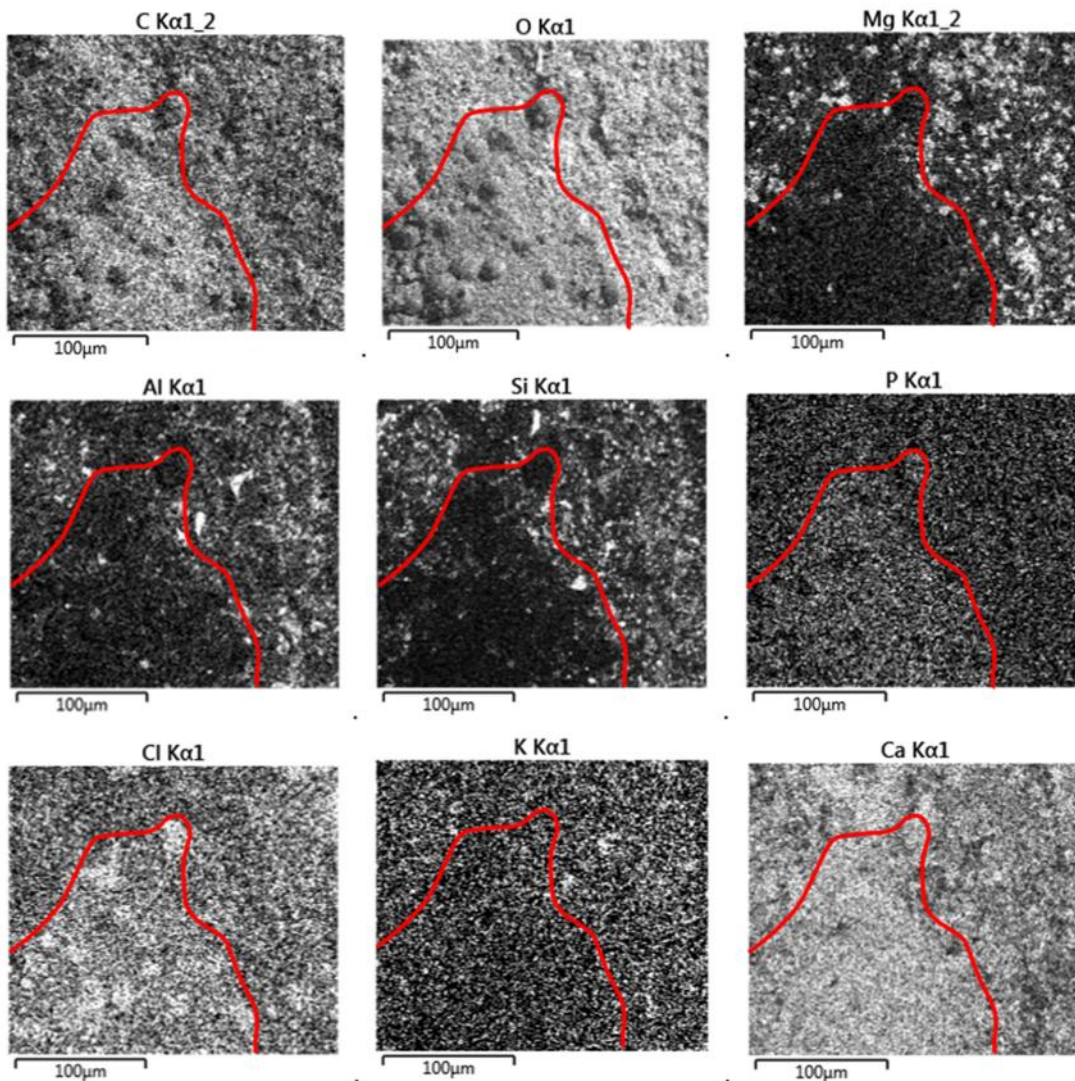


**Figure 93. Elemental mapping of 1 cycle bio-treated aggregate**

Based on the elemental analysis of 10 cycles' bio-treated aggregate, more Cl and P, less Mg and Si were detected (Figure 94). Cl and P come from bio-treatment coating, Mg and Si come from aggregates themselves. So the 10 cycles' bio-treatment has thick coating layer than 1-treatment. The thicker layer obscures more of the underlying aggregate.

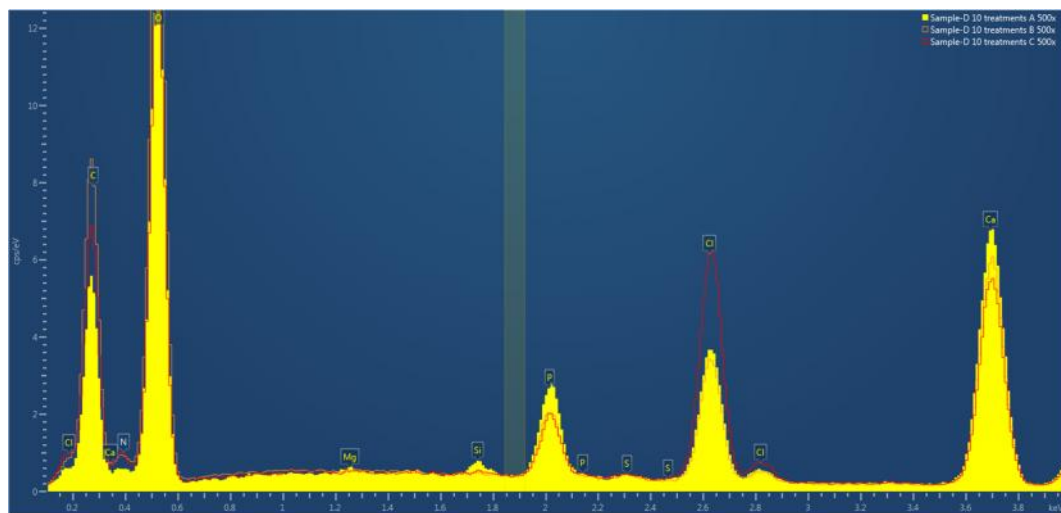


**Figure 94. Elemental composition of 10 cycles bio-treated aggregate**

Theoretically, the elemental constituents of bio-treatment zone contain Cl and P. These two elements were already detected in bio-treatment coating. However, there was no obvious presenting of Cl and P in the bio-treatment coating layer.

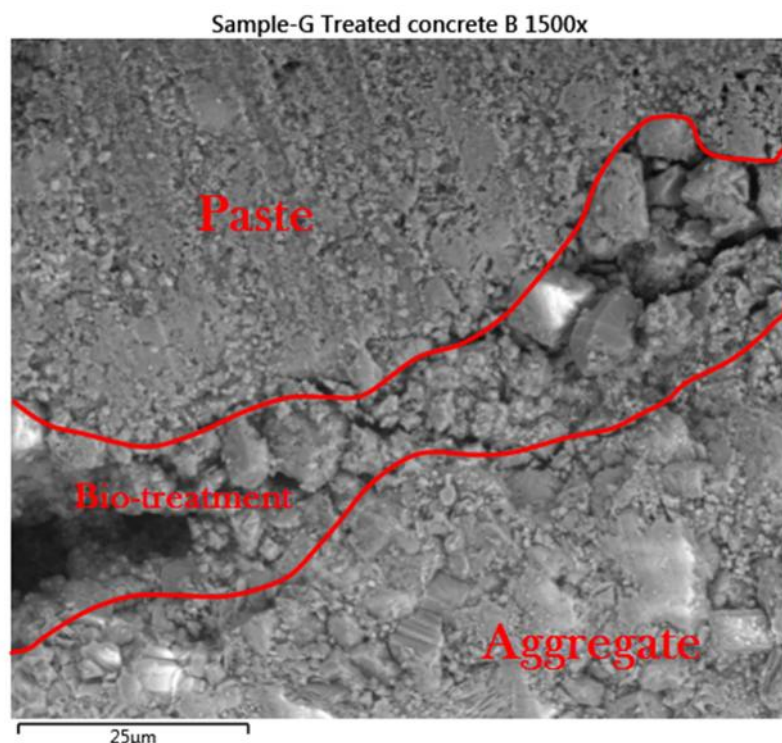


**Figure 95. SEM of 5 cycles' bio-treated concrete**

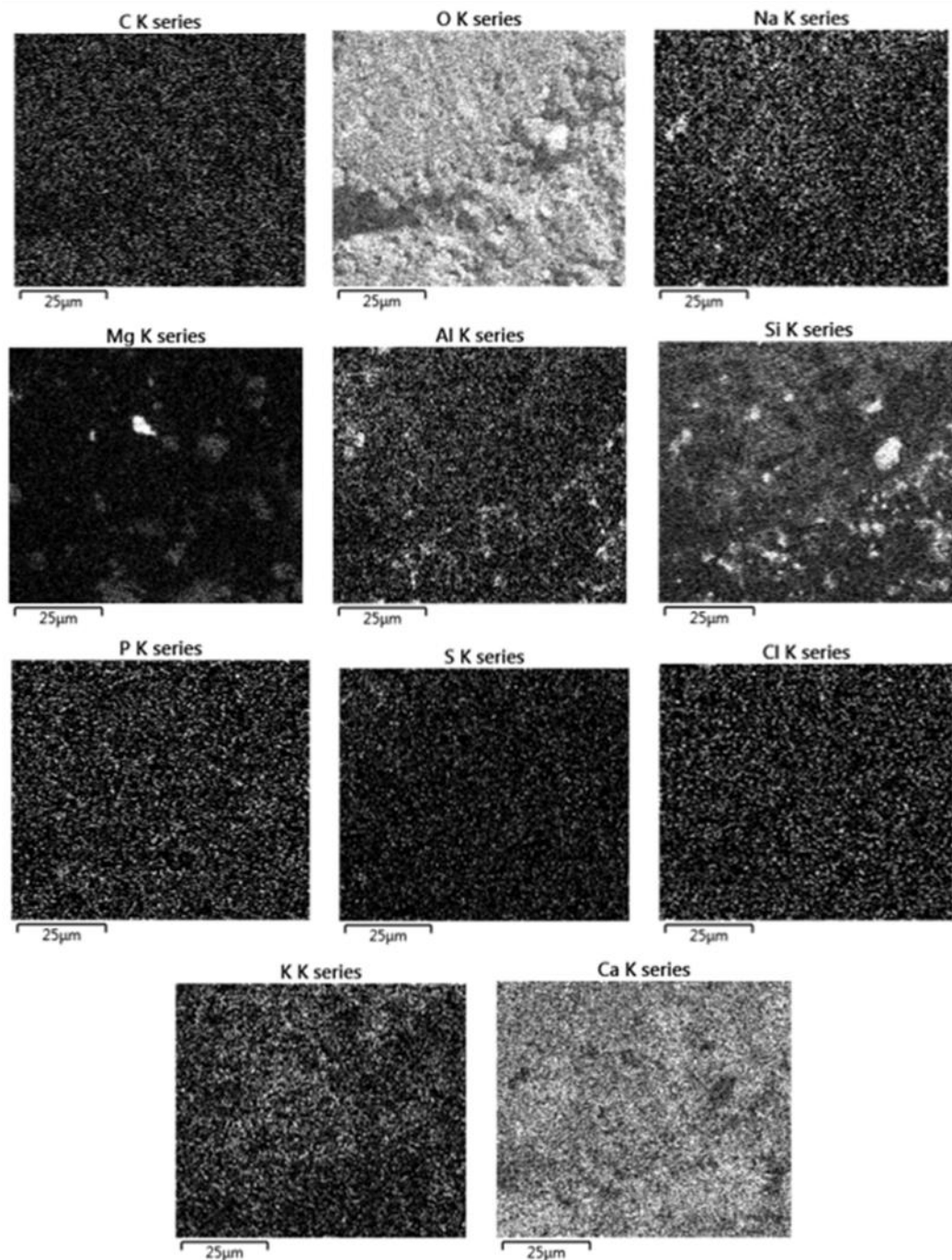


**Figure 96. Elemental mapping of 5 cycles' bio-treated concrete**

To confirm if cement cause the disappearing of Cl and P, we put bio-treated aggregates expose to cement for 20 minutes, and then wash out the cement. After conducting SEM and

EDS, we found the bio-treatment coating still existed, Cl and P were also detected under the bio-treatment coating (Figure 97, Figure 98).

The reason why Cl and P disappear is not clear now. Further elemental analysis needs to be investigated in future research.

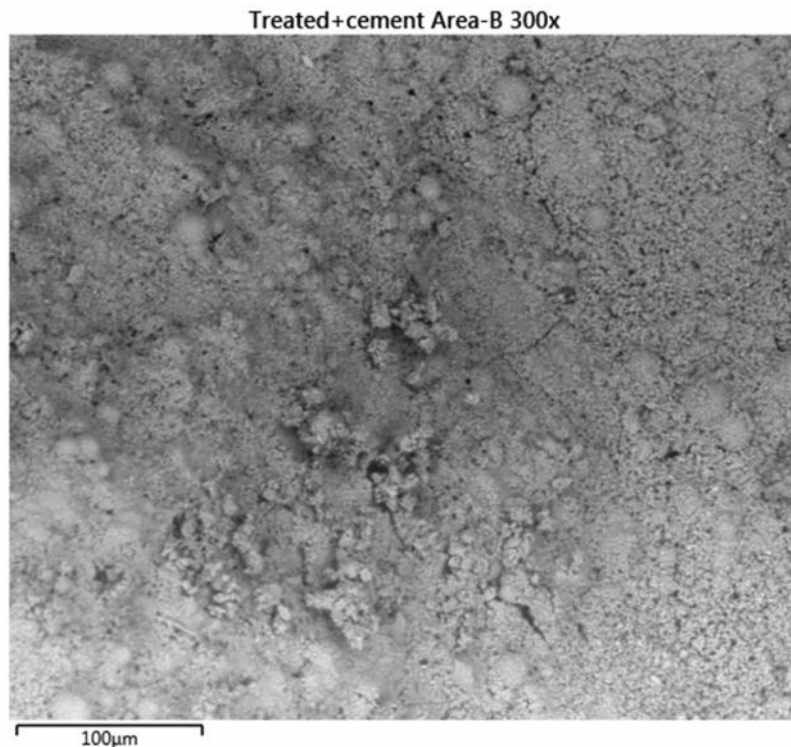


**Figure 97. SEM of bio-treated aggregate exposed to cement**

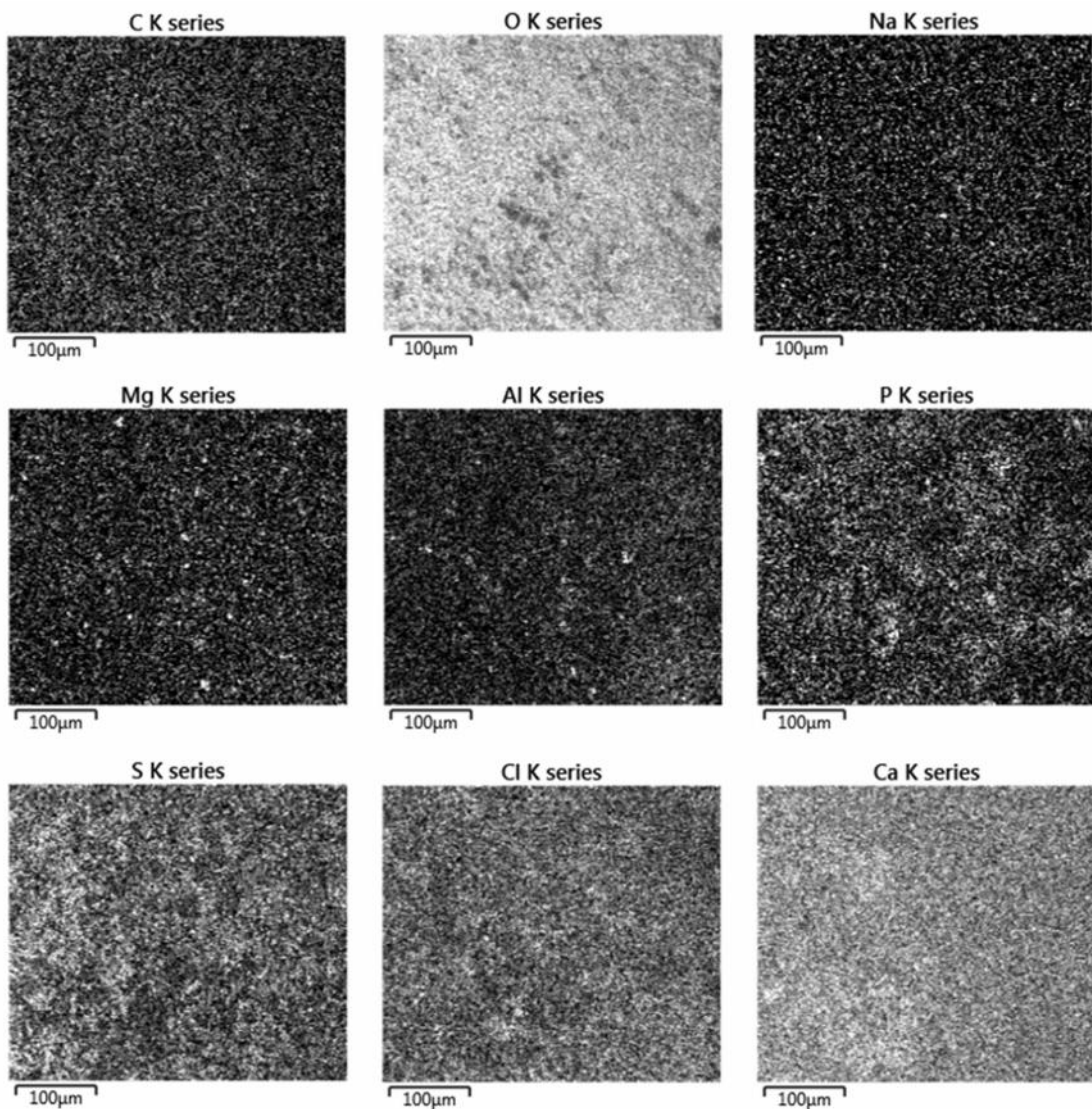


**Figure 98. Elemental mapping of bio-treated aggregate exposed to cement**

## CHAPTER 6. CONCLUSIONS AND RECOMMENDATIONS

This chapter presents an overview of the conclusions based on lab tests of material strength and pore-related analysis of geomaterials subjected to microbially induced precipitation using *Bacillus pasteurii*. Laboratory bio-stabilization experiments were conducted that involved treating silica sands and soils to increase strength and aggregates to improve quality. The results showed that bio-stabilization increased the strength of silica sand and soil samples and decreased the porosity of aggregates. For Portland cement concrete made with treated aggregate, the freeze-thaw performance increased.

### Key findings from soil strength tests

- Bio-treatment increased the average unconfined compressive strength of silica sand samples 3–6 times. Remarkably, after double bio-treatment the unconfined compressive strength of oven-dried silica sand increased from 0 to 38,700 psf.
- NH<sub>4</sub>Cl can replace (NH<sub>4</sub>)<sub>2</sub>SO<sub>4</sub> in preparing liquid medium. The microorganisms grow well and the bio-stabilization effect is slightly better when NH<sub>4</sub>Cl liquid medium is used.
- Bio-stabilization improved the strength of the silica sands more than the natural soils with higher amounts of silt and clay size particles.
- High temperature drying and more treatment cycles will influence the effect of bio-stabilization. The higher the curing temperature the higher the strength. Further, strength increased with increased number of treatment cycles.
- Overall, there seems to be great promise in using bio-treatment in soil improvement, but more research is needed to develop full-scale applications.

### Key findings from aggregate tests

- Bio-stabilization reduces the porosity of concrete pavement coarse aggregate by microbially induced precipitation. After 6-cycles of bio-treatments, mercury intrusion volume decreased from 0.0697 mL/g to 0.0199 mL/g. The pores were seemingly plugged by bio-precipitates. Bio-stabilization also had the effect of decreasing the pore size diameter of the aggregate.

- Less pore volume means less water penetrates in aggregates. Less water penetrates in aggregates reduces harmful freezing and thawing effects. Based on freeze-thaw and dynamic modulus results, bio-stabilization appears to be effective at reducing the impact of freezing and thawing and increases the durability of concrete by about 30%. Although improvement was observed, the magnitude of improvement is less than what is needed to ensure suitable performance in concrete using very porous aggregates.
- The compressive strength of bio-treated aggregate concrete is lower than untreated concrete after 7 days and 14 days wet curing. However after 28 days wet curing, the compressive strength of bio-treated aggregate concrete is similar to untreated concrete.
- Six-cycle bio-treatment is a boundary of workability for reducing coarse aggregate porosity. After six cycles of bio-treatment, the porosity of coarse aggregate increases. SEM suggests that the bio-treatment layer itself is porous in some areas while other areas appear to be solid. Additional research is needed to understand this phenomenon.
- The soundness of aggregate test showed that the bio-treated aggregate has 20% less mass loss compared to the untreated aggregate. These results reinforced the concrete freeze-thaw test results that bio-treatment of aggregate improves durability.

### **Summary of conclusions**

The goal of this study was to test bio-stabilization, a new geomaterials improvement technology. The research objectives were to develop a standard procedure for bacteria cultivation and bio-treatment method for geomaterials, review the literature to compare the effects of chemical and biological soil stabilizers, test the strength and other geotechnical properties of treated materials, and analyze the micro-structures of untreated and bio-treated samples. The bio-stabilization test results verified improvements based on increases in the unconfined compressive strength of soil and increased durability of aggregate and Portland cement concrete.

## **Recommendations**

Experiments involving biological processes for soil strengthening have been largely confined to laboratory studies of the precipitation of carbonate as a cementation material in sands and as a pore filler in aggregates. Much more research is needed to fully evaluate the full potential for soil stabilization and improvement and for their use as a pavement material, the potential uniformity of the treatment zone in field, and the longevity of the treated geomaterials.

### **Recommendations for future research**

- Estimate the number of bio-treatment cycles that can make soil samples achieve maximum strength.
- Replace  $\text{CaCl}_2$  in the treatment medium with other chemicals that will not negatively impact concrete durability.
- Run freezing and thawing tests for more concrete beams to obtain repeatable and more reliable data.
- Understand whether the bio-treatment microorganism is still alive after application in the field and develop in situ living conditions for the microorganism.
- Test other types of microorganisms that may be capable of producing useful precipitates.
- Full-scale field testing is needed and should involve:

Designing, building, and testing a large-scale incubator and distribution system;  
 Preparing a field quantity of *Bacillus pasteurii* in  $\text{NH}_4\text{Cl}$  culture medium;  
 Collecting soil samples before and after bio-treatment; and  
 Applying bio-stabilization medium to an unpaved gravel road.

## WORKS CITED

- AASHTO. (2004). "Standard method of test for soundness of aggregate by freezing and thawing." Annual book of AASHTO standards, AASHTO T103-91, Washington, D.C.
- ASTM. (2009). "Standard test method for density, relative density (specific gravity), and absorption of coarse aggregate." Annual book of ASTM standards, ASTM C127-01, West Conshohocken, PA.
- ASTM. (2009). "Standard test method for resistance to degradation of small-size coarse aggregate by abrasion and impact in the Los Angeles machine." Annual book of ASTM standards, ASTM C131-06, West Conshohocken, PA.
- ASTM. (2009). "Standard test method for air content of freshly mixed concrete by the pressure method." Annual book of ASTM standards, ASTM C231-97, West Conshohocken, PA.
- ASTM. (2009). "Standard test method for microscopical determination of parameters of the air-void system in hardened concrete." Annual book of ASTM standards, ASTM C457-98, West Conshohocken, PA.
- ASTM. (2009). "Standard test method for resistance of concrete to rapid freezing and thawing." Annual book of ASTM standards, ASTM C666, West Conshohocken, PA.
- ASTM. (2009). "Standard test method for density and unit weight of soil in place by the sand-cone method." Annual book of ASTM standards, ASTM D1556-07. West Conshohocken, PA.
- ASTM. (2009). "Standard test method for unconfined compressive strength of cohesive soil." Annual book of ASTM standards, ASTM D2166-06, West Conshohocken, PA.
- ASTM. (2009). "Standard practice for classification of soils for engineering purposes (unified soil classification system)." Annual book of ASTM standards, ASTM D2487-11, West Conshohocken, PA.
- ASTM. (2009). "Standard test method for determination of pore volume and pore volume distribution of soil and rock by mercury intrusion porosimetry." Annual book of ASTM standards, ASTM D4404-10, West Conshohocken, PA.
- America Type Culture Collection (2011) "ATCC medium 1376".  
[<http://www.atcc.org/Attachments/2613.pdf>](http://www.atcc.org/Attachments/2613.pdf) (Accessed: April 10, 2012).
- Bachmeier, K.L., Williams, A.E., Warmington, J.R., and Bang, S.S. (2001). "Urease activity in microbiologically-induced calcite precipitation." *Journal of Biotechnology*. 93, 171–181.
- Bang, S.S., and Ramakrishnan, V. (2001). "Microbiologically-enhanced crack remediation (MECR)," *Proceedings of the International Symposium on Industrial Application of Microbial Genomes*, Daegu, Korea. 3–13.
- Burbank, M.B., Weaver, T.J., Green, T.L., Williams, B.C., and Crawford, R.L. (2011). "Precipitation of calcite by indigenous microorganisms to strengthen liquefiable soils." *Geomicrobiology Journal*, 28:301–312.

- Cayan, D.R., Bromirski, P.D., Hayhoe, K., Tyree, M., Dettinger, M.D., Flick, R.E. (2008). “Climate change projections of sea level extremes along the California coast.” *Climate Change* 87, S57–S73.
- Chu, J., Ivanov, V., He, J., Naeimi, M., Li, B. and Stabnikov, V. (2011). “Development of Microbial Geotechnology in Singapore”. *Geo-Frontiers* 2011. 4070–4078.
- DeJong, J.T., Fritzges, M.B. and Nusslein, K. (2006). “Microbially induced cementation to control sand response to undrained shear”. *Journal of Geotechnical and Geoenvironmental Engineering*, 132(11): 1381-1392.
- DeJong, J.T., Mortensen, B.M., Martinez, B.C., and Nelson, D.C. (2010). “Bio-mediated soil improvement”. *Ecological Engineering*, 36(2), 197–210.
- Goldstein, G.I., Newbury, D.E., Echlin, P., Joy, D. C., Fiori, C., and Lifshin, E. (1981). Scanning electron microscopy and x-ray microanalysis. New York: Plenum Press.
- Gray, D.H. and Sotir, R.B. (1996). “Soil Bioengineering Plant Species.” Biotechnical and Soil Bioengineering Slope Stabilization, Appendix 1, pages 360-362.
- Iowa Department of Transportation. (2000). “Method test for determining the pore index of aggregates.” Test Method No. Iowa 219-C.
- Iowa Department of Transportation. (2010). “Source approvals for aggregates.” Level I & II aggregate reference manual, 2011–2012.
- Ivanov, V., and Chu, J. (2008). “Application of microorganisms to geotechnical engineering for bioclogging and biocementation of soil in situ”. *Reviews in Environmental Science and Biotechnology*, 7:139–153.
- Jonkers, H.M., and van Loosdrecht, M.C.M. (2010). “Editorial BioGeoCivil Engineering”. *Ecological Engineering* 36, 97-98.
- Karol, R.H. (2003). *Chemical grouting and soil stabilization*. Marcel Dekker. New York.
- Li, S. (2011). “Bio-treatment for subgrade stabilization”. Strategic Highway Research Program SHRP2 R02 Technology #45.
- Meyer, F.D., Bang, S., Min, S., Stetler, L.D. and Bang, S.S. (2011). “Microbiologically-induced soil stabilization: application of sporasarcina pasteurii for fugitive dust control”. *Geo-Frontiers* 2011. pp. 4002-4011.
- Mitchell, J.K., Hon.M.ASCE, Santamarina J.C., and M.ASCE (2005). “Biological Considerations in Geotechnical Engineering”. *Journal of Geotechnical and Geoenvironmental Engineering*, 131(19): 1222-1233.
- NRC. (2006). Geological and Geotechnical Engineering in the New Millennium: Opportunities for Research and Technological Innovation, National Research Council, National Academies Press, Washington, DC.
- Perkins, S.S., Gyr, P., and James, G. (2000). “The influence of biofilm on the mechanical behavior of sand.” *ASTM Geotechnical Testing Journal*, 23(3), 300–312.

- Ramakrishnan, V., Panchalan, R.K., and Bang, S.S. (2005). "Improvement of concrete durability by bacterial mineral precipitation", ICF XI-11th International Conference on Fracture, March 20-25, Turin, Italy.
- Roberts, F.L.; Kandhal, P.S.; Brown, E.R.; Lee, D.Y. and Kennedy, T.W. (1996). Hot Mix Asphalt Materials, Mixture Design, and Construction. National Asphalt Pavement Association Education Foundation. Lanham, MD.
- The Aberdeen Group. (1988). D-cracking pavement: causes are understood but treatment choices are few. Publication # C880845.
- Van der Ruyt, M. and Van der Zon, W. (2009). "Biological in situ reinforcement of sand in near-shore areas". *Geotechnical Engineering*, 162(1): 81-83.
- Vernon, J.M. and Wendell, D. (1982). "Durability of concrete and the Iowa pore index test". *Transportation Research Record*, 853: 25–30.
- Whiffin, V.S., van Paassen, L.A., Harkes, M.P. (2007). "Microbial carbonate precipitation as a soil improvement technique". *Geomicrobiol. J.* 25 (5), 417–423.
- Wood, D.M., Meadows, A., Murray, J.M.H. and Meadows, P.S. "Effect of Fungal and Bacterial Colonies on Slope Stability." *Vegetation and slopes* (1995) 1: 46-51.
- Wu, Y.; Parker, F. and Kandhal, K. (1998). Aggregate Toughness/Abrasion Resistance and Durability/Soundness Tests Related to Asphalt Concrete Performance in Pavements. NCAT Report 98-4. National Center for Asphalt Technology. Auburn, AL.
- Yang, I. C.-Y., Li, Y., and Yen, T. F. (1993). "Subsurface application of slime-forming bacteria in soil matrices." *Applied Biotechnology for Site Remediation*, Hinchee et al., eds., 268–274.

## APPENDIX A. UNCONFINED COMPRESSIVE STRENGTH

The following tables summarize the unconfined compressive strengths of bio-treated materials. The three post processing conditions are saturated with water, air-dried, and oven-dried. Air-dried soil samples were placed outside on a dry day. Oven-dried samples were heated at three temperatures: 38°C, 60°C, and 110°C. Single-treated samples were treated for 5 days, and double-treated samples were treated for 10 days.

**Table 25. Compressive strengths of silica sand treated with NH<sub>4</sub>Cl without bacteria**

Silica sand	Reading	Force (lbs)	Strength (psf)	Average (psf)
<b>Saturated</b>				
Sample 1	6	—	—	—
Sample 2	2	—	—	
Sample 3	2	—	—	
<b>Air-dried</b>				
Sample 4	31	—	—	—
Sample 5	26	—	—	
Sample 6	27	—	—	
<b>Oven-dried (110°C)</b>				
Sample 7	46	—	—	962.7
Sample 8	53	13.2	1275.0	
Sample 9	67	16.7	1613.0	

Note: the empty values mean there is no corresponding force when gauge reading is below 50.

**Table 26. Compressive strengths of silica sand after single bio-treatment with NH<sub>4</sub>Cl**

Silica sand	Reading	Force (lbs)	Strength (psf)	Average (psf)
<b>Saturated</b>				
Sample 10	7	—	—	—
Sample 11	16	—	—	
Sample 12	9	—	—	
<b>Air-dried</b>				
Sample 13	75	18.6	1796.0	568.2
Sample 14	26	—	—	
Sample 15	67	16.7	1613.0	
<b>Oven-dried (110°C)</b>				
Sample 16	182	44.9	4336.0	3894.7
Sample 17	102	25.3	2443.0	
Sample 18	206	50.8	4905.0	

Note: the empty values mean there is no corresponding force when gauge reading is below 50.

**Table 27. Compressive strengths of silica sand after double bio-treatment with NH<sub>4</sub>Cl**

Silica sand	Reading	Force (lbs)	Strength (psf)	Average (psf)
<b>Saturated</b>				
Sample 19	11	—	—	—
Sample 20	6	—	—	
Sample 21	19	—	—	
<b>Air-dried</b>				
Sample 22	59	14.7	1419.0	1815.0
Sample 23	91	22.6	2182.0	
Sample 24	77	19.1	1844	
<b>Oven-dried (110°C)</b>				
Sample 25	1331	338	32638.0	38,672.7
Sample 26	1428	363.7	35119.0	
Sample 27	1942	499.8	48261.0	

Note: the empty values mean there is no corresponding force when gauge reading is below 50.

**Table 28. Compressive strength of SM soil after single bio-treatment with NH<sub>4</sub>Cl**

SM or A-2-4(0)	Reading	Force (lbs)	Strength (psf)	Average (psf)
<b>Saturated</b>				
Sample 55	5	—	—	—
Sample 56	2	—	—	
Sample 57	0	—	—	
<b>Air-dried</b>				
Sample 58	46	—	—	—
Sample 59	37	—	—	
Sample 60	0	—	—	
<b>Oven-dried (110°C)</b>				
Sample 61	79	19.6	1893.0	1761.0
Sample 62	65	16.2	1564.0	
Sample 63	76	18.9	1825.0	

Note: the empty values mean there is no corresponding force when gauge reading is below 50.

**Table 29. Compressive strength of SM soil after double bio-treatment with NH<sub>4</sub>Cl**

SM or A-2-4(0)	Reading	Force (lbs)	Strength (psf)	Average (psf)
<b>Saturated</b>				
Sample 64	9	—	—	—
Sample 65	13	—	—	
Sample 66	15	—	—	
<b>Air-dried</b>				
Sample 67	56	14.0	1352.0	1452.0
Sample 68	61	15.2	1468.0	
Sample 69	64	15.9	1535.0	
<b>Oven-dried (110°C)</b>				
Sample 70	96	23.8	2298.0	1973.0
Sample 71	92	22.8	2202.0	
Sample 72	59	14.7	1419.0	

Note: the empty values mean there is no corresponding force when gauge reading is below 50.

**Table 30. Compressive strength of silica sand treated with (NH<sub>4</sub>)<sub>2</sub>SO<sub>4</sub> without bacteria**

Silica sand	Reading	Force (lbs)	Strength (psf)	Average (psf)
<b>Saturated</b>				
Sample 28	6	—	—	—
Sample 29	3	—	—	
Sample 30	21	—	—	
<b>Air-dried</b>				
Sample 31	43	—	—	—
Sample 32	39	—	—	
Sample 33	37	—	—	
<b>Oven-dried (110°C)</b>				
Sample 34	51	12.7	1226.0	408.7
Sample 35	44	—	—	
Sample 36	47	—	—	

Note: the empty values mean there is no corresponding force when gauge reading is below 50.

**Table 31. Compressive strength of silica sand after single bio-treatment with  $(\text{NH}_4)_2\text{SO}_4$** 

Silica sand	Reading	Force (lbs)	Strength (psf)	Average (psf)
<b>Saturated</b>				
Sample 37	2	—	—	—
Sample 38	11	—	—	
Sample 39	0	—	—	
<b>Air-dried</b>				
Sample 40	68	16.9	1632.0	1702.7
Sample 41	61	15.2	1468.0	
Sample 42	84	20.8	2008.0	
<b>Oven-dried (110°C)</b>				
Sample 43	453	111.6	10776.0	8091.7
Sample 44	231	57.0	5504.0	
Sample 45	336	82.8	7995.0	

Note: the empty values mean there is no corresponding force when gauge reading is below 50.

**Table 32. Compressive strength of silica sand after double bio-treatment with  $(\text{NH}_4)_2\text{SO}_4$** 

Silica sand	Reading	Force (lbs)	Strength (psf)	Average (psf)
<b>Saturated</b>				
Sample 46	10	—	—	—
Sample 47	9	—	—	
Sample 48	17	—	—	
<b>Air-dried</b>				
Sample 49	75	18.6	1796.0	2037.0
Sample 50	89	22.1	2134.0	
Sample 51	91	22.6	2182.0	
<b>Oven-dried (110°C)</b>				
Sample 52	759	186.8	18038.0	18537.0
Sample 53	894	222.0	21437.0	
Sample 54	679	167.1	16135.0	

Note: the empty values mean there is no corresponding force when gauge reading is below 50.

**Table 33. Compressive strength of SM soil after single bio-treatment with  $(\text{NH}_4)_2\text{SO}_4$** 

<b>SM or A-2-4(0)</b>	<b>Reading</b>	<b>Force (lbs)</b>	<b>Strength (psf)</b>	<b>Average (psf)</b>
<b>Saturated</b>				
Sample 73	8	—	—	—
Sample 74	16	—	—	
Sample 75	7	—	—	
<b>Air-dried</b>				
Sample 76	55	13.7	1323.0	441.0
Sample 77	46	—	—	
Sample 78	41	—	—	
<b>Oven dried (<math>110^\circ\text{C}</math>)</b>				
Sample 79	90	22.3	2153.0	2147.0
Sample 80	98	24.3	2346.0	
Sample 81	81	20.1	1941.0	

Note: the empty values mean there is no corresponding force when gauge reading is below 50.

**Table 34. Compressive strength of SM soil after double bio-treatment with  $(\text{NH}_4)_2\text{SO}_4$** 

<b>SM or A-2-4(0)</b>	<b>Reading</b>	<b>Force (lbs)</b>	<b>Strength (psf)</b>	<b>Average (psf)</b>
<b>Saturated</b>				
Sample 82	17	—	—	—
Sample 83	11	—	—	
Sample 84	0	—	—	
<b>Air-dried</b>				
Sample 85	61	15.2	1468.0	1680.0
Sample 86	72	17.9	1728.0	
Sample 87	77	19.1	1844.0	
<b>Oven dried (<math>110^\circ\text{C}</math>)</b>				
Sample 88	101	25.0	2414.0	2478.0
Sample 89	94	23.3	2250.0	
Sample 90	116	28.7	2771.0	

Note: the empty values mean there is no corresponding force when gauge reading is below 50.

We also prepared double bio-treated samples with NH<sub>4</sub>Cl in order to examine the effect of lower temperatures oven-dried.

**Table 35. Compressive strength of silica sand after double bio-treatment with NH<sub>4</sub>Cl**

Silica sand	Reading	Force (lbs)	Strength (psf)	Average (psf)
<b>Oven-dried (38°C)</b>				
Sample 91	51	12.7	1226.0	408.7
Sample 92	31	—	—	
Sample 93	44	—	—	
<b>Oven-dried (60°C)</b>				
Sample 94	14	—	—	940.0
Sample 95	67	16.7	1613.0	
Sample 96	50	12.5	1207.0	

Note: the empty values mean there is no corresponding force when gauge reading is below 50.

## APPENDIX B. CONCRETE COARSE AGGREGATE PROPERTIES

The following tables summarize the properties of untreated and treated coarse aggregate.

**Table 36. Specific gravity and absorption of untreated aggregate**

<b>Untreated aggregate</b>			
	<b>Mass 1 (g)</b>	<b>Mass 2 (g)</b>	<b>Average</b>
<b>A (oven dry in air)</b>	4333.6	3345.2	
<b>B (SSD in air)</b>	4530.2	3466.1	
<b>C (saturated in water)</b>	2736.6	2109.6	
<b>Specific gravity (SSD)</b>	2.53	2.56	2.54
<b>Absorption (%)</b>	4.54%	3.61%	4.08%

**Table 37. Specific gravity and absorption of bio-treated aggregate**

<b>Bio-treated aggregate</b>	
	<b>Mass (g)</b>
<b>A (oven dry in air)</b>	4837.5
<b>B (SSD in air)</b>	5046.9
<b>C (saturated in water)</b>	3061.1
<b>Specific gravity (SSD)</b>	2.54
<b>Absorption (%)</b>	4.33%

## APPENDIX C. CONCRETE MIX DESIGN

**Table 38. Untreated concrete mix design sheet**

Catalog number	Regular concrete	TRIAL #	_____
Mixture ID	Batch size: 0.8 ft <sup>3</sup>		
<b>Mix Date:</b>	<b>2/5/2013</b>		
<b>WHEN USING THE AGGREGATE IN THE BIN:</b>	Coarse Aggregate (Dry):	50.05	lb
<b>Stir the aggregate to obtain a homogenous mix. Run moisture content. Let's say the sand has moisture of a%:</b>	Fine Aggregate (Dry):	34.51	lb
<b>So the aggregate you are going to weigh will</b>	Cement:	16.71	lb
	<b>Waterproofer</b>		lb
	SILICA FUME		lb
4×8 cylinders= 5 3×4×16 beams= 3	Air Entrainer : Micro air	7.00	ml
	Water to be added	<b>10.16</b>	lb

**Table 39. Bio-treated aggregate concrete mix design sheet**

Catalog number	Bio-concrete	TRIAL #	_____
Mixture ID	Batch size: 0.8 ft <sup>3</sup>		
<b>Mix Date:</b>	<b>2/5/2013</b>		
<b>WHEN USING THE AGGREGATE IN THE BIN:</b>	Coarse Aggregate (Dry):	50.27	lb
<b>Stir the aggregate to obtain a homogenous mix. Run moisture content. Let's say the sand has moisture of a%:</b>	Fine Aggregate (Dry):	34.59	lb
<b>So the aggregate you are going to weigh will</b>	Cement:	16.71	lb
	<b>Waterproofer</b>		lb
	SILICA FUME		lb
4×8 cylinders= 5	Air Entrainer : Micro air	7.00	ml
3×4×16 beams= 3	Water to be added	<b>10.07</b>	lb

## APPENDIX D. INDEX PROPERTIES OF CONCRETE

**Table 40. Index properties of untreated concrete**

<b>Untreated Concrete</b>	
Slump (in.)	2
Mix temperature (°F)	60
Container (lbs)	7.85
Container+concrete (lbs)	43.25
Air content (%)	5
Container volume (ft <sup>3</sup> )	0.25
Unit weight (lbs/ft <sup>3</sup> )	141.6
Left water (mL)	110
Beam weight (g)	7129.4

**Table 41. Index properties of bio-treated aggregate concrete**

<b>Bio-treated aggregate concrete</b>	
Slump (in.)	6
Mix temperature (F)	62.5
Container (lbs)	7.85
Container+concrete (lbs)	42.7
Air content (%)	6.7
Container volume (ft <sup>3</sup> )	0.25
Unit weight (lbs/ft <sup>3</sup> )	139.4
Left water (mL)	541
Beam weight (g)	7018.6

## APPENDIX E. COMPRESSIVE STRENGTH OF CONCRETE

**Table 42. Compressive strength of untreated concrete**

<b>Untreated Concrete</b>		
<b>Curing period (days)</b>	<b>Force (lbs)</b>	<b>Strength (psi)</b>
7	50610.0	4028.0
14	51870.0	4128.0
28	58460.0	4652.0
	57340.0	4563.0
Average (28)	57900.0	4607.5

**Table 43. Compressive strength of bio-treated aggregate concrete**

<b>Bio-treated aggregate concrete</b>		
<b>Curing period (days)</b>	<b>Force (lbs)</b>	<b>Strength (psi)</b>
7	45630.0	3631.0
14	48430.0	3854.0
28	59460.0	4732.0
	56910.0	4528.0
Average (28)	58185.0	4630.0

## APPENDIX F. FREEZING AND THAWING RAW DATA

**Table 44. Freezing and thawing raw data**

<b>Mix Date</b>	5-Feb			5-Feb		
<b>Curing Date</b>	6-Feb			6-Feb		
<b>Date in F/T Chamber</b>	20-Feb			20-Feb		
<b>Beam ID</b>	U-1	U-2	U-3	T-1	T-2	T-3
<b>Before F/T</b>	<b>Date</b>	20-Feb				
	<b>Weight (g)</b>	7377.45	7387.21	7369.29	7214.84	7189.44
	<b>Frequency (Hz)</b>	1.575	1.563	1.562	1.473	1.475
<b>30 F/T cycles</b>	<b>Date</b>	26-Feb				
	<b>Weight (g)</b>	7357.5	7403	7380.5	7176.7	7162.1
	<b>Frequency (Hz)</b>	1.522	1.506	1.495	1.417	1.419
	<b>f</b>	-0.053	-0.057	-0.067	-0.056	-0.056
	<b>p<sub>c</sub>=n<sub>1</sub><sup>2</sup>/n<sup>2</sup>*100</b>	93.38	92.84	91.61	92.54	92.55
	<b>Average p<sub>c</sub></b>	92.61			92.97	
	<b>w</b>	-19.95	15.79	11.21	-38.14	-27.34
<b>60 F/T cycles</b>	<b>Date</b>	4-Mar				
	<b>Weight (g)</b>	7280.2	7349.7	7352.2	7084	7088.1
	<b>Frequency (Hz)</b>	1.47	1.422	1.406	1.365	1.391
	<b>f</b>	-0.105	-0.141	-0.156	-0.108	-0.084
	<b>p<sub>c</sub>=n<sub>2</sub><sup>2</sup>/n<sup>2</sup>*100</b>	87.11	82.77	81.02	85.87	88.93
	<b>Average p<sub>c</sub></b>	83.64			87.64	
	<b>w</b>	-97.25	-37.51	-17.09	-130.84	-101.34
<b>90 F/T cycles</b>	<b>Date</b>	10-Mar				
	<b>Weight (g)</b>	7187.4	7283.3	7282.4	6990.4	7036
	<b>Frequency (Hz)</b>	1.299	1.137	1.137	1.242	1.337
	<b>f</b>	-0.276	-0.426	-0.425	-0.231	-0.138
	<b>p<sub>c</sub>=n<sub>2</sub><sup>2</sup>/n<sup>2</sup>*100</b>	68.02	52.92	52.99	71.09	82.16
	<b>Average p<sub>c</sub></b>	57.98			76.18	

	<b>w</b>	-190.05	-103.91	-86.89	-224.44	-153.44	-177.5
<b>120 F/T cycles</b>	<b>Date</b>	16-Mar					
	<b>Weight (g)</b>	6902.2	7121.7	6725.7	6847.4	6947.6	6888.9
	<b>Frequency (Hz)</b>	1.015			1.073	1.244	1.101
	<i>f</i>				-0.4	-0.231	-0.365
	$p_c = n_2^2 / n^2 * 100$				53.06	71.13	56.40
	<b>Average p<sub>c</sub></b>				60.20		
	<b>w</b>	-475.25	-265.51	-643.59	-367.44	-241.84	-296
<b>150 F/T cycles</b>	<b>Date</b>	22-Mar					
	<b>Weight (g)</b>	6412.1	5534.4	5889.8	6577.6	6847.6	6701.7
	<b>Frequency (Hz)</b>					1.046	
	<i>f</i>					-0.429	
	$p_c = n_2^2 / n^2 * 100$					50.29	
	<b>Average p<sub>c</sub></b>						
	<b>w</b>	-965.35	-1852.81	-1479.49	-637.24	-341.84	-483.2

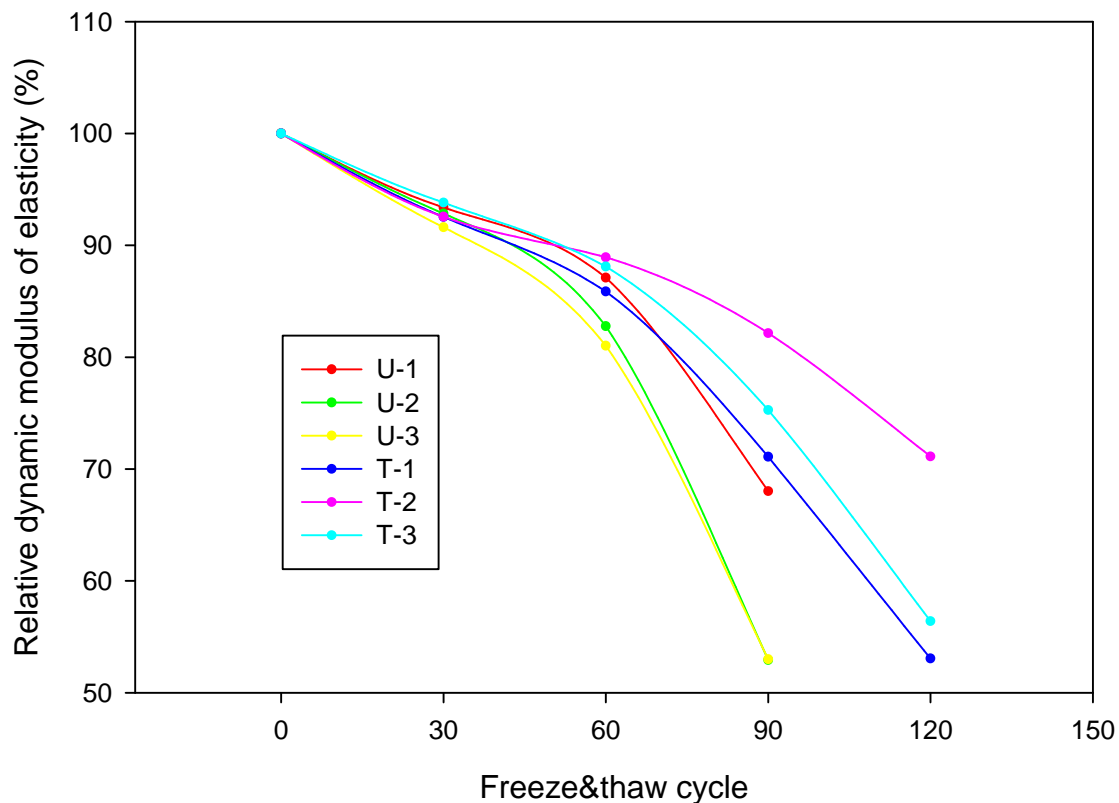


**Figure 99. Variation of relative dynamic modulus after freeze and thaw**

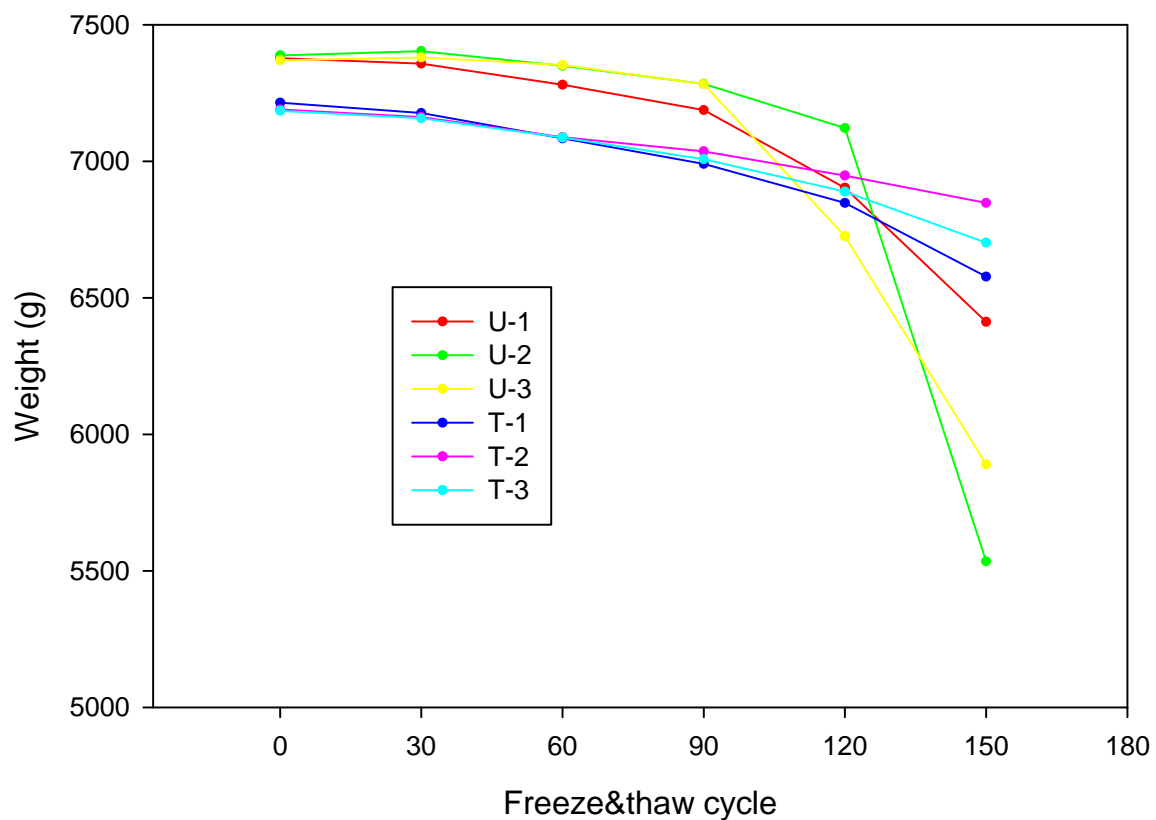


**Figure 100. Variation of weight after freeze and thaw**

120

## **APPENDIX G. MERCURY INTRUSION POROSIMETRY RAW DATA**

**Figure 101** MIP data of raw aggregates

**Figure 102** MIP data of 1-treatment aggregates

**Figure 103.** MIP data of 2-treatment aggregates

**Figure 104.** MIP data of 3-treatment aggregates

**Figure 105** MIP data of 4-treatment aggregates

**Figure 106** MIP data of 5-treatment aggregates

**Figure 107.** MIR data of 6 treatment aggregates

Micrometrics Instrument Corporation		Micrometrics Instrument Corporation		Micrometrics Instrument Corporation		Micrometrics Instrument Corporation		Micrometrics Instrument Corporation		Micrometrics Instrument Corporation	
Autosizer Serial: 121/2/2 Page 1		Autosizer Serial: 121/2/2 Page 1		Autosizer Serial: 121/2/2 Page 1		Autosizer Serial: 121/2/2 Page 1		Autosizer Serial: 121/2/2 Page 1		Autosizer Serial: 121/2/2 Page 1	
Sample: Bulk-Heated-7		Sample: Bulk-Heated-7		Sample: Bulk-Heated-7		Sample: Bulk-Heated-7		Sample: Bulk-Heated-7		Sample: Bulk-Heated-7	
Operator: CB		Operator: CB		Operator: CB		Operator: CB		Operator: CB		Operator: CB	
Submitter: Iowa State University		Submitter: Iowa State University		Submitter: Iowa State University		Submitter: Iowa State University		Submitter: Iowa State University		Submitter: Iowa State University	
File: C:\0900\DATA\0121\2013\09\13\00044A.SMP		File: C:\0900\DATA\0121\2013\09\13\00044A.SMP		File: C:\0900\DATA\0121\2013\09\13\00044A.SMP		File: C:\0900\DATA\0121\2013\09\13\00044A.SMP		File: C:\0900\DATA\0121\2013\09\13\00044A.SMP		File: C:\0900\DATA\0121\2013\09\13\00044A.SMP	
HP Analysis: 2/21/2013 Sample No: W_4245g		HP Analysis: 2/21/2013 Sample No: W_4245g		HP Analysis: 2/21/2013 Sample No: W_4245g		HP Analysis: 2/21/2013 Sample No: W_4245g		HP Analysis: 2/21/2013 Sample No: W_4245g		HP Analysis: 2/21/2013 Sample No: W_4245g	
HP Analysis: 2/21/2013 Corrective/None		HP Analysis: 2/21/2013 Corrective/None		HP Analysis: 2/21/2013 Corrective/None		HP Analysis: 2/21/2013 Corrective/None		HP Analysis: 2/21/2013 Corrective/None		HP Analysis: 2/21/2013 Corrective/None	
Report Tr: 2/21/2013 Show Neg/No		Report Tr: 2/21/2013 Show Neg/No		Report Tr: 2/21/2013 Show Neg/No		Report Tr: 2/21/2013 Show Neg/No		Report Tr: 2/21/2013 Show Neg/No		Report Tr: 2/21/2013 Show Neg/No	
Summary Report		Tabular Report		Cumulative Intrusion vs Pore size		Incremental Intrusion vs Pore size		Cumulative Pore Area vs Pore size		Differential Intrusion vs Pore size	
Penetrometer parameters											Log Differential Intrusion vs Pore size
Pressure [Pa]	0.5	Depth [m]	0.392	Stem, Solid		Penetrometer		Pore size [nm]		Intrusion for Cycle 1	
0.5130E+00	348.28E+00	2.36E-31	0.0	0.0		0.0000E+00		μm²		0.0000E+00	
0.5784E+00	28.47E+00	0.0000E+00	3.11E-06	5.11E-06		3.11E-06		μm²		3.11E-06	
0.6429E+00	21.93E+00	0.0000E+00	1.24E-05	1.78E-05		1.78E-05		μm²		1.78E-05	
0.7074E+00	16.39E+00	0.0000E+00	2.04E-05	2.48E-05		2.48E-05		μm²		2.48E-05	
0.7719E+00	11.85E+00	0.0000E+00	2.84E-05	3.28E-05		3.28E-05		μm²		3.28E-05	
0.8364E+00	8.31E+00	0.0000E+00	3.64E-05	4.08E-05		4.08E-05		μm²		4.08E-05	
0.8999E+00	5.77E+00	0.0000E+00	4.44E-05	4.84E-05		4.84E-05		μm²		4.84E-05	
0.9644E+00	3.23E+00	0.0000E+00	5.24E-05	5.64E-05		5.64E-05		μm²		5.64E-05	
1.0289E+00	1.79E+00	0.0000E+00	6.04E-05	6.44E-05		6.44E-05		μm²		6.44E-05	
1.0934E+00	9.55E-01	0.0000E+00	6.84E-05	7.24E-05		7.24E-05		μm²		7.24E-05	
1.1579E+00	4.99E-01	0.0000E+00	7.64E-05	8.04E-05		8.04E-05		μm²		8.04E-05	
1.2224E+00	2.45E-01	0.0000E+00	8.44E-05	8.84E-05		8.84E-05		μm²		8.84E-05	
1.2869E+00	1.01E-01	0.0000E+00	9.24E-05	9.64E-05		9.64E-05		μm²		9.64E-05	
1.3514E+00	4.67E-02	0.0000E+00	1.004E-04	1.044E-04		1.044E-04		μm²		1.044E-04	
1.4159E+00	2.33E-02	0.0000E+00	1.084E-04	1.124E-04		1.124E-04		μm²		1.124E-04	
1.4804E+00	1.19E-02	0.0000E+00	1.164E-04	1.204E-04		1.204E-04		μm²		1.204E-04	
1.5439E+00	6.55E-03	0.0000E+00	1.244E-04	1.284E-04		1.284E-04		μm²		1.284E-04	
1.6084E+00	3.81E-03	0.0000E+00	1.324E-04	1.364E-04		1.364E-04		μm²		1.364E-04	
1.6729E+00	1.97E-03	0.0000E+00	1.404E-04	1.444E-04		1.444E-04		μm²		1.444E-04	
1.7374E+00	9.43E-04	0.0000E+00	1.484E-04	1.524E-04		1.524E-04		μm²		1.524E-04	
1.7999E+00	4.71E-04	0.0000E+00	1.564E-04	1.604E-04		1.604E-04		μm²		1.604E-04	
1.8644E+00	2.35E-04	0.0000E+00	1.644E-04	1.724E-04		1.724E-04		μm²		1.724E-04	
1.9289E+00	1.17E-04	0.0000E+00	1.724E-04	1.804E-04		1.804E-04		μm²		1.804E-04	
1.9934E+00	5.85E-05	0.0000E+00	1.804E-04	1.884E-04		1.884E-04		μm²		1.884E-04	
2.0579E+00	2.92E-05	0.0000E+00	1.884E-04	1.964E-04		1.964E-04		μm²		1.964E-04	
2.1224E+00	1.46E-05	0.0000E+00	1.964E-04	2.044E-04		2.044E-04		μm²		2.044E-04	
2.1869E+00	7.31E-06	0.0000E+00	2.044E-04	2.124E-04		2.124E-04		μm²		2.124E-04	
2.2514E+00	3.65E-06	0.0000E+00	2.124E-04	2.204E-04		2.204E-04		μm²		2.204E-04	
2.3159E+00	1.83E-06	0.0000E+00	2.204E-04	2.284E-04		2.284E-04		μm²		2.284E-04	
2.3804E+00	9.17E-07	0.0000E+00	2.284E-04	2.364E-04		2.364E-04		μm²		2.364E-04	
2.4439E+00	4.58E-07	0.0000E+00	2.364E-04	2.444E-04		2.444E-04		μm²		2.444E-04	
2.5084E+00	2.39E-07	0.0000E+00	2.444E-04	2.524E-04		2.524E-04		μm²		2.524E-04	
2.5729E+00	1.25E-07	0.0000E+00	2.524E-04	2.604E-04		2.604E-04		μm²		2.604E-04	
2.6374E+00	6.25E-08	0.0000E+00	2.604E-04	2.684E-04		2.684E-04		μm²		2.684E-04	
2.6999E+00	3.13E-08	0.0000E+00	2.684E-04	2.764E-04		2.764E-04		μm²		2.764E-04	
2.7644E+00	1.56E-08	0.0000E+00	2.764E-04	2.844E-04		2.844E-04		μm²		2.844E-04	
2.8289E+00	7.8E-09	0.0000E+00	2.844E-04	2.924E-04		2.924E-04		μm²		2.924E-04	
2.8934E+00	3.9E-09	0.0000E+00	2.924E-04	3.004E-04		3.004E-04		μm²		3.004E-04	
2.9579E+00	1.95E-09	0.0000E+00	3.004E-04	3.084E-04		3.084E-04		μm²		3.084E-04	
3.0224E+00	9.75E-10	0.0000E+00	3.084E-04	3.164E-04		3.164E-04		μm²		3.164E-04	
3.0869E+00	4.875E-10	0.0000E+00	3.164E-04	3.244E-04		3.244E-04		μm²		3.244E-04	
3.1514E+00	2.4375E-10	0.0000E+00	3.244E-04	3.324E-04		3.324E-04		μm²		3.324E-04	
3.2159E+00	1.21875E-10	0.0000E+00	3.324E-04	3.404E-04		3.404E-04		μm²		3.404E-04	
3.2804E+00	5.99375E-11	0.0000E+00	3.404E-04	3.484E-04		3.484E-04		μm²		3.484E-04	
3.3439E+00	3.00E-11	0.0000E+00	3.484E-04	3.564E-04		3.564E-04		μm²		3.564E-04	
3.4084E+00	1.50E-11	0.0000E+00	3.564E-04	3.644E-04		3.644E-04		μm²		3.644E-04	
3.4729E+00	7.5E-12	0.0000E+00	3.644E-04	3.724E-04		3.724E-04		μm²		3.724E-04	
3.5374E+00	3.75E-12	0.0000E+00	3.724E-04	3.804E-04		3.804E-04		μm²		3.804E-04	
3.5999E+00	1.875E-12	0.0000E+00	3.804E-04	3.884E-04		3.884E-04		μm²		3.884E-04	
3.6544E+00	9.375E-13	0.0000E+00	3.884E-04	3.964E-04		3.964E-04		μm²		3.964E-04	
3.7089E+00	4.6875E-13	0.0000E+00	3.964E-04	4.044E-04		4.044E-04		μm²		4.044E-04	
3.7634E+00	2.34375E-13	0.0000E+00	4.044E-04	4.124E-04		4.124E-04		μm²		4.124E-04	
3.8179E+00	1.171875E-13	0.0000E+00	4.124E-04	4.204E-04		4.204E-04		μm²		4.204E-04	
3.8724E+00	5.859375E-14	0.0000E+00	4.204E-04	4.284E-04		4.284E-04		μm²		4.284E-04	
3.9269E+00	2.9296875E-14	0.0000E+00	4.284E-04	4.364E-04		4.364E-04		μm²		4.364E-04	
3.9814E+00	1.464875E-14	0.0000E+00	4.364E-04	4.444E-04		4.444E-04		μm²		4.444E-04	
4.0359E+00	7.314875E-15	0.0000E+00	4.444E-04	4.524E-04		4.524E-04		μm²		4.524E-04	
4.0894E+00	3.6574875E-15	0.0000E+00	4.524E-04	4.604E-04		4.604E-04		μm²		4.604E-04	
4.1439E+00	1.82874875E-15	0.0000E+00	4.604E-04	4.684E-04		4.684E-04		μm²		4.684E-04	
4.1984E+00	9.14374875E-16	0.0000E+00	4.684E-04	4.764E-04		4.764E-04		μm²		4.764E-04	
4.2529E+00	4.572174875E-16	0.0000E+00	4.764E-04	4.844E-04		4.844E-04		μm²		4.844E-04	
4.3074E+00	2.3860875E-16	0.0000E+00	4.844E-04	4.924E-04		4.924E-04		μm²		4.924E-04	
4.3619E+00	1.24304375E-16	0.0000E+00	4.924E-04	5.004E-04		5.004E-04		μm²		5.004E-04	
4.4164E+00	6.21521875E-17	0.0000E+00	5.004E-04	5.084E-04		5.084E-04		μm²		5.084E-04	
4.4709E+00	3.107609375E-17	0.0000E+00	5.084E-04	5.164E-04		5.164E-04		μm²		5.164E-04	
4.5244E+00	1.553704875E-17	0.0000E+00	5.164E-04	5.244E-04		5.244E-04		μm²		5.244E-04	
4.5779E+00	7.768524875E-18	0.0000E+00	5.244E-04	5.324E-04		5.324E-04		μm²		5.324E-04	
4.6314E+00	3.8842624875E-18	0.0000E+00	5.324E-04	5.404E-04		5.404E-04		μm²		5.404E-04	
4.6849E+00	1.94213124875E-18	0.0000E+00	5.404E-04	5.484E-04		5.484E-04		μm²		5.484E-04	
4.7384E+00	9.71065624875E-19	0.0000E+00	5.484E-04	5.564E-04		5.564E-04		μm²		5.564E-04	
4.7919E+00	4.855328124875E-19	0.0000E+00	5.564E-04	5.644E-04		5.644E-04		μm²		5.644E-04	
4.8454E+00	2.4276640625E-19	0.0000E+00	5.644E-04	5.724E-04		5.724E-04		μm²		5.724E-04	
4.8989E+00	1.2138320625E-19	0.0000E+00	5.724E-04	5.804E-04		5.804E-04		μm²		5.804E-04	
4.9524E+00	6.0691660625E-20	0.0000E+00	5.804E-04	5.884E-04		5.884E-04		μm²		5.884E-04	
5.0059E+00	3.0345830625E-20	0.0000E+00	5.884E-04	5.964E-04		5.964E-04		μm²		5.964E-04	
5.0594E+00	1.5172915625E-20	0.0000E+00	5.964E-04	6.044E-04		6.044E-04		μm²		6.044E-04	
5.1129E+00	7.5864575625E-21	0.0000E+00	6.044E-04	6.124E-04		6.124E-04		μm²		6.124E-04	
5.1664E+00	3.7932285625E-21	0.0000E+00	6.124E-04	6.204E-04		6.204E-04		μm²		6.204E-04	
5.2199E+00	1.8966145625E-21	0.0000E+00	6.204E-04	6.284E-04		6.284E-04		μm²	</td		

**Figure 108.** MIP data of 7-treatment aggregates

**Figure 100.** MIR data of 8 treatment aggregates

**Figure 110.** MIR data of 9 treatments at a reactor

Figure 111. MIP data of 10 treatment aggregates.

## APPENDIX H. PLAN FOR FIELD TESTING

In order to test the feasibility of applying microbially induced precipitation in situ, I designed a field-use system that consists of an incubator tank and a distribution system (Figure 112). The incubator tank will be used to culture and store the microorganism in the incubation medium, and the distribution system will be used to apply the bio-stabilization medium to an unpaved gravel road.

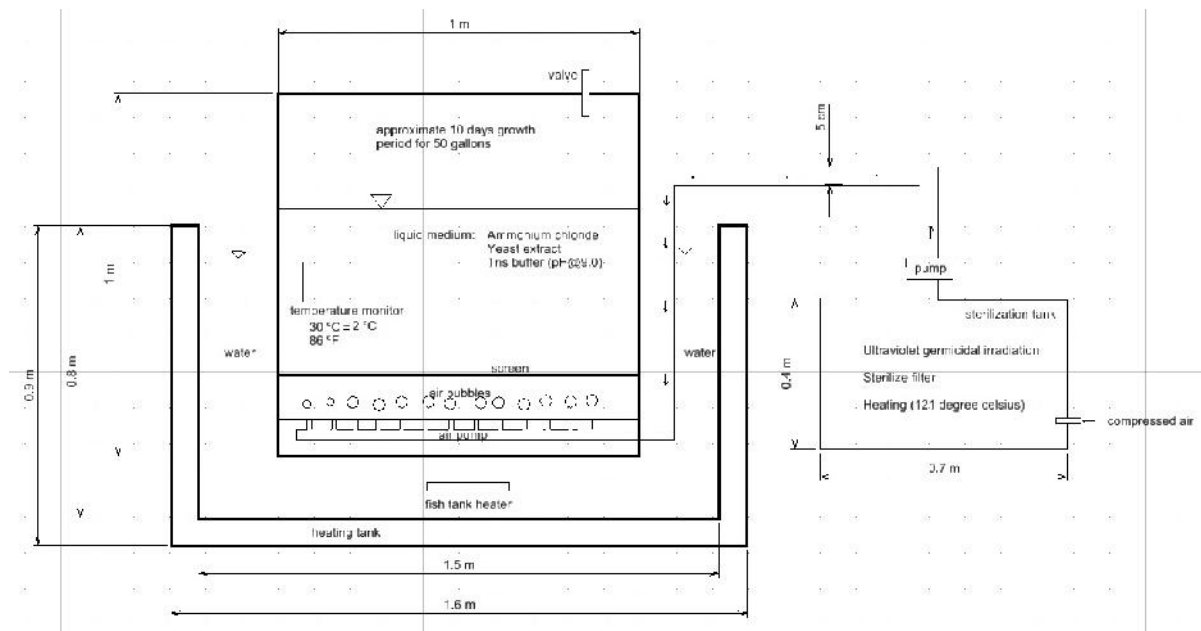


**Figure 112. Schematic diagram of field-use bio-stabilization equipment**